Distinct Neuronal Cell Types in the Rat Auditory Brainstem Exhibit Genetic Response and Synaptic Plasticity Upon Novel Sensory Input

Inauguraldissertation
zur
Erlangung der Doktorwürde
der Fakultät für Biologie
der Albert-Ludwigs-Universität
Freiburg im Breisgau

vorgelegt von

Adrian Reisch
aus Basel (CH)

September 2006

Dekan der Fakultät:	Prof. Dr. Georg Fuchs
Promotionsvorsitzender:	Prof. Dr. Samuel Rossel
Betreuer und Referent der Arbeit:	Prof. Dr. Robert-Benjamin Illing
Koreferent:	Prof. Dr. Klaus Vogt
3. Prüfer:	Prof. Dr. Ad Aertsen
Tag der Verkündigung des Prüfungsergebnisses:	13. Dezember 2006

Declaration

Hereby I declare that this submission is my own work and that, to the best of my knowledge and belief, it contains no material previously published or written by another person, nor material which has to a substantial extent been accepted for the award of any other degree or diploma of the university or another institute of higher learning, except where acknowledgments had been made in the text. The project was supervised by Prof. Dr. Dr. h.c. Roland Laszig and Prof. Dr. Robert-Benjamin Illing. The preparations of the cochlea slices were done by Ingeborg Hirschmüller-Ohmes.

Acknowledgements

First of all I would like to thank Prof. Dr. Robert-Benjamin Illing for his support and encouragement throughout the thesis. I warmly thank Prof. Dr. Dr. h.c. Roland Laszig for his helpfulness and giving me the opportunity to work in the university ENT clinic Freiburg.

Thanks to all members of the neurobiological research laboratory for the numerous discussions and the support. I thank the electrical facility, the ERA laboratory, and the animal facility within the university clinic of Freiburg for their support. Especially I would like to thank Peter Pedersen, the only person I know which can manufacure cochlear implants for rats and the man who had a practical solution for almost all problems concerning stimulation and recordings.

Cochlear Implants and stimulation equipment was kindly provided by Cochlear AG. I kindly thank Dr. Horst Hessel (Hannover) and Herbert Mauch (Basel) from Cochlear AG for their expertise and help.

A PhD scholarship provided by the Deutsche Forschungsgesellschaft is gratefully acknowledged and I wish to thank especially all members of the Freiburg Neuroscience Graduate School for support and interesting discussions.

Finally, special acknowledgments to my family and friends for their encouragement.

1. Summary

The central nuclei of the auditory brainstem are interconnected by excitatory as well as inhibitory ascending, descending, and commissural pathways. In these different nuclei, various neuronal cell types exist. Classically, neurons have been characterized by their morphological appearance. Here, their axonal connections were determined by tracer application in combination with immunocytochemistry to identify the major neuronal cell types of the dorsal (DCN) and ventral cochlear nucleus (VCN), the lateral superior olive (LSO), the medial superior olive (MSO), and the central nucleus of the inferior colliculus (CIC) of the rat to re-evaluate the major cell types of the auditory brainstem in terms of their projection pattern and molecular profile. As molecular markers, the neurotransmitters glutamate, glycine, and GABA, as well as the calcium-binding proteins (CaBPs) parvalbumin (PV), calretinin (CR), and calbindin-D28k (CB) were visualized with fluorescent antibodies. The obtained data were successfully related to the morphological cell types previously described and a so far unrecognized type of neuron in the LSO that forms a descending pathway heading for the VCN was discovered. Moreover, the thesis provides first evidence for the existence of glycinergic neurons in the rat CIC. In the CIC, the large neuronal population of GABAergic cell bodies always contained PV, whereas GABAergic neurons in VCN and LSO were always devoid of CaBPs.

Repetitive patterns of novel sensory activity may induce plastic reconstruction processes of neurons and their communication network in the adult mammalian brain. Expression of the immediate early genes (IEGs) c-fos and egr-1 is a major indicator for the initial step of neuronal remodeling as both encode transcription factors that trigger cascades of activity-dependent protein synthesis. Following spectrally and temporally precisely defined electrical intracochlear stimulation (EIS) that corresponded to physiological acoustic stimulation and lasted for two hours under anesthesia, those neuronal types that express IEGs in VCN, DCN, LSO, and CIC of the rat were characterized. Patterned activation of sensory afferents affected only neuronal sub-populations, but not non-neuronal cells. Specific glutamatergic and glycinergic cells responded in all four areas, whereas GABAergic neurons failed to do so except for DCN. Combining immunocytochemistry with axonal tracing, commissural VCN cells and neurons of the descending auditory system were identified to respond to EIS with IEG expression, while principal LSO cells projecting to the contralateral

CIC as well as collicular efferents of the DCN did not. In total, less than 50% of the identified neurons turned up expression of IEG transcription factors as a consequence of stimulation. The pattern of IEG expression caused by unilateral EIS in the auditory brainstem suggests that dominant sensory activity may quickly initiate a facilitation of central pathways serving the active ear at the expense of those serving the unstimulated ear.

C-Fos, as a part of the AP-1 transcription factor complex, has the ability to induce the growth and plasticity-associated protein GAP-43, which is involved in structural synaptic rearrangements. When extending the time frame of stimulation from two hours to seven days in unanesthetized and freely moving animals, molecular changes beyond IEG expression were detected. Increased levels of GAP-43 and the polysialylated form of the neural cell adhesion molecule (PSA-NCAM) were observed in the anteroventral cochlear nucleus (AVCN) of the stimulated side, strongly indicating activity-dependent structural rearrangements of synapses. In the AVCN of the unstimulated side, but also in DCN and posteroventral cochlear nucleus (PVCN) on both sides, these two plasticity-associated molecules remained at control levels. In the LSO, GAP-43 but not PSA-NCAM showed increased levels on the stimulated side. It seems therefore likely, that GAP-43 positive fibers originate from the LSO and project to AVCN to mediate structural plasticity caused by increased and novel afferent activity.

2. Introduction

2.1. Central Auditory System

The central auditory system of the mammalian brain serves analysis and feature detection of the acoustic environment. These fundamental functions are shared by specific types of neurons arrayed in various nuclei and connected by a complex network of ascending, descending, and commissural pathways (for review c.p. Malmierca, 2003). The auditory brainstem consists of four large nuclei which are all divided into further sub-nuclei (Fig. 1). Sound-induced movements of the tympanic membrane lead to pressure changes in the fluid-filled cochlea which are translated into electrical information that reaches the brain via spiral ganglion neurons forming the auditory nerve. Acoustic information arrives in the cochlear nucleus complex (CNC), passes trough the superior olivary complex (SOC), the dorsal (DNLL) and ventral nucleus of the lateral lemniscus (VNLL) to reach the inferior colliculus (IC). From CNC, auditory information is processed via three different pathways. The dorsal acoustic stria (DAS) and the intermediate acoustic stria (IAS) mainly provide input to the contralateral nuclei of the lateral lemniscus (NLL) and IC (Fig. 1). The ventral acoustic stria (VAS) or trapezoid body (TB) processes information to the SOC on both sides. When leaving the brainstem, auditory information transverses the medial geniculate body (MGB) of the thalamus to arrive in the primary auditory cortex (AC).

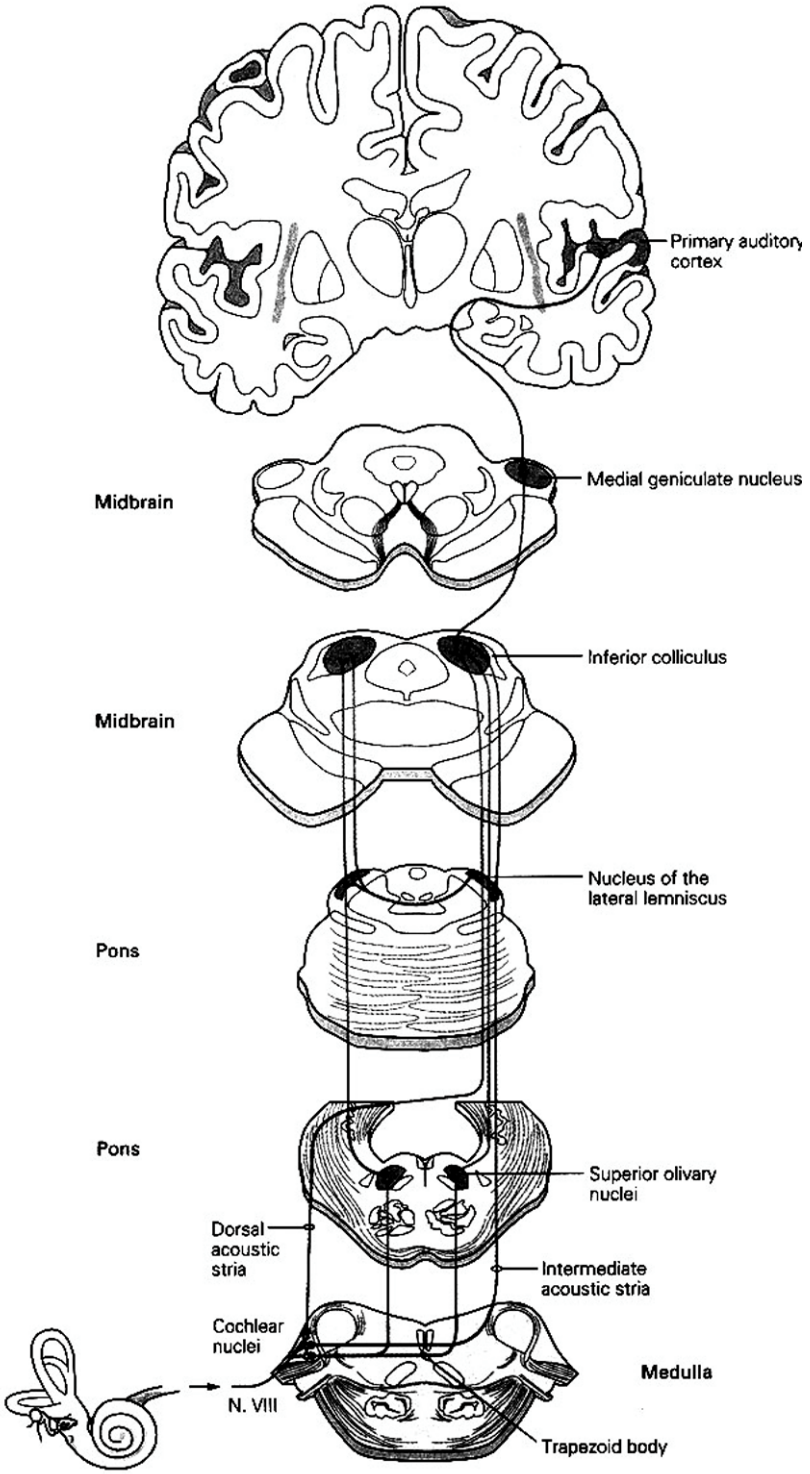

Figure 1: The central auditory pathways of the mammalian brain. Auditory nerve fibers from the cochlea terminate in CNC. Neurons of the CNC send their axons to various centers in the brain via three main pathways: 1) the DAS, 2) the IAS, and 3) the VAS or TB. Neuronal cells in SOC receive input via the VAS and project, along with neurons of the CNC, to the IC via the lateral lemniscus. Cells of the IC send their axons to the MGB, while the axons of MGB neurons terminate in the primary AC (from Kandel et al., 2000).

2.1.1. Spiral Ganglion of the Cochlea

The pinna of the outer ear is designed to collect sounds from a wide area of the environment. Via the auditory canal, sound reaches the tympanic membrane (tympanum), which is connected to the ossicles (maleus, incus, and stapes) of the middle ear (Fig. 2A). These three middle ear bones transfer sound induced deflections of the tympanic membrane to the fluid-filled cochlea, leading to pressure changes. The basilar membrane of the cochlea (Fig. 2B) is deflected by these pressure changes and acoustic information is translated into electrical impulses by mechanoelectrical transduction of inner hair cells (IHCs). Cila of the IHCs undergo displacement by the deflecting basilar membrane, causing K^+ channels to open. Massive influx of K^+ ions into the hair cells leads to depolarization, that generates action potentials. This electrical information is processed to the distal part of the spiral ganglion neurons, which build the auditory nerve with their distal and proximal appendices. The auditory nerve connects IHCs of the cochlea with neurons in CNC. Acoustic stimulation of a distinct frequency excites maximal motion at a particular position on the basilar membrane. Low-frequency sounds excite the basilar membrane near the apex, high-frequency sounds excite the membrane at its base (Fig. 2C). This tonotopic organisation of the cochlea is also represented in the nuclei of the auditory brainstem. Outer hair cells (OHCs) do not directly process auditory information but serve as amplificators by enhancing the deflection of the basilar membrane or as silencers of extremely strong inputs by minimizing baslilar membrane deflection.

2.1.2. Cochlear Nucleus Complex

All fibers of the auditory nerve terminate in one of the three sub-nuclei of the CNC; the dorsal (DCN), the anteroventral (AVCN), or the posteroventral cochlear nucleus (PVCN). AVCN and PVCN together form the ventral cochlear nucleus (VCN). The distribution of the auditory information into three parallel channels is based on the separation of the CNC into these three sub-nuclei. Three parallel auditory nerve tracts, the DAS, the IAS, and the VAS form three separate pathways trough the auditory brainstem, before information leaves the brainstem via IC.

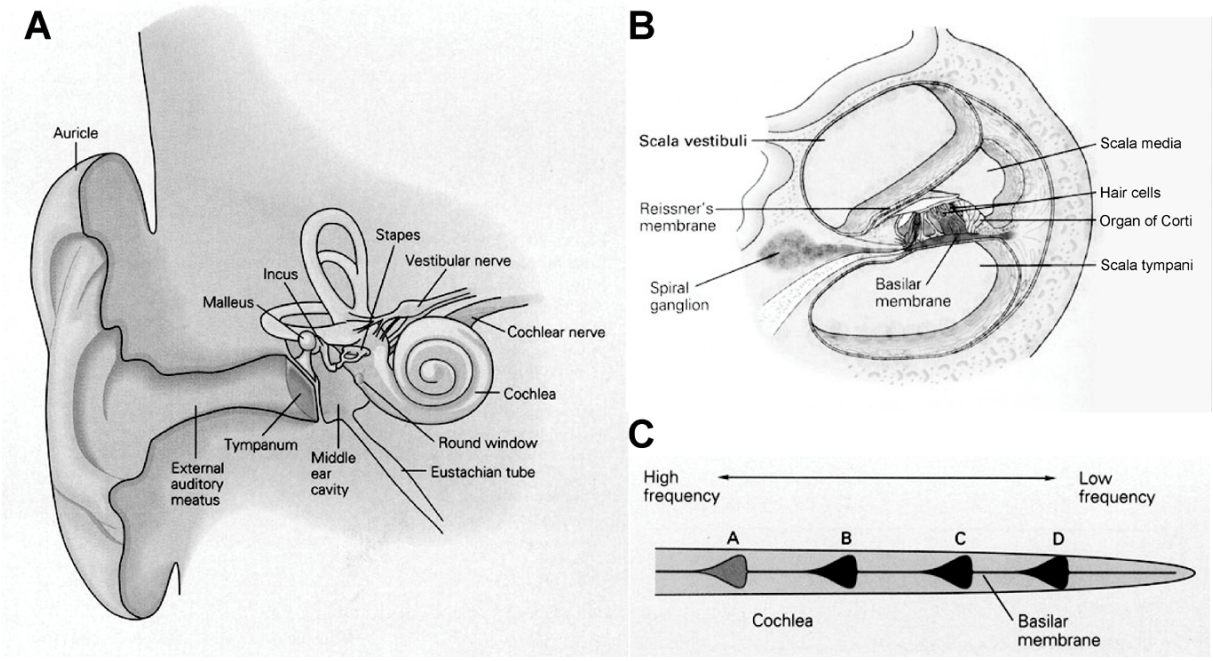

Figure 2: The mammalian ear. A: Vibrations of the tympanic membrane (tympanum) are conveyed by the three middle ear bones malleus, incus, and stapes. The stapes pushes against the oval window of the cochlea to stimulate the inner ear. B: The oval window is connected to the scala vestibuli and pressure changes caused by movements of the stapes lead to deflections of the basilar membrane. Hair cells translate mechanical sound information into electrical signals that are sent to the brain by neurons of the spiral ganglion. C: Each frequency of stimulation excites maximal motion at a particular position along the basilar membrane. Low-frequency sound excites the basilar membrane near the apex, high-frequency sound excites the membrane at its base (from Kandel et al., 2000).

The DAS originates from fusiform and giant cells in DCN, projecting mainly via the contralateral NLL to the IC (Osen, 1972; Oliver, 1984). Fusiform neurons mediate excitation (Oliver, 1985) while giant cells mediate inhibition (Adams, 1979; Alibardi, 2000). There is also a frequency specific projection from the DCN to the ipsilateral VCN that originates from vertical cells and mediates inhibition (Saint Marie et al., 1991; Zhang and Oertel, 1993). One of the distinguishing features of the DCN is its diversity in cell types, the majority of which are interneurons that create inhibitory local neuronal circuits (Osen et al., 1990; Kolston et al., 1992; Ottersen et al., 1995). In the rat, the DCN is organized in layers lying in the horizontal plane (Malmierca, 2003) and tonotopically organized with high frequencies represented in the dorso-medial part and low frequencies in the ventro-lateral part.

The main projection of the IAS is formed by the large axons of octopus cells in PVCN, that target the contralateral VNLL (Warr, 1966; Friauf and Ostwald, 1988; Schofield and Cant, 1997). A small collateral projection of octopus neurons also projects to the perolivary regions. Octopus cells receive input from several spiral ganglion neurons of different frequency specificity and therefore respond stronger to defined frequency spectra than to pure tones. Glutamatergic octopus cells are relatively few and they are easily identified by their compact, island-like location, their ovoid shape of the somata, their eccentric nuclei, and their distinctive dendritic morphology (Alibardi, 1998b).

Multipolar type II neurons in the VCN, whose axons also leave via the IAS, target the contralateral CNC (Doucet and Ryugo, 1997; Doucet et al., 1999). The axons also give rise to extensive collateral branches within the parent VCN and send widespread terminations to the ipsilateral DCN. In both, ispilateral and contralateral CNC, the axon terminals contain pleomorphic or flattened synaptic vesicles, consistent with an inhibitory effect on the target cells (Smith and Rhode, 1989; Alibardi, 1998a).

The VAS originates from spherical bushy, globular bushy, and multipolar cells of the VCN and processes auditory information to the SOC on both sides (Harrison and Warr, 1962; Friauf and Ostwald, 1988). Bushy cells are mainly located in the AVCN, in the anterior PVCN some globular bushy cells are additionally found. Large presynaptic structures of spiral ganglion neurons, the endbulbs of held, terminate directly on the soma of bushy cells (Sento and Ryugo, 1989). A single action potential on the presynaptic ending is able to spill enough neurotransmitter to depolarize the postsynaptic cell to threshold. Therefore, this type of connection is perfectly suited to process neuronal signals that are temporally coupled to the sound phase without loss of temporal information. The large myelin sheet of the bushy cell axons, which enables a fast conduction of action potentials, allows conservation of the temporal structure of acoustic information. Axons of spherical bushy cells terminate in the ipsilateral lateral superior olive (LSO) and in the medial superior olive (MSO) on both sides of the brainstem (Warr, 1966; Cant, 1984; Friauf and Ostwald, 1988). Axons of globular bushy cells innervate the lateral nucleus of the trapezoid body (LNTB) as well as the medial nucleus of the trapezoid body (MNTB; Henkel and Gabriele, 1999). The VCN is strictly tonotopically organized with high frequencies represented in the dorsal part and low frequencies represented in the ventral part.

2.1.3. Superior Olivary Complex

The three main nuclei of the SOC are more diffusely than sharply separated from the environment. MSO, LSO, and MNTB mainly receive inputs from bushy cells (Warr, 1966; Friauf and Ostwald, 1988; Henkel and Gabriele, 1999). An essential function of the SOC is sound localization (van Adel and Kelly, 1998). Calculation of the space-coordinates of a sound source is based on the detection of differences in intensity and time of an auditory event between left and right ear.

The MSO mainly serves to localize sound sources in the horizontal plane by the temporal phase difference of the sound event (Masterton et al., 1975). The MSO mainly consists of multipolar neurons projecting to DNLL (Oliver and Shneiderman, 1989) and IC (Henkel and Spangler, 1983) on the same side.

The LSO mainly serves to calculate information about the direction of sound sources from intensity differences at the two ears. Principal neurons of the LSO are multipolar and receive excitatory input from spherical bushy cells of the ipsilateral AVCN (Warr, 1966; Cant, 1984; Osen, 1988) and additionally inhibitory input of neurons from the MNTB (Moore and Caspary, 1983; Saint Marie et al., 1989; Adams and Mugnaini, 1990). By this mixture of ipsilateral excitatory and contralateral inhibitory input, the ground-level activity of LSO principal neurons is increased, if the sound source is located ipsilaterally and decreased if it is located contralaterally (Finlayson and Adam, 1997). The MNTB serves to reform the excitatory glutamatergic projection of the AVCN neurons (Henkel and Gabriele, 1999) into an inhibitory glycinergic projection. The LSO is tonotopically organized, with isofrequency bands arranged in the dorsal-ventral axis. In the rat, the LSO is S-shaped and structured in a lateral, an intermediate, and a medial limb. Low frequencies are represented laterally, high frequencies medially.

The SOC is also a major source for descending pathways projecting back to the cochlea. These olivocochlear connections can be anatomically divided in two different systems; the lateral olivocochlear (LOC) and the medial olivocochlear (MOC) system (Warr et al., 1986). Small neurons of the LOC system are located in the LSO and dispersed over the full frequency area (Warr, 1975; Warr and Guinan, 1979). There are at least two sub-populations of LOC neurons. Cholinergic cells additionally express calcitonin gene-related peptide (CGRP), GABAergic neurons are CGRP negative (Vetter et al., 1991). Axons of both sub-populations project to the region of the IHCs in the cochlea, where they synapse on the

radial spiral ganglion fibers immediately underneath the IHCs (Warr and Guinan, 1979; Guinan et al., 1983). In the rat, LOC neurons exclusively project to the cochlea on the same side (White and Warr, 1983; Aschoff and Ostwald, 1988) and there are no collateral projections to VCN (Horváth et al., 2000). Functionally viewed, LOC neurons guide back part of the auditory information that is processed via ipsilateral VCN to the SOC, to the cochlea. This feedback loop may function as a safety mechanism protecting IHCs from damage caused by high-intensity noise (Robertson and Anderson, 1994). Outside the LSO, in the perolivary regions, one can find the so called shell neurons, that are interpreted as an additional LOC system (Warr et al., 1997). Like LOC neurons, axons of shell LOCs are very thin and project back to IHCs of the ipsilateral cochlea (Kraus and Illing, 2005). A frequency specificity is just hardly recognizable and the function of these cells is fairly unknown.

MOC neurons are localized in the ventral nucleus of the trapezoid body (VNTB), medial to the MSO, projecting to both cochleae. A small part of fibers projects in an uncrossed pathway to the ipsilateral cochlea, the larger part in a crossed pathway to the contralateral cochlea (Aschoff and Ostwald, 1988) The myelinated MOC axons form synapses directly at the basis of OHCs. A large part of the projection contacts cells of the middle frequency range of the cochlea. Contrarily to LOC neurons, collateral connections of MOC neurons form excitatory connections to VCN multipolar cells (Horváth et al., 2000). There is only one population of triangular-shaped MOC neurons, all cholinergic and CGRP negative. In the rat, they are located in VNTB tonotopically arranged from medial to lateral corresponding to the frequency areas of the cochlea from high to low (Vetter and Mugnaini, 1992). Activation of the MOC system leads to inhibition of OHCs. The release of the neurotransmitter acetylcholine at presynaptic terminals directly at the basis of OHCs increases the conductance of Ca^{2+}-dependent K^+ channels, leading to increased K^+ influx and therefore to depolarization of OHCs. This inhibits the active oscillation of the OHCs reducing the vibration of the basilar membrane. A mechanism for sound protection of the MOC system is very likely (Kukawa and Liberman, 1997). Additionally the MOC system increases the dynamic range of the auditory system by actively increasing or decreasing the sensitivity for hearing of OHCs compared to sound intensity.

2.1.4. Inferior Colliculus

The IC is the largest auditory center of the brainstem, separated into several sub-nuclei, and it is also the last nucleus before centrally processing informations reach the thalamus. The central nucleus of the inferior colliculus (CIC), the largest of the IC sub-nuclei, is surrounded by several smaller nuclei, which lie sheet-like on the borders of the spherical central area. The CIC mainly receives projections originating in DNLL and LSO on both sides, from ipsilateral VNLL and MSO, as well as from contralateral CNC (Coleman and Clerici, 1987; Oliver et al., 1999; Casseday et al., 2002). To which amount the monaural and binaural inputs converge in CIC is still not completely clarified.

The major ascending projection of the CIC leads to the ipsilateral MGB. The ventral division of the MGB receives a topographical projection which preserves tonotopicity and provides short latency responses (Calford and Aitkin, 1983). Although the majority of this projection is probably glutamatergic and excitatory, a strong GABAergic and inhibitory input to the MGB has been demonstrated (Winer et al., 1996; Peruzzi et al., 1997). There is a strong glutamatergic projection trough the commissure of the CIC (Saint Marie, 1996; Zhang et al., 1998), but the existence of a GABAergic projection has also been described (Gonzales-Hernandez et al., 1996). Neurons projecting trough the commissure of the CIC can therefore mediate inhibitory as well as excitatory effects on their contralateral counterparts (Malmierca et al., 2005). Additionally, many interneurons assume strong neuronal interconnections in the CIC itself (Osen, 1972). The CIC has a characteristic laminar organization (Faye-Lund and Osen, 1985; Malmierca et al., 1993) that constitutes the structural basis for its tonotopic organization (Ryan et al., 1988; Kelly et al., 1991; Friauf, 1992). High frequencies are represented in the ventro-medial region, low frequencies in the dorso-lateral area of the CIC.

2.1.5. Medial Geniculate Body of the Thalamus

The MGB lies in the postero-lateral surface of the thalamus as a round eminence and represents the main auditory center of the thalamus, the last center for auditory processing before inputs reach the AC. The MGB contains three main sub-divisions; ventral (MGBv), dorsal (MGBd), and medial (MGBm); each defined on the basis of cytoarchitecture and fiber connections (LeDoux et al., 1985; Clerici et al., 1990; Winer et al., 1999). On the basis of cytoarchitectonic, connectional, and functional features, it has been suggested that MGBv has a purely acoustic function (LeDoux et al., 1987; Bordi and LeDoux, 1994), while MGBd is involved in acoustic attention and MGBm in multisensory arousal and emotional auditory learning (Herkenham, 1980; Bordi and LeDoux, 1994; Linke, 1999).

2.1.6. Primary Auditory Cortex

The AC represents the site of termination of fibers ascending from the MGB and shows large variations between species. Based on Nissl-stained and Golgi-impregnated material, Games and Winer (1988) analyzed the neuronal architecture of the central core region in the adult rat. They distinguished six distinct layers extending over 1.1-1.2 mm. Layer I extends about 140 μm from the pial surface and contains very few neurons. Layer II is densely packed with many small neurons and is 125 μm thick. Layer III is populated by both pyramidal and nonpyramidal neurons whose dendritic arbors are heterogenous in orientation and extends over 190 μm. In layer IV, neurons are smaller, stellate in shape, and more densely packed than in layer III. Layer IV is only about 100 μm thick. Layer V is thickest and represents about 25% (270 μm) of the total. It begins approximately midway and possesses a lower neuronal packing density and larger cells than layer IV. The main cell type consists of pyramidal cells, which are larger and more numerous in the lower than in the upper half of layer V. Layer V is of particular interest because its cells form part of the projection to the thalamus, subthalamic nuclei, and contralateral cortex through the corpus callosum (Moriizumi and Hattori, 1996; Saldana et al., 1996; Hefti and Smith, 2000). Finally, layer VI contains both pyramidal cells and nonpyramidal cells that are closely packed. It is 245 μm thick and represents about 22% of the cortical depth.

2.2. The Cochlear Implant

2.2.1. An Introduction to the Cochlear Implant

Cochlear Implant (CI) users can, due to deafness caused by loss of hair cells, only hear by the aid of this inner ear prothesis. The cause for deafness is very often a genetic disposition for prelingual deaf people, whereas postlingual deafening is mostly the result of a noise exposure for long time, a hearing trauma or other pathological processes. Contrary to the loss of other sensory perceptions, deafness results in the total loss of verbal social interactions. Postlingual deafened persons are suddenly pushed out of their habituated acoustical environment. Deaf born children get no chance to enter the world of hearing without CIs. The CI enables deaf children and adults to overcome the verbal communication handicap with a high probability (Marangos and Laszig, 1996).

During implantation of the CI, the electrode carrier is inserted via the round window into the cochlea and wires there around the modiolus (Fig. 3A). A crucial prerequisite for the CI therapy are intact spiral ganglion neurons in the cochlea. Activation of CI electrodes generates electrical fields that induce action potentials in the intramodial spiral ganglion cells of the acoustic nerve (Fig. 3B). The temporal and local patterns of the electric fields are mainly responsible for the hearing (Kral et al., 1998) and are generated by changing combinations of active electrodes. The basics for electrode activation are calculated from acoustic signals of the environment in the mobile speech processor and sent to the implanted receiver by radio signals.

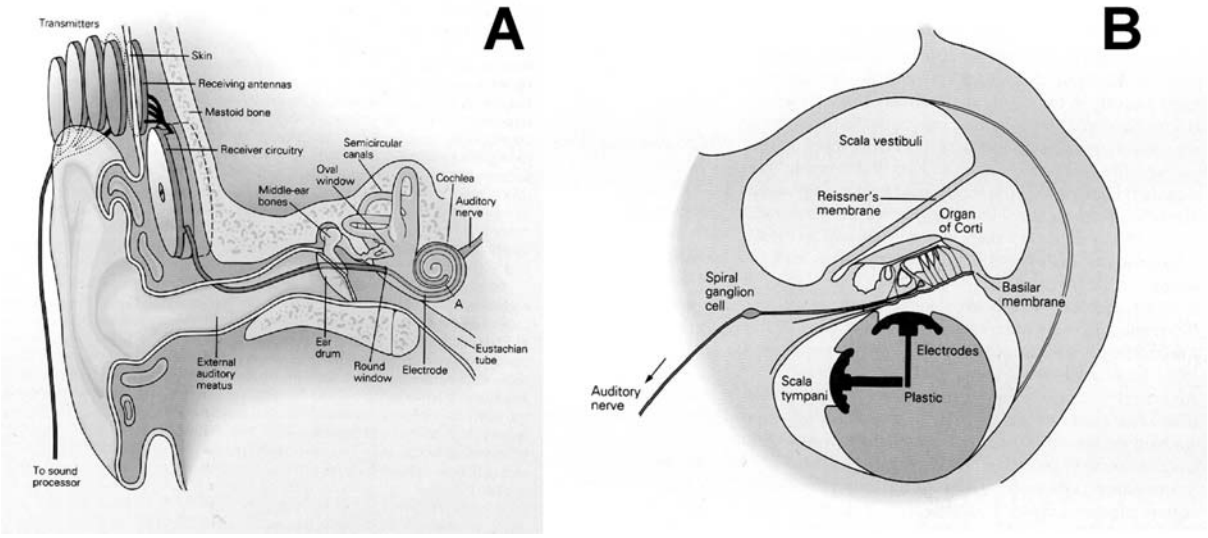

Figure 3: The Cochlear Implant. A: Position of the electrode carrier in the cochlea. B: Cross section of the cochlea showing the placement of the electrode array. Current flow between an electrode pair excites the auditory nerve fibers directly, causing them to fire action potentials (from Kandel et al., 2000).

2.2.2. Adaptation of the Nervous System to the Cochlear Implant

In the more than 20 years of experience with CIs, important parameters, either favoring or refusing implantation, appeared. In deaf born children, it is considered as most successful to implant as soon as possible (Shepherd et al., 1997; Robinson, 1998). Age is here the limiting factor for the operation and today implantations are mostly performed with children in their second year of age, since younger children can not be operated. In deaf adult, the time that passes from deafening to implantation is the critical determinant. The sooner the operation, the better the chances to succeed in gaining back normal hearing. If a critical time window passed, in both cases a CI therapy is unsuccessful (Robinson, 1998; Ponton et al., 1999). The reason for this unsuccessfulness is probably a loss of sensory evoked activity in the auditory system, which leads to changes in the functional organization of the auditory brainstem (Moore et al., 1997; Ponton et al., 1999).

After CI implantation, readjustments of stimulation parameters are necessary in the phase of rehabilitation. The optimal adjustment is in general only valid for a distinct but constantly increasing postoperative time interval. The stepwise adaptation of the auditory system onto the stimulation parameters points towards that the auditory system adapts only slowly to novel sensory situations after a longer hearing break. This phenomenon resembles learning of a novel complex motion, which can only be performed optimally after learning the necessary basic movements.

Understanding structural and functional relationships in auditory neurons necessary to translate CI signals into hearing is a central object of science. By knowing which activity patterns induce neuronal plasticity and by identifying molecules that play key roles during physiological and morphological adaptation, plastic events in the nervous system could be influenced and directed. This knowledge could speed up the success of therapy and allow a more effective use of the CI. The time point of implantation could be fixed more flexible and parameters that are important for the adaptation of the novel hearing technique could be influenced optimally.

2.3. Neuronal Plasticity

In the 20th century, the image of the function of the brain was enhanced by the idea of learning-related structural dynamics of the nervous system. A first thesis was postulated in 1949 by Donald Hebb with the theory of synaptic plasticity. The main prediction of this theory was that in two connected nerve cells, a memory to a distinct state of activity is saved by structural adaptations. The two rules postulated by Hebb were as follows: Cells that fire together, wire together, and: Cells that fire out of sync, lose their link. In the 70s, Hubel and Wiesel showed with a pioneering study in the field of plasticity, how strong the functional anatomy of central structures depends on sensorial experience during critical phases. The physiological equivalent of the Hebbian synapse, the so called long-term potentiation (LTP) was discovered shortly afterwards by Bliss and Lomo (1973). These experiments represented the first scientific proves of activity-dependent structural plasticity in the central nervous system (CNS). In the beginning, many neuroscientists were convinced that neuronal plasticity only plays a role in the developmental stages of an organism. Later, when it was shown that

plastic processes also occur in the adult CNS (Kaas et al., 1983; Clark et al., 1988), many people were convinced that neuronal plasticity is restricted to the cortex. Acceptance of the concept of subcortical plasticity has been slow, but due to a variety of crucial experiments (Darlington et al., 1991; Illing and Horváth, 1995; Palmer et al., 1998; Jain et al., 2000), even the brainstem has finally been included into the plastic brain.

Plasticity is a crucial sign for the adaptability of the CNS to novel situations. The potential of neuronal plasticity is primarily determined by the ontogenetic state of the organism and secondarily by the cerebral hierarchy. The nervous system of the young organism has a higher potential for plasticity than the adult. Nevertheless, the key molecules that take part in plastic processes are mostly the same. The actual science in the field of neuronal plasticity tries to discover circumstances, signaling pathways, and molecules that trigger, guide or inhibit plastic processes (Darlington et al., 1991).

2.3.1. Activity-Dependent Plasticity

At the beginning of plastic neuronal processes, there is mostly a change in the "used" activity pattern of the nerve cell (Hess et al., 1995; Zhu et al., 1995; 1997). This change in activation can be determined either by intrinsic developmentally related factors (Goodman and Shatz, 1993), or by external sensory factors (Hubel and Wiesel, 1970). Pathological processes may also induce plastic events in the brain (Bledsoe et al., 1995; Hughes et al., 1999). The loss of natural, sensory evoked excitatory patterns of auditory neurons can for example lead to changes in their physiological identity, but also to degeneration of the affected nerve cells (Kim et al., 1997; Morest et al., 1998). If sensory systems affected by an acoustic deprivation are artificially stimulated afterwards, the physiological function of auditory neurons can be conserved (Hartshorn et al., 1991; Matsushima et al., 1991) and the degeneration of the affected structures is significantly attenuated (Lousteau, 1987; Leake et al., 1999). Stimulation with a CI immediatelly after deafening showed that the nervous system is able, after a phase of adaptation, to accept the electrically evoked signals as a substitute for the natural sensory evoked signals of the inner ear and to recognize them as relevant auditory information (Marangos and Laszig, 1996).

Brief high-frequency stimulation of a neural pathway can induce long-lasting increases in synaptic efficacy (Bliss and Lomo, 1973). This so called LTP provides an experimental analogue of learning-induced changes in synaptic connectivity. This activity-dependent synaptic potentiation occurs within milliseconds and can persist for many hours in the anaesthetized animal and even for days to weeks when induced in the awake animal (for review c.p. Bliss and Collingridge, 1993). The early component of LTP is protein synthesis independent, the late phase of LTP depends on changes in gene expression and protein synthesis (Huang et al., 1994; Nguyen et al., 1994; Barea-Rodriguez et al., 2000). Signalling molecules which link the activity that induces LTP to the nucleus by activating key transcription factors play an important role for the transition of early LTP into late LTP (Abraham and Williams, 2003; Pittenger and Kandel, 2003; Lynch, 2004). Another molecule important for LTP is the protein kinase C (PKC; Linden and Routtenberg, 1989; Bliss and Collingridge, 1993; Malenka and Nicoll, 1999), which changes the state of activity of plasticity-associated proteins via phosphorylation. In the latest phase of LTP, morphological changes that include growth of new synapses, enlargement of preexisting synapses, and splitting of single postsynaptic densities into two functional synapses take place (Yuste and Bonhoeffer, 2001; Abraham and Williams, 2003).

2.3.2. Immediate Early Genes: The First Molecular Indicators for Plasticity

Expression of immediate early genes (IEGs) is an integral step in molecular signaling cascades triggered by specific patterns of neuronal activity to initiate LTP. The emergence of the IEG transcription factors c-Fos (Morgan and Curran, 1989) and Egr-1 (Sukhatme et al., 1988), also known as Zif-268 (Christy et al., 1988), NGFT-A (Milbrandt, 1987) or Krox 24 (Lemaire et al., 1988), is indicative for neurons in the adult mammalian brain to be transformed into a state of plasticity (Cole et al., 1989; Rampon et al., 2000). C-Fos expression in the CNC is strongly increased following stimulation with novel sounds (Hillman et al., 1997) or after electrical stimulation of the cochlea (Saito et al., 2000; Illing et al., 2002). Beyond CNC, neurons throughout the ascending auditory system ranging from SOC (Adams, 1995), DNLL (Saint Marie et al., 1999a), CIC (Ehret and Fischer, 1991; Friauf, 1995), and MGB (Rouiller et al., 1992) to AC (Zuschratter et al., 1995; Geissler and Ehret, 2004) may respond to acoustic or electric stimulation of the ear with a tonotopically specific

up-regulation of c-Fos. The expression of c-Fos is especially strong when a novel stimulus is presented (Hillmann et al., 1997) or when the stimulus is behaviourally relevant (Carretta et al., 1999). The continuous repetition of a stimulus let the c-Fos expression decrease compared to a unique presentation of the stimulus (Keilmann and Herdegen, 1996; 1997).

Like c-Fos, the expression of Egr-1 is also stimulation-dependent (Chaudhuri, 1997) and represents a molecular marker for the induction of LTP (Cole et al., 1989; Bramham et al., 1996). Egr-1 is ascribed to induce structural rearrangements of neurons after LTP (Platenik et al., 2000) and plays a major role in the stimulation-dependent development of cortical structures (Kaplan et al., 1995). Both transcription factors, c-Fos and Egr-1 are co-regulated very often in the nervous system (Sukhatme et al., 1988).

2.3.3. Activity-Dependent Morphological Rearrangements Mediated by GAP-43 and PSA-NCAM

C-Fos is a monomeric part of the activator protein 1 (AP-1) dimer (Herdegen and Leah, 1998), which can regulate the transcription of the gap-43 gene via an AP-1 binding site in its promotor region (de Groen et al., 1995). However, the direct influence of c-Fos on the expression of the growth and plasticity-associated protein GAP-43 has never been shown. So far it is not known weather neurons expressing c-Fos upon stimulation do necessarily also up-regulate GAP-43 afterwards or weather they do not. GAP-43 is a phosphoprotein which is expressed at high levels during development of the CNS (Benowitz et al., 1988). In vitro studies have shown that the expression of GAP-43 correlates with axonal outgrowth (Skene and Willard, 1981; Goslin et al., 1988; Mahalik et al., 1992) and forms a major component in the growth cone (de Graan et al., 1985; Meiri et al., 1998). In most neurons, high levels of GAP-43 mRNA correlate with late stages of axon formation and synaptogenesis (Mahalik et al., 1992). GAP-43 is enriched at the interface between receptors and cytoskeleton, and its phosphorylation state influences cytoskeletal dynamics, including actin polymerization (Meiri and Gordon-Weeks, 1990; Aigner and Caroni, 1993; He et al., 1997). GAP-43 is activated via phosphorylation on serin41 (Meiri et al., 1998; Van Hooff et al., 1988) that is induced by PKC, which is activated by increased intracellular calcium levels (Schaechter and Benowitz, 1993; Oehrlein et al., 1996; Kleschevnikov and Routtenberg, 2001).

Phosphorylation of GAP-43 is increased rapidly and persistently during electrically induced LTP (Gianotti et al., 1992), whereas low-frequency, non-potentiating stimulation does not increase GAP-43 phosphorylation, and phosphorylation of GAP-43 is not elevated when high-frequency stimulation does not produce potentiation (Lovinger et al., 1986). Genetic overexpression of GAP-43 dramatically enhanced learing and LTP in transgenic mice. If the overexpressed GAP-43 was precluded to be phosphorylated by PKC, then no learning enhancement was found (Routtenberg et al., 2000). In Addition, mice lacking GAP-43 display defects in neuronal pathfinding during early development (Strittmatter et al., 1995). Recently it was shown, that increased GAP-43 expression is correlated with LTP-like potentiation in hippocampus of guinea-pigs (Chirwa et al., 2005; Williams et al., 2006).

The neural cell adhesion molecule (NCAM), a member of the Ig superfamily expressed on the surface of most neuronal cells, is involved in cell-cell interactions during brain development, synaptic plasticity, and regeneration (Schachner, 1997; Ronn et al., 2000). The unusual carbohydrate polysialic acid (PSA), attached uniquely to NCAM through a developmentally regulated process, modulates neuronal cell interactions (for review c.p. Kiss and Rougon, 1997). PSA is constituted of long chains of α2-8 sialic acids and is therefore highly negatively charged. A prevailing view is that PSA-NCAM could interfere with the adhesive properties of other adhesion molecules, thus promoting remodeling of synaptic membranes (Rutishauser et al., 1988; Rutishauser and Landmesser, 1996). In the nervous system, PSA-NCAM has been shown to promote plasticity in cell-cell interactions, especially during axonal pathfinding or branching (Rutishauser and Landmesser, 1996; Walsh and Doherty, 1996). PSA is abundant in embryonic tissues, but its level decreases progressively during development. In the adult brain, mainly the regions of persistent morphological or physiological plasticity retain PSA expression (Seki and Arai, 1993; Rutishauser and Landmesser, 1996). Enzymatic removal of NCAM-associated PSA and genetic ablation of polysialyltransferase ST8SiaIV, which is required for polysialylation of NCAM in the adult hippocampus, leads to impairment of LTP (Becker et al., 1996; Muller et al., 1996; Eckhardt et al., 2000).

In the adult rat, the dorsal vagal complex expresses high levels of GAP-43 (Kruger et al., 1993) and PSA-NCAM (Bonfanti et al., 1992) that could subserve structural reorganizations and synaptic plasticity in response to afferent activity. Electrical stimulation of the vagal afferents causes a rapid decrease of PSA-NCAM, which may be associated with long-term depression (Bouzioukh et al., 2001), a form of activity-dependent decrease in synaptic efficacy. Continued co-expression of PSA-NCAM and GAP-43 is related to remarkable capacities for morphological plasticity in the adult rat (Alonso et al., 1997). Because the capacities of morphological plasticity of immature neurons in the developing CNS appear intimately related to the co-expression of PSA-NCAM and GAP-43 by these neurons, it could logically be assumed that the same properties would apply to specific neurons of the adult CNS that continue to co-express these two embrionic molecules.

3. Motivation and Aims

3.1. Classification of Neuronal Cell Types by Molecular Markers

In the first study, neuroanatomical tract tracing was combined with immuno-histochemistry against neurotransmitters and calcium-binding proteins (CaBPs) for the first time. In this comprehensive study, six of the most relevant neuronal markers were linked to different morphological cell types, based partly on their connections. In the adult mammalian brain, the CaBPs parvalbumin (PV; Heizmann, 1984), calretinin (CR; Rogers, 1987), and calbindin-D28k (CB; Bredderman and Wasserman, 1974) are expressed exclusively in neurons. The neuronal populations in various auditory brainstem regions of the adult rat exhibit unique patterns of CaBP expression (Friauf, 1993; Friauf, 1994; Lohmann and Friauf, 1996). CaBPs protect neurons against harmful consequences of overexcitation (Rogers, 1989) and contribute to synaptic plasticity (Molinari et al., 1996; Caillard et al., 2000). However, it is known only from a few of the morphologically identified neurons which CaBPs they contain. Neuronal cell types were mapped according to their expression of these three CaBPs together with the neurotransmitters glutamate, glycine and GABA. As reviewed (Malmierca, 2003), glutamatergic, glycinergic and GABAergic neurons cover close to all neurons in the investigated areas. Differentiating the numerous cell types that have been identified in the mammalian auditory brainstem in a variety of other studies using these techniques alone, is an important endeavor. Identification of specific neuronal types in different parts of the nervous system will contribute to a better understanding of both physiological and anatomical results.

3.2. Immediate Early Gene Expression Upon Acute Electrical Intracochlear Stimulation

In the neurobiolgical research laboratory of the ENT clinic Freiburg, molecular changes in the auditory nervous system are investigated with the background of perfecting CI therapy. Activity-dependent plasticity is induced by electrical stimulation of the auditory nerve in the cochlea. Expression of IEG transcription factors c-Fos and Egr-1 serves as

marker for these stimulation-dependent molecular changes and were described in previous studies of the Illing laboratory (Illing and Michler, 2001; Illing et al., 2002). In these two, as well as in a variety of other studies (Vischer et al., 1995; King et al., 1996; Saito et al., 1999), the plastic response of the auditory system onto novel stimuli was clearly shown. However, it is as yet unclear how large the share of affected neurons is, and if the affected neurons constitute specific sub-populations related to their morphology, molecular type, or axonal projection. In order to determine if afferent activity has general or specific consequences for the neural network of the auditory brainstem, neurons expressing IEGs upon a strictly controlled electrical intracochlear stimulation (EIS) were determined by their molecular or projectional type. In this second study, it was investigated which of the neuronal cell types identified in the first study expressed IEGs upon EIS and which do not.

3.3. Activity-Dependent Synaptic Plasticity Induced by Chronic Electrical Intracochlear Stimulation

In previous work, it was shown that unilateral deafening trough cochleotomy, a operative remove of the cochlea, leads to massive changes in auditory brainstem neurons after several days. Cochleotomy leads to complete disruption of auditory input and as consequence, a variety of molecular and structural changes occur in the auditory brainstem areas. The IEG product c-Jun is expressed in neurons that form the olivocochlear bundle (Kraus and Illing, 1998; 2005), the plasticity marker GAP-43 is re-expressed in the auditory brainstem (Illing and Horváth, 1995; Illing et al., 1997; Kraus and Illing, 2004), and GAP-43 mRNA is upregulated in particular neurons of the auditory brainstem (Illing et al., 1999). Unilateral loss of sensory activation by cochleotomy as well as a substitution for it by EIS entail specific molecular, ultrastructural, and morphological changes to central auditory neurons (Illing and Reisch, 2006). So far, activity-dependent neuronal network dynamics upon EIS were only studied in a small time window. Two hours of stimulation are sufficient to induce IEG transcription factors, but way to low for structural synaptic rearrangements to occur. Based on the knowledge obtained from cochleotomy-induced synaptic plasticity, it seems logical that such structural rearrangements occur after several days. To investigate stimulation-dependent plasticity beyond IEG expression, chronic EIS lasting seven days was performed.

4. Material and Methods

Adult Wistar rats aged seven to nine weeks were used for all experiments. Care and use of the animals as reported here were approved by Regierungspräsidium, Freiburg, Germany, permission number 37/9185.81/1/267.2. The rats were anesthetized with an intraperitoneal injected mixture of ketamine (50 mg/kg, Ketanest, Parke-Davis, Ann Arbor, MI) and xylazine (5 mg/kg, Rompun, Bayer-Leverkusen, Germany) for ear bone removal, tracer injection, and implantation for chronic stimulation. For acute EIS, anesthesia was done with urethane (1.5g/kg i.p.). Before fixation of the brain by transcardial perfusion, rats were given a lethal dose of pentabarbital (0.6 ml/kg of Narcodorm-n, Alvetra GmbH, Neumünster, Germany, i.p.).

4.1. Immunohistochemistry and In Situ Hybridization

Animals were deeply anaesthetized with pentabarbital and transcardially perfused with one liter of ice-cold fixative solution containing 4% paraformaldehyde, 15% piciric acid, and 0.1% glutaraldehyde in 0.1 M phosphate buffered saline (PBS) at pH 7.4 for one hour as described before (Illing et al., 1997). Brain and cochleae were removed from the skull. For cryoprotection, brains were soaked overnight in 0.1 M PBS at pH 7.4 containing 30% sucrose. Cochleae were decalcified in PBS containing 8% EDTA for one week at 37°C before being soaked in sucrose. The brains were cryo-cut into frontal sections of 20 µm for fluorescence immunocytochemisty (Illing and Reisch, 2006) and into sections of 30 µm for immunostaining with diaminobenzidine (DAB; Illing et al., 1997). Cochleae were cut into sections of 50 µm longitudinal to the modiolus (Michler and Illing, 2002).

Immunocytochemistry was performed using antibodies raised against the following amino acids and proteins: c-Fos (raised in rabbit, 0.1 µg/ml, Santa Cruz Biotechnology, Santa Cruz, CA, No. Sc-253, Fleischmann et al., 2000), Egr-1 (raised in rabbit, 0.02 µg/ml, Santa Cruz Biotechnology, No. Sc-110, Sukhatme et al., 1988), c-Jun (raised in rabbit, 1:2000, Calbiochem, Cambridge, MA, No. PC06, Arndt and Fink, 1986), glutamate (raised in mouse, 5.8 µg/ml, Sigma-Aldrich, St. Louis, MO, No. G9282, Storm-Mathisen et al., 1983; or raised in rabbit, 3.9 µg/ml, Sigma-Aldrich, No. G6642, Ottersen and Storm-Mathisen, 1985), GABA

(raised in mouse, 0.02 µg/ml, Acris, Hiddenhausen, Germany, No. BM124, Halasy et al., 1992; Szabat et al., 1992; or raised in rabbit, 0.05 µg/ml, Sigma-Aldrich, No. A-2052), glycine (raised in rabbit, 1:2000, Chemicon, Temecula, CA, No. AB139, Gates et al., 1996; Kalloniatis and Fletcher 1993), CB (raised in mouse, 0.43 µg/ml, Sigma-Aldrich, No. C-8666, Celio, 1990; Friauf, 1993), PV (raised in mouse, 1:15000, Sigma-Aldrich, No. P-3171, Celio and Heizmann, 1982; Celio et al., 1988), CR (raised in rabbit, 1:5000, Swant, Bellinzona, Switzerland, No. 7696, Schwaller et al., 1993; Lohmann and Friauf 1996), glial fibrillary acidic protein (GFAP, raised in rabbit, 0.82 µg/ml, Sigma-Aldrich, No. G 9269), GAP-43 (raised in mouse, 1:5000, Chemicon, No. MAB347, Goslin et al., 1988), PSA-NCAM (raised in mouse, 1:5000, Chemicon, No. MAB5324, Rougon et al., 1982).

4.1.1. Fluorescence Immunostaining

After incubation for 48 to 72 hours, secondary antibodies matching the species of the primary antibody and labeled either with Cy3 (5 µg/ml, Sigma-Aldrich, sheep anti-rabbit IgG (whole molecule), No. C2306, Sargent, 1994) or Alexa Fluor 488 (10 µg/ml, Molecular Probes, Eugene, OR; goat anti-mouse IgG (H+L), No. A11045, Ausubel et al., 1992, or goat anti-rabbit IgG (H+L), No. A11046, Ausubel et al., 1992) were employed to visualize the binding sites of the primary antibodies. Double staining was achieved either by exposing sections simultaneously to two primary antibodies raised in different species or, alternatively, by sequentially applying primary antibodies of the same species. The sequential technique was used for experiments combining staining with antibodies against c-Fos, Egr-1, CR, and glycine, all raised in rabbit. Brain sections were exposed to the first primary and the corresponding secondary antibody as described. Unbound sites of the first primary antibody were blocked with 2% normal rabbit serum before applying the second primary antibody that was subsequently visualized with a matching secondary antibody bearing a label different from the first one.

The specificity of the antibodies that I used was already shown in previous studies (see above). Nevertheless, various controls were applied to check the specificity again in this approach. First, I applied two primary antibodies A and B, in various combinations, with only one secondary antibody that matched only primary antibody A, but not B. This resulted in fluorescence labeled structures stained only for antibody A but not B, clearly showing the

specificity of the secondary antibody for the appropriate primary antibody. As a second control, I applied two primary antibodies and no secondary antibody, which resulted in no fluorescence labeling at all. This test was done to exclude detection of unspecific fluorescence originating from the specimen itself. As a last control, I checked brain areas in double labeled sections outside the investigated areas. Singly labeled structures were always found for both antibodies in at least one of the areas. It clearly showed the specificity of secondary antibody A for primary antibody A and secondary antibody B for primary antibody B, excluding cross-reactivity.

4.1.2. Immunostaining with Diaminobenzidine

For immunostaining with DAB, series of free-floating sections were exposed to 0.05% H_2O_2, PBS containing 1% milk powder, and finally to blocking buffer containing 5% nonimmune bovine serum, 5% normal horse serum, and 0.05% Triton X-100 in PBS, all for 30 minutes at room temperature. Subsequently, sections were exposed to primary antibodies. After incubation times of 48 to 72 hours at 4°C, biotinylated secondary antibodies and the avidin-biotin technique (Vector Laboratories, Burlingame, CA) were employed to visualize the binding sites of the primary antibodies with DAB (0.05%; Sigma-Aldrich) and ammonium nickel sulfate (0.3%) for intensification of the reaction product.

4.1.3. In Situ Hybridization

The procedure followed for in situ hybridization has been done as previously described (Illing et al., 1999). Sections of 30 µm were cryo-cut and collected in 4% paraformaldehyde in PBS. Sections were washed in PBS and treated in 0.2 N hydrochloric acid and in 50mM Tris-buffer containing 5mM EDTA and proteinase K (30 µg/ml) at 37°C. Subsequently, sections were rinsed in PBS containing 0.2% glycine, followed by another fixation step in 4% paraformaldehyde containing PBS, both at room temperature. Following washing in PBS, the sections were exposed to 0.1 M triethanol amine/ 0.9% sodium chloride (TEA) and incubated in 0.25% acetic anhydride in TEA, followed by rinses in PBS. The sections were then prehybridized at 68°C in a mixture of 50% formamid, 23% distilled water,

20% 20xSSC, 10% dextransulfate, 2% 50xDenhardt's, 2.5% salomon sperm-DNA (denaturated), and 2.5% E. coli-tRNA. Hybridization was done overnight at 68°C in the same solution to which 0.02 ng/µl of digoxigenin-coupled riboprobe to GAP-43 mRNA were added. Digoxigenin-labeled sense and antisense riboprobes were synthesized from a full length plasmid, kindly gifted from Dr. Pico Caroni, Basel, by help of Dr. J. Kapfhammer, Basel, using digoxigenin-11-UTP (Boehringer, Mannheim, Germany). After several posthybridization washing steps, sections were transferred to Tris-buffered saline (TBS, 0.1 M Tris buffer at pH 7.5 and 0.15 M NaCl). Following incubation in 0.3% Triton X-100 and 3% normal sheep serum in TBS, GAP-43 mRNA molecules were detected with a sheep anti-digoxigenin antibody tagged with alkaline phosphatase (1:2000; Boehringer) and stained with nitroblue tetrazolium.

4.2. Axonal Tracing

Labeling of neurons projecting to CIC, to VCN, or of olivocochlear neurons (Horváth et al., 2000) was achieved using either Fast Blue (FB; Sigma-Aldrich) or Dextran-tetramethyl-rhodamine (Fluoro-Ruby; Molecular Probes) as retrograde axonal tracers. Tracer injections to CIC were done stereotaxically (0.2 mm lateral, 2.0 mm rostral, and 5.0 mm dorsal to interaural zero, according to Paxinos and Watson, 1982). Three injections forming a triangle with a side-length of 0.5 mm centered at the determined coordinate (see above) were made to cover the whole CIC in the rostral-caudal and sagital plane. To cover the whole depth of CIC, I applied four times 50 µl of tracer at each injection site, starting at 5.0 mm dorsal to interaural zero, moving up to 3.5 mm with steps of 0.5 mm between each of the four applications. I applied 600 µl of tracer in total for the whole CIC, which was sufficient to cover the whole nucleus (Fig. 4A). Octopus neurons projecting to VNLL were never labeled, providing good evidence that just CIC, but not adjacent areas were covered with tracer.

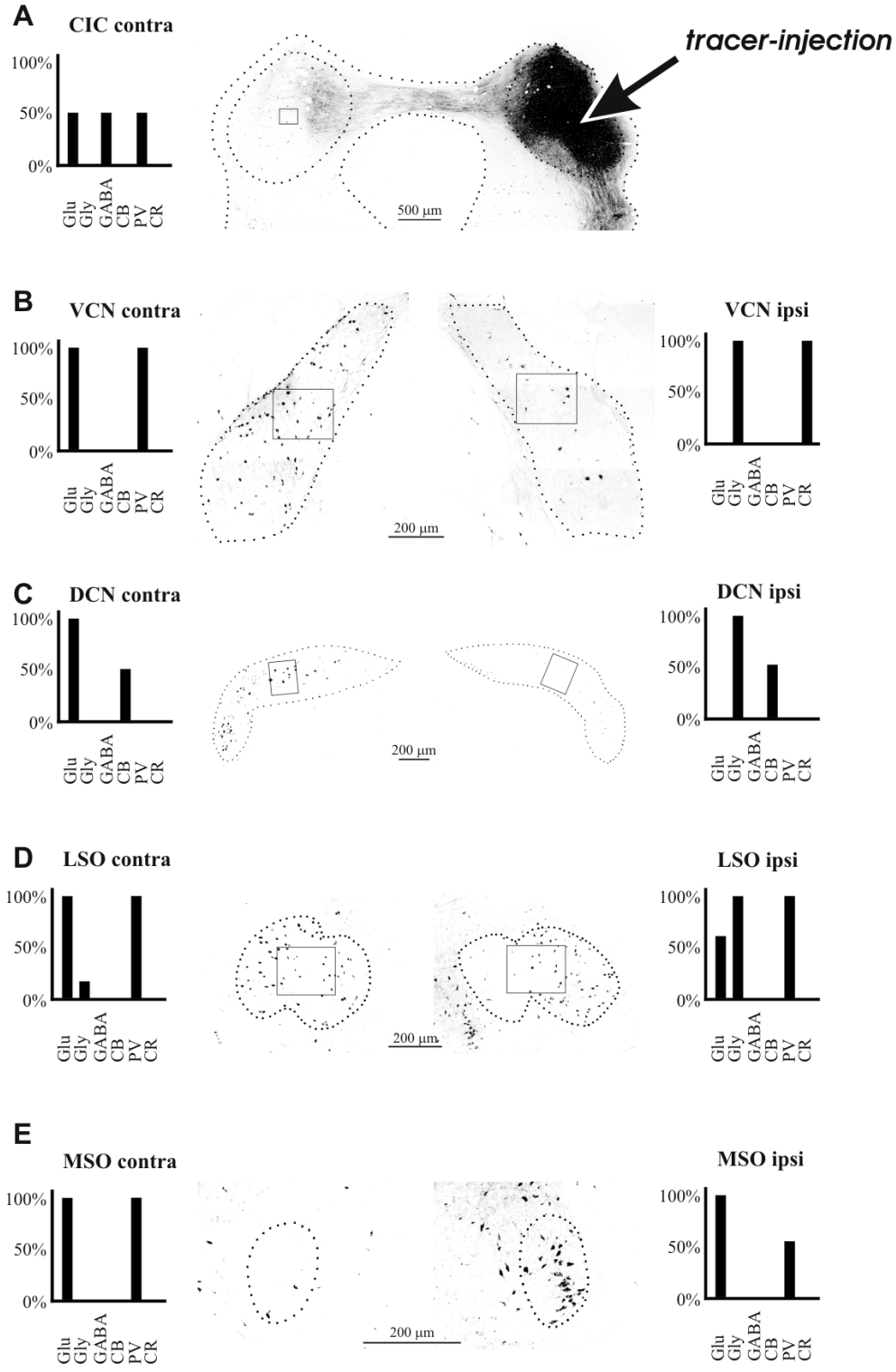

Figure 4: Tracer injection into CIC. A: Tracer injection into the right CIC covered the whole nucleus. Neurons from the contralateral CIC (left) sent commissural fibers to CIC where tracer injection occurred. One half of these cells was glutamatergic, the other half GABAergic and PV positive as shown in the diagram on the left. The window in the ipsilateral CIC shows the field for cell counting. B: Many neurons from the contralateral VCN (left), all glutamatergic and PV positive, projected to the CIC. From the ipsilateral VCN (right), only few

glycinergic and CR positive cells sent their axon to the CIC, where tracer injection occurred. The windows show the counting fields located in the dorso-medial VCN. C: Similar to VCN, many neurons from contralateral DCN (left), but only few from ipsilateral DCN (right) projected to CIC. Contralaterally projecting cells were all glutamatergic and half of them were CB containing. Neurons projecting ipsilaterally were all glycinergic and 50% also CB positive. The windows show the fields for cell counting. D: In the medial half of the LSO (counting fields), the contralateral projection was stronger than the one to the ipsilateral CIC. All tracer labeled neurons were PV positive. Those projecting contralaterally were to 100% glutamatergic and to some part glycine stained, the cells projecting ipsilaterally were all glycinergic, but showed to 60% glutamate immunoreactivity. E: MSO neurons projected mainly to the ipsilateral CIC and were all glutamatergic. The few cells projecting contralaterally were all PV stained, those projecting ipsilaterally to 50%.

The VCN was approached under vision after a hole was made through the occipital bone (Kraus and Illing, 2004). Flocculus and paraflocculus were aspirated to expose the CNC. 150 µl of a saturated solution of the tracer were pressure injected through a glass micropipette with a tip diameter of about 50 µm. Application of tracer in that way guaranteed that only the VCN itself, but not medially passing fibers outside VCN came in contact with tracer. To exclude the possibility of tracer uptake by passing fibers and to evaluate the extent of tracer diffusion, injection sites were checked in brain sections under the microscope (Fig. 5A).

Application of FB to the cochlea was performed using a retroauricular approach (Horváth et al., 2000). A small hole was drilled centered over the middle turn into the cochlear wall and FB was tamped into it. The opening was closed with surgical bone wax and the bulla was filled with Gelfoam. In all tracing experiments, rats recovered and survived for seven to ten days until they were exposed to EIS or perfused directly.

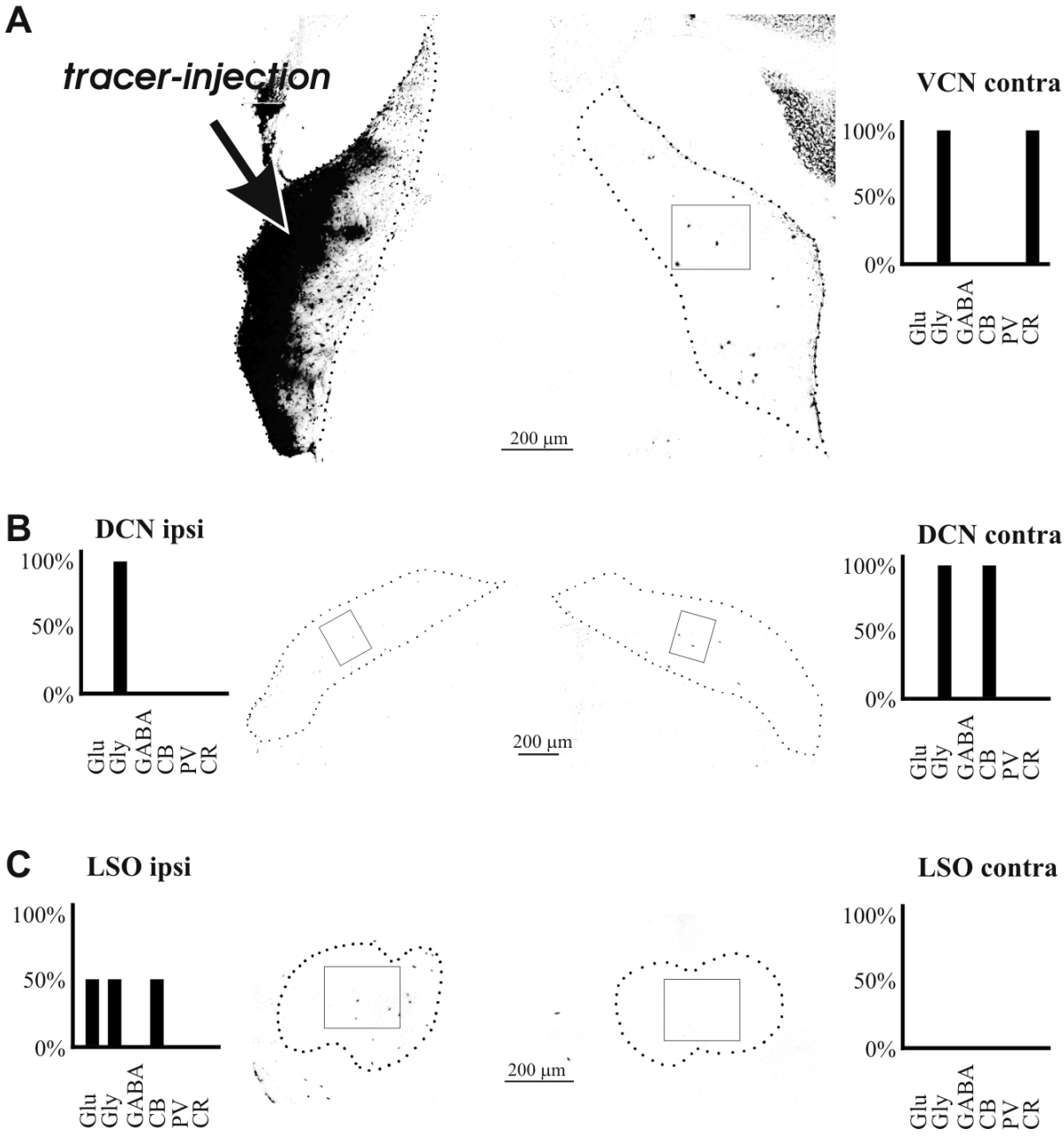

Figure 5: Tracer injection into VCN. Tracer injection into the left VCN covered large part of the nucleus, but did not reach passing fibers outside VCN. Large commissural neurons from the contralateral VCN (right) projected to the VCN where tracer injection occurred. These neurons were all glycinergic and CR positive. B: Projection neurons from the ipsilateral DCN (left), were all glycinergic, DCN neurons projecting contralaterally were also all glycinergic, but additionally CB immunoreactive. C: Small neurons from the medial part of the ipsilateral LSO (left) sent their axon to VCN and where therefore stained by tracer. 50% of these cells were glutamatergic and CB immunostained, the other 50% were glycinergic. The LSO on the contralateral side (right) showed no projection to VCN. Windows show the fields for cell counting.

4.3. Electrical Intracochlear Stimulation

4.3.1. Acute Stimulation in Anesthetized Rats

To reduce the level of hearing-dependent spiking activity in the auditory system, the tympanic membrane was disrupted and the malleus was removed bilaterally two days before EIS. Judging from the auditory brainstem response (ABR), loss of middle ear transmission led to an immediate and sustained rise of hearing threshold by 50 dB (Michler and Illing, 2002). The cochlea was exposed using a retroauricular surgical approach. A hole was drilled into the bony wall of the basal cochlea to insert the electrode carrier. Bipolar stimulation was applied using a cochlear implant (Model CI24M), run by the Nucleus Implant Communicator, both kindly provided by Cochlear AG (Basel, Switzerland). The ABR was recorded by placing steel needle electrodes subcutaneously at vertex and mastoids to corroborate for the correct placement of the stimulation electrodes and to determine an appropriate current level. The ABR was visualized using an averager (Multiliner E; Evolution 1.70c; Toennies, Würzburg, Germany), calculating mean amplitudes over 500 sweeps in a frequency band between 0.1 and 3 kHz. The aim was to obtain an initial ABR amplitude in the range of 5 to 10 μV, corresponding to acoustically evoked amplitudes of 30 to 60 dB (Fig. 6A). EIS was applied unilaterally at the left side for two hours. Frequency of the biphasic stimulation remained constant at 50 Hz and pulse width was set to 50 μs, while the current level was varied between 260 and 950 μA between experiments to compensate for variations in electrode position. These stimulation parameters were optimized in previous studies (Illing and Michler, 2001; Illing et al., 2002). Throughout the period of stimulation, a duty cycle of 50% with 30 seconds stimulation alternating with 30 seconds pause was set to minimize adaptation of the system onto the stimulus. The ABR was recorded every 15 minutes to verify unchanged electrode positioning and sustained effective stimulation of the central auditory system (Fig. 6B).

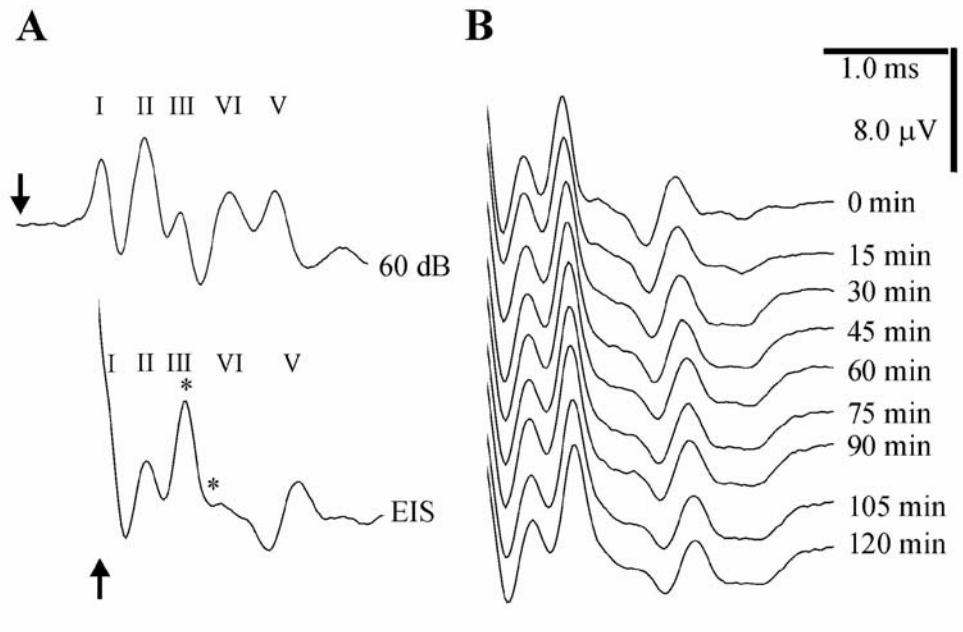

Figure 6: ABR induced by acoustical and electrical stimulation. A: Acoustically ABR induced with a 60 dB tone stimulation (top), and electrically evoked ABR (EABR) at comparable amplitude (bottom) on which the present study is based. Arrows indicate stimulus onset, and ABR and EABR shifted against each other to match corresponding waves. Positive peaks of ABR recording are numerated according to Buchwald and Huang (1975). Asterisks indicate the interval for amplitude measurements between peak III and peak IV. B: EABR of a representative experiment taken every 15 minutes to verify effective stimulation over the full two hours of stimulation.

4.3.2. Chronic Stimulation Experiments in the Awake Animal

To extend the time frame from two hours under anesthesia to seven days in the awake animal, a setup for chronic EIS was developed. The same stimulation program and parameters as for the acute EIS were used. From a conventional Cochlear Implant, the first two electrodes were clamped and this so called “implant in a box” was connected to the implant on the rats head.

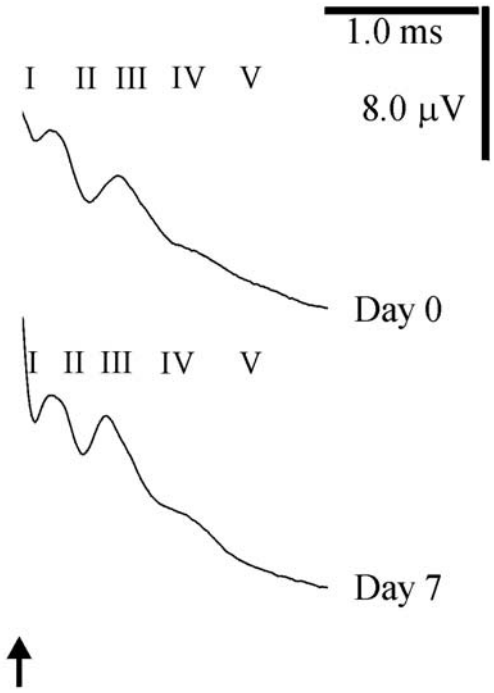

Figure 7: ABR measurements during chronic EIS lasting 7 days. Recordings of ABR amplitudes at the beginning (day 0) and end (day 7) proved the continuity of stimulation for the whole experiment. Arrow: trigger onset.

Middle ear bones were removed on both sides immediately before implantation. The skin on the rats head was opened and four holes were drilled into the skull to fix the implant. Then the same retroauricular approach as for acute EIS was used to access the cochlea. The implant was fixed on the rats skull and the electrode carrier of a conventional implant, kindly provided by Cochlear AG, was guided subcoutaneously to the cochlea. The electrode carrier was inserted into the basal cochlea and fixed with 4% agar in 0.9% sodium chloride solution, which sealed the cochlea and avoided loss of haemolymph trough the hole drilled for the electrode carrier. Wounds were surgically closed, the implant was connected, and ABR responses were measured (Fig. 7). Then the rats were put into the chronic stimulation box (Fig. 8). After survival times of seven days with uninterrupted stimulation, rats were anesthetized and ABR responses were measured again (Fig. 7). The Implant was removed and animals were perfused immediately.

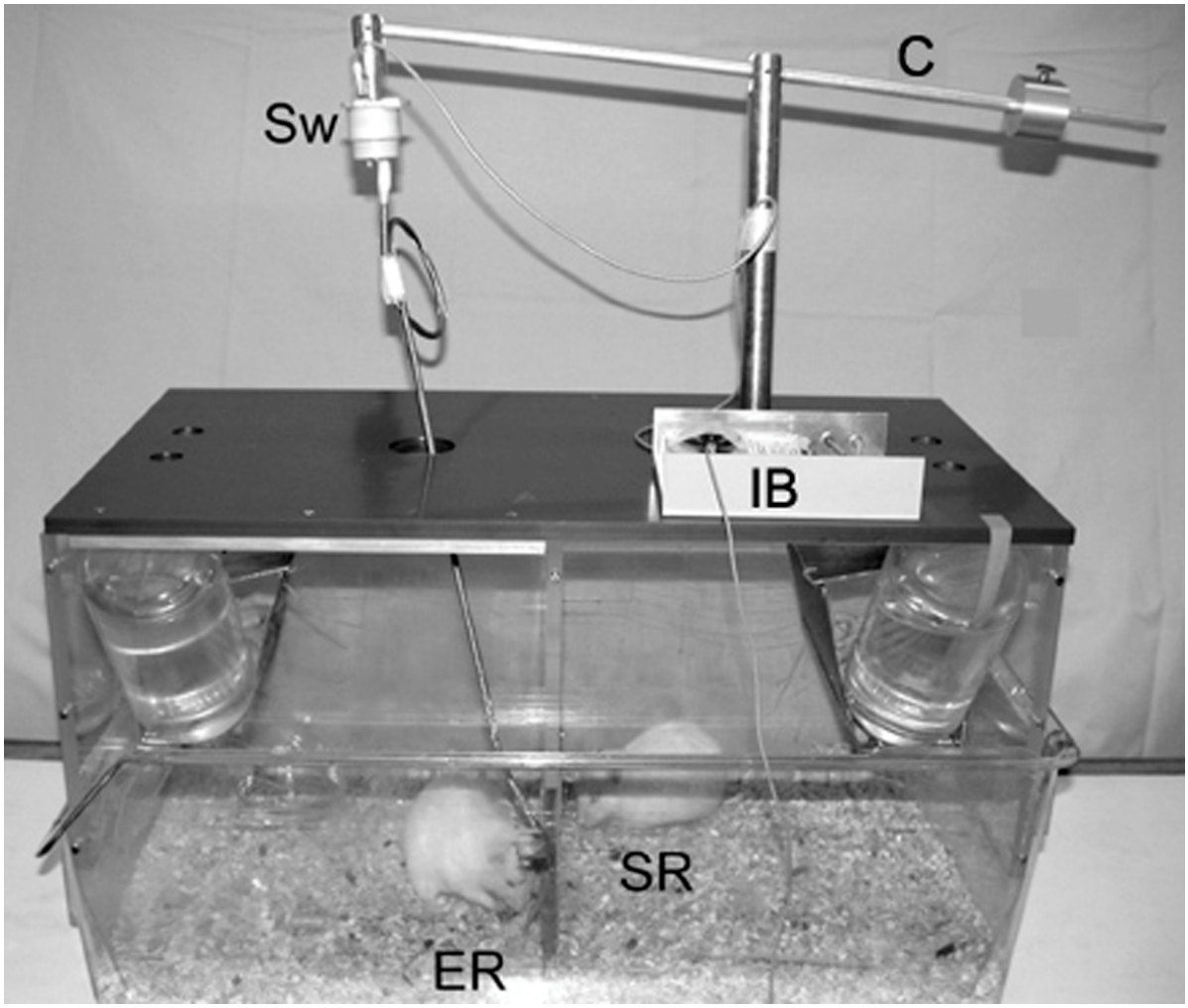

Figure 8: Setup for chronic stimulation experiments. ER: experimental rat, SR: social rat, IB: implant in a box, Sw: swivel. C: cradle-arm.

4.4. Quantification and Statistical Analysis

4.4.1. Analysis of Fluorescence Staining

Patterns of fluorescence staining were visualized under a fluorescence microscope using appropriate fluorescence filter sets (set No. 10 for the green channel, set No. 15 for the red channel, set No. 02 for the blue channel, Zeiss, Jena, Germany). Counting of neuronal cell bodies was based on two different animals and at least two brain sections per animal for each combination of markers or marker and tracer, respectively. In LSO, MSO, and CIC, neuronal

cell types were described to be rather evenly distributed, which was confirmed qualitatively by inspecting the entire area of the respective nuclei in the sections. A sufficiently large counting field and a central position for it was considered as appropriate to reproduce reasonable numbers. In DCN, counting fields were positioned to include equal lengths of the layers. In VCN, local differences in the composition of cell types do exist, most pronounce for the octopus cells forming a rather compact cell group at the junction of PVCN and AVCN. I determined the octopus cell region in a serial volumetric reconstruction to comprise between 10 and 15% of VCN. Since only 40% of neurons in the octopus cell region were octopus cells itself, intermingled by 60% of other neurons, I ended up with 5% octopus cells in the entire VCN. The quantitative data do not distinguish between globular and spherical bushy cells. The counting was done under an epi-fluorescence microscope using high magnification objectives (x 40 or x 100), which allowed for focusing through the sections to distinguish true marker co-localization from stained elements on different depth levels. Evaluation and counting were strictly confined to a counting field of 180 μm times 220 μm in the evaluated brainstem areas (Fig. 4; Fig 5). Since this counting-field had the same size in all investigated areas, the total number of neurons counted per section were similar in VCN, DCN, LSO, and CIC, although the total number of neurons of the whole area dramatically varied between these regions. The MSO was to small to apply the defined counting-field and was therefore counted entirely.

Attempting to generate a practical classification of cell types in each region of the auditory brainstem based on various pairs of double staining, three counting criteria were introduced. First, if two marker proteins or amino acids appeared to be co-localized in less than 5% of the neurons stained for either marker, the two populations were classified as non-overlapping. Without this criterion, one may have ended up with types represented by single neurons. Second, since local EIS led to IEG expression in tonotopically restricted regions, evaluation was based on determining how many of the IEG positive neurons showed a specific second marker, but not the inverse. I avoided to elaborate on the question how many neurons of a second-marker population also contained IEG, as this number could, due to regionally sub-optimal stimulation of neurons, turn out to be very small without reflecting true relationships. Third, for tracing experiments, immunostained cell bodies or cellular nuclei only closer than 50 μm from tracer-filled cells were counted as singly stained. This criterion was based on the assumption that immunoreactive cells would have been retrogradely labeled

if they had an axon ending in the region of tracer injection known to be tonotopically connected to the analyzed region.

The numbers of cells stained for either one or two markers were counted and averaged for each combination of staining across all analyzed sections and experiments. Diameters of neuronal somata were measured on photographs in anaySIS (Soft Imaging System GmbH, Münster, Germany) to determine the mean diameter ± standard error of mean of the cell bodies. For statistical evaluation, I used the unpaired two-tailed Student's t-test, with significance levels set to $p < 0.05$. Photographic documentation was done with a digital camera (Axiocam; Zeiss) and assembled with Photoshop 6.0 (Adobe, San Jose, CA) and Corel Draw 8.0 (Corel Corporation, Ottawa, Canada) to produce multicolor pictures.

4.4.2. Gray-Value Density Measurements

Images visualized under a microscope were documented using a digital camera (Axiocam; Zeiss) aided by imaging software (Axiovision; Zeiss), with a resolution of 1,300 x 1,030 pixels in 8-bit gray tone scale. Assembling and lettering of these images was done with Adobe Photoshop 6.0 and Corel Draw 8.0.

The intensity of GAP-43 and PSA-NCAM immunoreactivity was quantitatively determined. Staining intensities were compared by evaluating the mean of the gray tone distribution in pictures of the appropriate area taken under strictly identical illumination conditions. The gray tone means were obtained from representative fields in sections across several experimental brains. Per animal, three to nine sections were analyzed on each side. Regions at the margin and areas obviously containing larger blood vessels were excluded from the measurement area.

Statistical comparisons were made on two levels. First, I determined in each animal if the staining levels, as indicated by the gray tone means, differed between ipsilateral and contralateral side with respect to EIS. Second, the average ratio of the right-to-left balance of the staining was calculated and compared in controls and in stimulated rats. For statistical evaluations the two-tailed Student's t-test, paired and unpaired, was used. The significance level was set to $p < 0.05$.

5. Results

5.1. Neuronal Cell Types in the Rat Auditory Brainstem as Defined by Molecular Profile and Axonal Projection

Neuronal cell types of the auditory brainstem were characterized according to their axonal destination and the molecular markers they contained. By fluorescence double staining experiments the number of neurons that appeared singly or double stained were determined. I always used two selected markers (Table 1), or one marker together with a tracer (Table 2), per experiment in various combinations and evaluated neurons in VCN, DCN, LSO, MSO, and CIC. Based on the evidence derived from previous work that glutamatergic, glycinergic and GABAergic neurons cover close to all neurons in the investigated areas, their sum, after subtracting neurons with dual transmitter contents, was set to 100%. The percentage of the diverse neuronal sub-populations was determined from the total number of neurons that were characterized.

Table 1
Combinations of antibodies used in the experimental animals

	Area	M927[b]	M928	M931	M932
Glu-Gly[a]	VCN	n=3[c]		n=3	
	DCN	n=3		n=3	
	LSO	n=3		n=3	
	MSO	n=3		n=3	
	CIC	n=3		n=3	
Glu-GABA	VCN	n=2		n=3	
	DCN	n=3		n=3	
	LSO	n=3		n=3	
	MSO	n=3		n=3	
	CIC	n=2		n=2	
Glu-PV	VCN		n=3		n=3
	DCN		n=3		n=3
	LSO		n=3		n=3
	MSO		n=3		n=3
	CIC		n=2		n=2
Glu-CR	VCN		n=2		n=3
	DCN		n=3		n=3
	LSO		n=3		n=3
	MSO		n=3		n=3
	CIC		n=2		n=2
Glu-CB	VCN		n=3		n=3
	DCN		n=3		n=3
	LSO		n=2		n=3
	MSO		n=2		n=3
	CIC		n=2		n=2
Gly-GABA	VCN	n=3		n=3	
	DCN	n=3		n=3	
	LSO	n=3		n=3	
	MSO	n=3		n=3	
	CIC	n=2		n=3	
Gly-PV	VCN	n=3		n=3	
	DCN	n=3		n=3	
	LSO	n=3		n=3	
	MSO	n=3		n=3	
	CIC	n=2		n=3	
Gly-CR	VCN	n=3		n=3	
	DCN	n=3		n=3	
	LSO	n=3		n=3	
	MSO	n=3		n=3	
	CIC	n=2		n=3	
Gly-CB	VCN	n=3		n=3	
	DCN	n=3		n=3	
	LSO	n=3		n=3	
	MSO	n=3		n=3	
	CIC	n=2		n=3	
GABA-PV	VCN		n=3		n=3
	DCN		n=3		n=3
	LSO		n=3		n=3
	MSO		n=3		n=3
	CIC		n=2		n=2
GABA-CR	VCN	n=4		n=3	
	DCN	n=3		n=3	
	LSO	n=3		n=3	
	MSO	n=3		n=3	
	CIC	n=3		n=3	
GABA-CB	VCN		n=3		n=3
	DCN		n=3		n=3
	LSO		n=3		n=3
	MSO		n=3		n=3
	CIC		n=2		n=2
PV-CR	VCN		n=3		n=3
	DCN		n=3		n=3
	LSO		n=3		n=3
	MSO		n=3		n=3
	CIC		n=2		n=3
CB-CR	VCN		n=3		n=3
	DCN		n=3		n=3
	LSO		n=3		n=3
	MSO		n=3		n=3
	CIC		n=3		n=3

[a] combination of antibodies used. [b] experimental rat number. [c] number of slices counted per animal. Glu = glutamate, Gly = glycine, PV = parvalbumin, CR = calretinin, CB = calbindin-D28k

Table 2
Combinations of immunocytochemical staining and tracer injections in the experimental animals

	Area	M894[b]	M902	M904	M907	M946	M951	M952	M965
Tracer ClCc-Glu[a]	VCN			n=4[c]	n=4				
	DCN			n=4	n=2				
	LSO			n=5	n=3				
	MSO			n=5	n=3				
Tracer ClCi-Glu	VCN			n=3	n=3				
	DCN			n=3	n=3				
	LSO			n=3	n=3				
	MSO			n=3	n=3				
Tracer ClCc-Gly	VCN			n=2	n=3				
	DCN			n=2	n=4				
	LSO			n=3	n=3				
	MSO			n=3	n=3				
Tracer ClCi-Gly	VCN			n=3	n=4				
	DCN			n=2	n=3				
	LSO			n=3	n=3				
	MSO			n=3	n=3				
Tracer ClCc-PV	VCN					n=3		n=2	
	DCN					n=3		n=3	
	LSO					n=3		n=2	
	MSO					n=3		n=2	
Tracer ClCi-PV	VCN					n=6		n=4	
	DCN					n=3		n=3	
	LSO					n=3		n=2	
	MSO					n=3		n=2	
Tracer ClCc-CR	VCN					n=3		n=2	
	DCN					n=3		n=3	
	LSO					n=3		n=3	
	MSO					n=3		n=3	
Tracer ClCi-CR	VCN					n=6		n=4	
	DCN					n=3		n=3	
	LSO					n=3		n=3	
	MSO					n=3		n=3	
Tracer ClCc-CB	VCN					n=3		n=3	
	DCN					n=3		n=3	
	LSO					n=3		n=2	
	MSO					n=3		n=2	
Tracer ClCi-CB	VCN					n=3		n=3	
	DCN					n=3		n=3	
	LSO					n=3		n=2	
	MSO					n=3		n=2	
Tracer VCN-Glu	VCNc	n=2	n=12						
	DCNc	n=2	n=5						
	LSOi	n=2	n=4						
	MSOc	n=2	n=4						
Tracer VCN-Gly	VCNc	n=2	n=3						
	DCNc	n=2	n=4						
	LSOi	n=2	n=4						
	MSOc	n=2	n=4						
Tracer VCN-PV	VCNc						n=3		n=3
	DCNc						n=3		n=2
	LSOi						n=5		n=4
	MSOc						n=5		n=4
Tracer VCN-CR	VCNc						n=3		n=3
	DCNc						n=3		n=2
	LSOi						n=3		n=2
	MSOc						n=3		n=2
Tracer VCN-CB	VCNc						n=3		n=3
	DCNc						n=2		n=2
	LSOi						n=3		n=2
	MSOc						n=3		n=2

[a] combination of tracer injection site and antibodies. [b] experimental rat number. [c] number of slices counted per animal. Glu = glutamate, Gly = glycine, PV = parvalbumin, CR = calretinin, CB = calbindin-D28k

5.1.1. Cell Types in the Ventral Cochlear Nucleus

In VCN, I identified a considerable number of neurons with glutamate immunoreactivity dispersed over the whole nucleus. Some of these glutamatergic cells appeared singly stained, others exhibited co-localization with CR, CB, or PV. Glutamate positive cells represented 75% of the VCN neurons identified by any molecular marker employed in this study. These glutamatergic neurons split up into four different subsets based on the co-expression of the CaBPs as follows: 5% of the glutamatergic VCN neurons did not contain any of these CaBPs (Fig. 9, sub-population 1). Another 5% were CB positive (Fig. 9, sub-population 2) and restricted to the octopus area of the PVCN. The remaining two sub-sets showed co-localization with PV (Fig. 9, sub-population 3, 45%) and CR (Fig. 9, sub-population 4, 20%), respectively, and were both distributed throughout VCN.

Cell Types in VCN

Glutamate[a]	42.0 ± 1.6[b]	n=28[c]	75%[d]
Glycine	6.8 ± 0.4	n=30	15%
GABA	6.1 ± 0.7	n=30	10%
CB	2.8 ± 0.6	n=24	5%
PV	26.0 ± 1.3	n=24	45%
CR	17.7 ± 1.0	n=30	35%
CIC contra	21.6 ± 2.6	n=26	35%
CIC ipsi	4.8 ± 1.3	n=39	5%
VCN contra	2.2 ± 0.4	n=37	5%

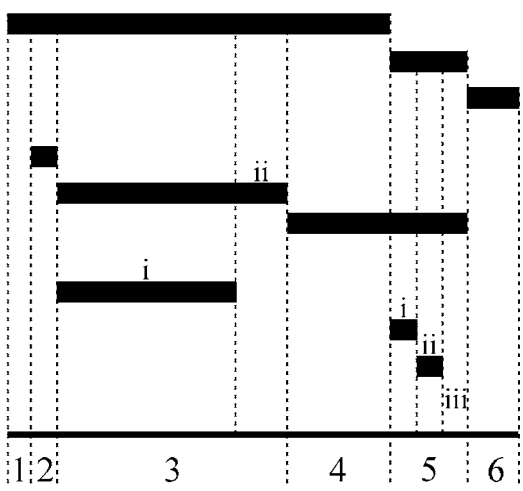

Figure 9: Immunocytochemically identified neuronal sub-populations in VCN. Based on the estimate that glutamatergic, glycinergic and GABAergic neurons cover close to all neurons in VCN, their sum was set to 100%. Six major molecular sub-populations of neurons (1 to 6) were identified. [a] Marker molecule or site of tracer application, respectively. [b] Average number of cells counted per section ± S.E.M. [c] Number of sections on which evaluation was based. [d] Percentage of neurons stained with markers or tracer within the total (100%) of evaluated cells.

Glycine positive neurons were less numerous than glutamatergic cells in VCN but also widely dispersed. Some of the glycinergic neurons had extraordinarily large cell bodies with a mean diameter of 18.3 ± 1.3 µm (ranges: 22.3 – 16.3 µm), while others were generally smaller with 11.2 ± 0.5 µm (ranges: 12.7 – 9.3 µm) mean diameter. Glycine positive neurons represented 15% of the VCN neurons and all of them showed immunoreactivity for CR (Fig. 9, sub-population 5) but not for other CaBPs. Conversely, the majority of CR positive cells were not immunopositive for glycine (Fig. 10A). GABAergic neurons of 4.9 ± 0.3 µm (ranges: 6.1 – 3.6 µm) mean diameter were scattered throughout VCN and exclusively singly stained. They represented 10% of the identified neurons in VCN (Fig. 9, sub-population 6).

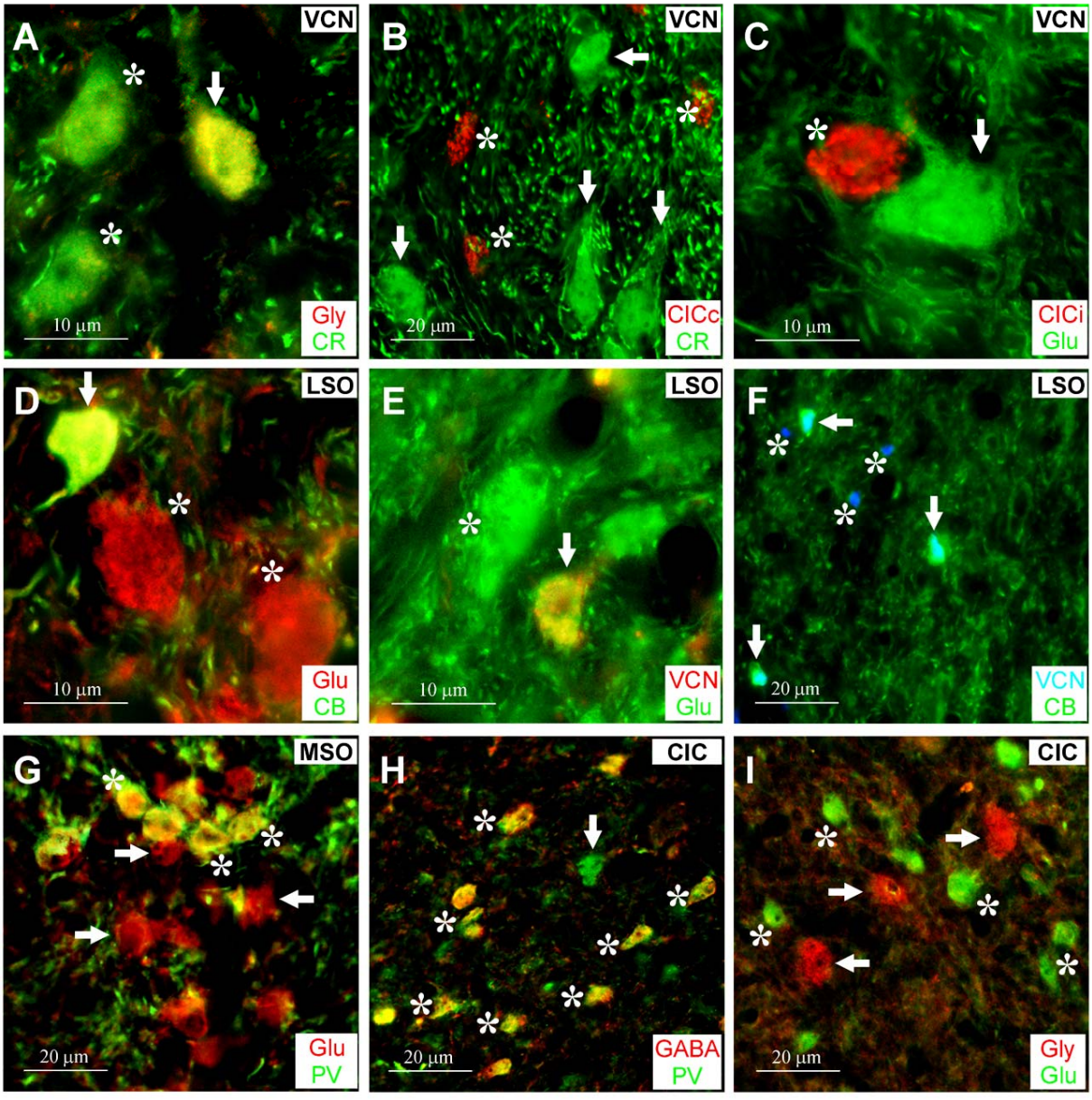

Figure 10: Exemplary illustrations of neuronal sub-populations in the auditory brainstem. A: All glycinergic neurons in VCN contained CR (arrow, yellow), but the majority of CR positive cells was singly stained (asterisks, green). The yellow color of the double stained soma indicates the co-expression of glycine (red) and CR (green). B: VCN neurons projecting to the contralateral CIC (asterisks, red) were never CR positive (arrow, green). C: Neurons of the VCN that sent their axons to the ipsilateral CIC (asterisks, red) were devoid of glutamate (arrow, green). D: Staining for CB (green) was restricted to small LSO neurons which proved to be glutamatergic (arrow, yellow). Large principal cells of LSO containing glutamate never showed CB immunoreactivity (asterisks, red). E: Small LSO neurons projecting to VCN (red) were positively stained for glutamate (arrow, yellow), whereas glutamatergic principal cells showed no tracer uptake (asterisk, green). F: One part of the small LSO neurons that sent their axons to the ipsilateral VCN was CB stained (arrows, green), whereas another part of the tracer filled somata was CB negative (asterisks, blue). G: Glutamatergic MSO neurons were to some part singly stained (arrows, red) and to some part co-localizing with PV (asterisks, yellow). In all experiments, I never observed somata singly stained for PV (green) in the MSO. H: All CIC GABAergic neurons exhibited PV staining (asterisks, yellow), while few PV containing cells were singly stained (arrow, green). I: In CIC, glutamate was expressed in medium sized somata that appeared always singly stained (asterisks, green). A few larger cell bodies were immunoreactive for glycine (arrows, red).

To further specify the neuronal sub-populations, axonal tracing was combined with immunocytochemistry. All VCN neurons projecting to the contralateral CIC contained both glutamate and PV (Fig. 4B), representing 35% of VCN neurons (Fig. 9, sub-population 3i). These neurons exhibited neither glycine nor CR immunoreativity (Fig. 10B). Ten percent of the cell bodies that were stained for both PV and glutamate do not send projections to the contralateral CIC (Fig. 9, sub-population 3ii); their axons must terminate in other regions. Neurons that project to the ipsilateral CIC contained glycine and CR (Fig. 9, sub-population 5i), but were neither immunopositive for glutamate (Fig. 10C) nor for PV.

The commissural connection to the contralateral VCN in the rat is established by glycinergic neurons with large somata (Doucet and Ryugo 1997; Alibardi, 1998a; Doucet et al., 1999). These commissural cells always contained CR and glycine (Fig. 5A), but not glutamate or PV (Fig. 9, sub-population 5ii). The glycinergic and CR immunoreactive neurons projecting to the ipsilateral CIC (Fig. 4B) and to the contralateral VCN (Fig. 5A) together represented 10% of the characterized VCN neurons. Another 5% of neurons immunoreactive for both glycine and CR apparently project to neither of these two areas (Fig. 9, sub-population 5iii); they may instead connect to DCN neurons.

5.1.2. Cell Types in the Dorsal Cochlear Nucleus

In DCN, glutamatergic neurons showed co-localization with CR as well as with CB, but co-localization with glycine, GABA, or PV immunoreactivity was never observed. Characterization of neuronal sub-sets from double staining studies revealed that 45% of all DCN neurons were glutamatergic neurons, splitting up into different sub-populations. Large and medium-sized neurons of 13.7 ± 0.5 μm (ranges: 18.1 – 9.3 μm) mean diameter that were singly stained for glutamate comprised 10% of all DCN neurons (Fig. 11, sub-population 1). Small glutamatergic neurons with a mean diameter of 4.7 ± 0.1 μm (ranges: 6.1 – 3.5 μm) representing a second sub-population of 25% identified DCN neurons, showed co-localization with CR (Fig. 11, sub-population 2), and were exclusively observed in the granular cell layer. Small fusiform cells with a mean diameter of 7.1 ± 0.3 μm (ranges: 8.6 – 5.8 μm) co-localized glutamate and CB, representing 10% of all DCN cells that were characterized (Fig. 11, sub-population 3).

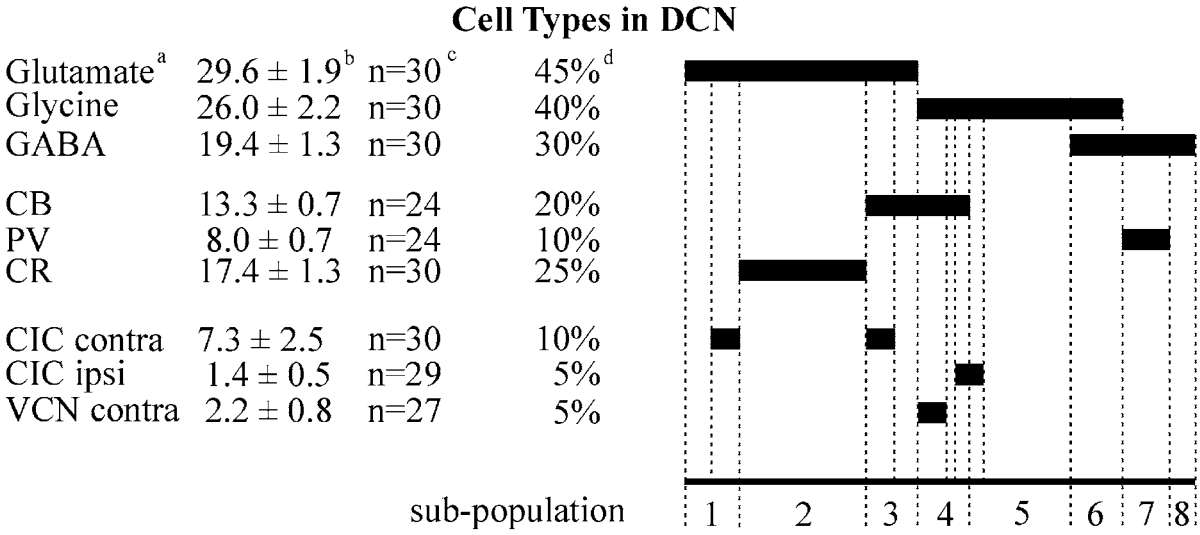

Figure 11: Immunocytochemically identified neuronal sub-populations in DCN. With glutamatergic, glycinergic and GABAergic neurons approximately forming 100% of DCN neurons, after subtracting neurons with dual transmitter contents, eight major molecular sub-populations of neurons (1 to 8) were identified. [a] Selected marker protein or site of tracer application, respectively. [b] Average number of cells counted per section ± S.E.M. [c] Number of sections on which evaluation was based. [d] Percentage of neurons stained with markers or tracer within the total of evaluated cells.

Glycinergic neurons of the DCN comprised 40% of the total population of neurons characterized and exhibited double staining with GABA or with CB. Hence, they split up into three distinct neuronal subsets. Ten percent of DCN neurons co-localized glycine and CB in particularly large somata of 13.1 ± 0.7 μm (ranges: 17.1 – 10.0 μm) mean diameter and were located in the deep layer (Fig. 11, sub-population 4). Cells at the boundaries between granular and superficial layer displayed immunoreactivity for GABA as well as glycine, representing another 10% of DCN neurons counted here (Fig. 11, sub-population 6). Additionally, I observed neurons in the deep layer with small somata of 8.2 ± 0.2 μm (ranges: 9.8 – 6.4 μm) mean diameter singly stained for glycine to constitute a subset comprising 20% of DCN neurons (Fig. 11, sub-population 5).

GABA stained DCN neurons showed immunoreactivity for PV, but not for other CaBPs used here. Ten percent of the identified neurons showed immunoreactivity for GABA in conjunction with PV (Fig. 11, sub-population 7) and were located in the superficial layer. Another 5% of DCN neurons, located in the granular layer, were singly stained for GABA (Fig. 11, sub-population 8).

From DCN, only 20% of the neuronal population sent projections to the CIC (Fig. 4C), or to the VCN (Fig. 5B), either ipsilaterally or contralaterally. Neurons projecting to the contralateral CIC exhibited glutamate immunoreactivity, whereas neurons projecting to the ipsilateral CIC were glycinergic cells. Additionally, half of the neurons projecting either to the ipsilateral or to the contralateral CIC showed co-localization with CB. By contrast, DCN cells projecting to the contralateral VCN all stained for CB and glycine, while neurons projecting to the ipsilateral VCN stained for glycine only.

5.1.3. Cell Types in the Lateral Superior Olive

Double staining of glutamatergic LSO neurons was observed with glycine, PV, and CB, but not with GABA immunoreactivity. CR immunoreactivity was restricted to fibers but absent from neuronal somata in the entire LSO. Of all neurons characterized by any of the markers used here, glutamatergic cells made up 65%. Glutamate staining was found in large and ovoid principal cells with a mean diameter of 10.6 ± 0.6 μm (ranges: 12.0 – 8.6 μm) as well as in small spherical neurons of 4.9 ± 0.3 μm (ranges: 5.9 – 4.2 μm) mean diameter. Again, I distinguished sub-sets of glutamatergic neurons, of which the neurons singly stained

for glutamate represented a minority of 5% of the identified LSO cells (Fig. 12, sub-population 1). CB was absent from large LSO principal cells, but present in glutamatergic neurons that appeared small and round (Fig. 10D). These small cells always and exclusively co-localized CB with glutamate, constituting another 15% of the identified LSO neuronal sub-sets (Fig. 12, sub-population 2). Co-localization of glutamate with PV occurred only in large principal neurons. This sub-set comprised 25% of LSO neurons (Fig. 12, sub-population 3). Twenty percent of LSO neurons showed a co-localization of glutamate and glycine (Fig. 12, sub-population 4). This co-localization was exclusively observed in LSO principal cells, all of which showed PV staining in addition.

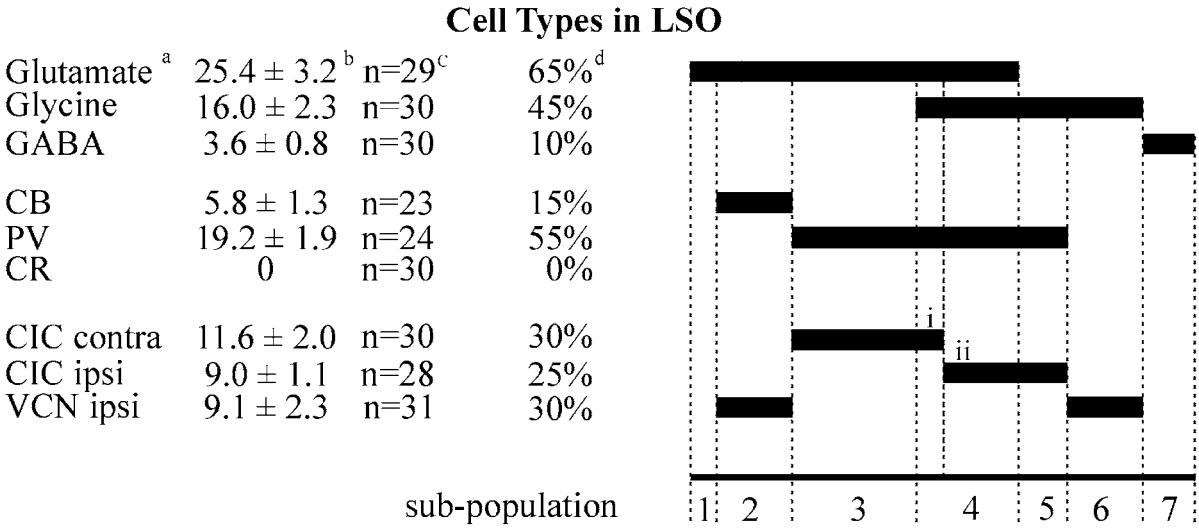

Figure 12: Immunocytochemically identified neuronal sub-populations in LSO. Seven major molecular sub-populations of neurons (1 to 7) were identified. [a] Selected marker protein or site of tracer application, respectively. [b] Average number of cells counted per section ± S.E.M. [c] Number of sections on which evaluation was based. [d] Percentage of neurons stained with markers or tracer within the total of evaluated cells.

The percentage of neurons co-localizing glycine with PV was higher than the amount of cells co-expressing glycine and glutamate. Therefore, a third sub-population of LSO principal neurons that was immunoreactive for glycine and PV, but not for glutamate (Fig. 12, sub-population 5) was introduced. However, glycine staining was not restricted to the large and spherical PV positive principal neurons. Glycine staining was also found in small and round cell bodies that did not show co-localization with any other marker (Fig. 12, sub-population 6). Small GABAergic LSO neurons with a mean diameter of 6.8 ± 0.2 μm (ranges: 7.9 – 4.8 μm) never exhibited colocalization with any of the other markers (Fig. 12, sub-population 7).

All LSO principal cells contained PV independent of their projection to either the ipsilateral or the contralateral CIC (Fig. 12). All neurons of the LSO constituting the projection to the contralateral CIC showed glutamate immunoreactivity (Fig. 4D). Additionally I detected neurons with the same axonal destination that also contained glycine. Twenty-five percent of all LSO neurons sent their axons to the contralateral CIC and were exclusively glutamatergic (Fig. 12, sub-population 3), while 5% co-localized glutamate with glycine (Fig. 12, sub-population 4i). All neurons projecting to the ipsilateral CIC contained glycine and PV, while 60% additionally contained glutamate (Fig. 4D). These neuronal sub-populations represented 10% (Fig. 12, sub-population 5) and 15% (Fig. 12, sub-population 4ii) of the entire LSO neuronal population, respectively.

When injecting tracer into VCN to study the commissural projection between the cochlear nuclei, a so far undescribed descending connection of the SOC was discovered. A projection from the LSO back to the ipsilateral VCN (Fig. 5C) that was constituted of both glutamatergic (Fig. 10E) and glycinergic neurons was found. Half of the cells projecting to the ipsilateral VCN also exhibited CB immunoreactivity (Fig. 10F). As indicated above, CB positive LSO neurons exclusively represented glutamatergic cells. In total, 30% of all LSO cells characterized here represented neurons that sent their axons to the ipsilateral VCN. Fifteen percent were glutamatergic, CB positive cells (Fig. 12, sub-population 2), the other 15% glycinergic neurons (Fig. 12, sub-population 6), both with small somata of 5.2 ± 0.2 μm (ranges: 5.9 – 4.2 μm) mean diameter.

5.1.4. Cell Types in the Medial Superior Olive

Neurons of the MSO were always positively stained for glutamate, but never for glycine or GABA. These glutamatergic neurons partially co-localized PV (Fig. 10G), but somata positively stained for CB or CR were never observed in the MSO. 40% of the identified neurons were singly stained for glutamate (Fig. 13, sub-population 1), while 60% additionally expressed PV (Fig. 13, sub-population 2).

Almost all of the MSO neurons, projected to the ipsilateral CIC (Fig. 4E). 40% of cells were only stained for glutamate (Fig. 13, sub-population 1), while 55% of neurons co-localized glutamate with PV (Fig. 13, subpopulation 2ii). These two sub-populations together represented 95% of the identified MSO neurons, all sending their axons to the ipsilateral CIC. 5% of the identified MSO neuronal cells projected to the contralateral CIC, all positively stained for glutamate and PV (Fig. 13, sub-population 2i).

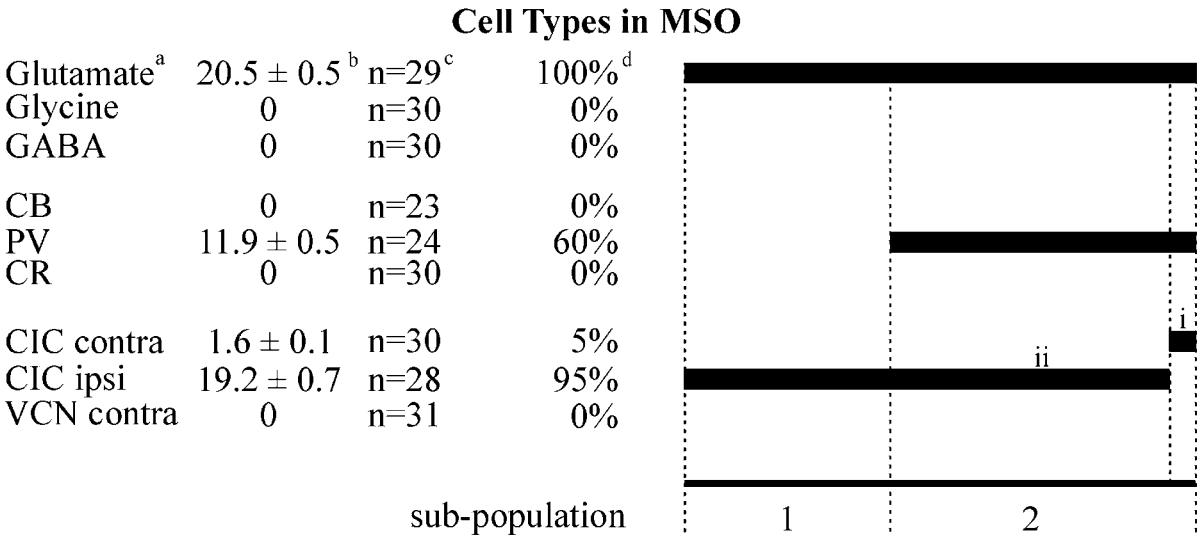

Figure 13: Immunocytochemically identified neuronal sub-populations in MSO. [a] Selected marker protein or site of tracer application, respectively. [b] Average number of cells counted per section ± S.E.M. [c] Number of sections on which evaluation was based. [d] Percentage of neurons stained with markers or tracer within the total of evaluated cells.

5.1.5. Cell Types in the Central Nucleus of the Inferior Colliculus

Neurons immunoreactive for glutamate were dispersed over the whole CIC with mean soma diameter of 5.9 ± 0.1 μm (ranges: 8.7 – 3.9 μm). Remarkably, all of them failed to express any other of the markers used in this study. I found this population to comprise 55% of identified CIC neurons (Fig. 14, sub-population 1). GABA positive cell bodies were, with a mean diameter of 10.6 ± 0.4 μm (ranges: 14.5 – 7.9 μm), larger and much more numerous in CIC as compared to GABAergic neurons in VCN (mean diameter: 4.9 ± 0.3 μm) and LSO (mean diameter: 7.1 ± 0.3 μm). GABAergic cells represented 35% of the CIC neurons. These cells always co-localized GABA with PV (Fig. 14, sub-population 3 + 4). However, not all PV positive neurons were also GABAergic (Fig. 10H), some appeared exclusively singly stained (Fig. 14, sup-population 5). In 10% of the identified CIC neurons GABA was co-localized with glycine (Fig. 14, sub-population 3). Glycinergic neurons have not been observed before in rat CIC (Fig. 14, sub-population 2 + 3). They were larger than glutamatergic cells, having somata of 10.2 ± 0.4 μm (ranges: 12.8 – 7.3 μm) mean diameter (Fig. 10I). I found cell bodies that were stained for either CR or CB at high densities in the dorsal and external cortex of the inferior colliculus, but rarely in CIC.

In total, less than 5% of all CIC cells characterized here represented commissural neurons. Half of these cells projecting to the contralateral CIC were glutamatergic, the other half GABAergic and PV positive (Fig. 4A).

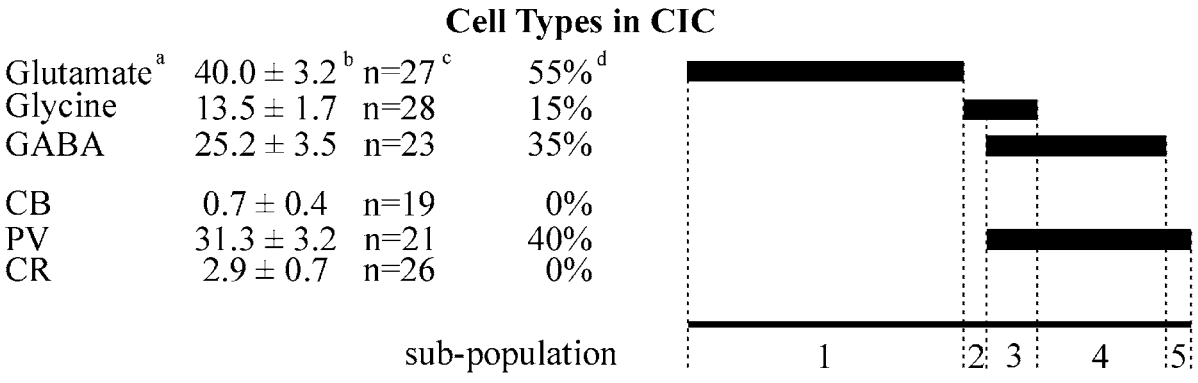

Figure 14: Immunocytochemically identified neuronal sub-populations in CIC. [a] Selected marker protein or site of tracer application, respectively. [b] Average number of cells counted per section ± S.E.M. [c] Number of sections on which evaluation was based. [d] Percentage of neurons stained with markers or tracer within the total of evaluated cells.

5.2. Specific Types of Neurons in the Rat Auditory Brainstem Invoke Immediate Early Gene Expression Upon Acute Electrical Intracochlear Stimulation

In this set of experiments, EIS was applied to stimulate the auditory system unilaterally for two hours. The investigations focused on the high-frequency areas of VCN, DCN, LSO, and CIC, originating from the basal cochlea. The stimulation resulted in a tonotopic expression of Egr-1 and c-Fos (Fig. 15A) in all four auditory brainstem areas. In MSO no stimulation-dependent IEG expression was detected. Cellular nuclei immunoreactive for Egr-1 always exhibited staining for c-Fos in VCN (100% in 5 sections), DCN (100%, n=6), LSO (100%, n=5), and CIC (97.1 ± 1.7%, n=5). This cellular co-expression was consistent with the locally matching up-regulation of both IEGs upon EIS as reported before (Illing et al., 2002). Therefore, further investigations were based on the marker c-Fos, implying that Egr-1 was co-expressed in neurons showing c-Fos. I performed various experiments with selected markers (Table 3) and axonal tracing (Table 4) to identify c-Fos expressing neurons in VCN, DCN, LSO, and CIC.

Table 3
Combinations of antibodies used in the experimental animals after acute EIS

	Area	M849[b]	M852	M856	M858	M871	M878	M887	M897	M937	M943
Glu - c-Fos[a]	VCN				n=4	n=6[c]		n=3			
	DCN					n=3		n=4			
	LSO					n=3		n=2			
	CIC					n=5		n=3			
Gly - c-Fos	VCN					n=4			n=5		
	DCN					n=3			n=3		
	LSO					n=3			n=7		
	CIC					n=4			n=3		
GABA - c-Fos	VCN					n=3	n=3		n=10		
	DCN						n=3		n=4		
	LSO						n=3		n=6		
	CIC						n=3		n=4		
PV - c-Fos	VCN		n=3	n=2							
	DCN		n=3	n=3							
	LSO		n=3	n=8							
	CIC		n=5	n=6							
CR - c-Fos	VCN							n=4	n=5		
	DCN							n=3	n=3		
	LSO							n=5	n=5		
	CIC							n=3	n=3		
CB - c-Fos	VCN	n=5		n=5							
	DCN	n=4		n=4							
	LSO	n=4		n=2							
	CIC	n=3		n=2							
GFAP - c-Fos	VCN									n=3	n=3
	DCN									n=3	n=3
	LSO									n=3	n=3
	CIC									n=3	n=3
Egr-1 - c-Fos	VCN							n=3	n=2		
	DCN							n=3	n=3		
	LSO							n=3	n=2		
	CIC							n=2	n=3		

[a] combination of antibodies used. [b] experimental rat number. [c] number of slices counted per animal. Glu = glutamate, Gly = glycine, PV = parvalbumin, CR = calretinin, CB = calbindin-D28k, GFAP = glial fibrillary acidic protein

Table 4
Combinations of immunocytochemical staining and tracer injections in the experimental animals after acute EIS

	Area	M908[b]	M914	M916	M918	M923	M929	M948	M951	M959
Tracer CICc-c-Fos[a]	VCN	n=3[c]			n=4					
	DCN	n=3			n=3					
	LSO	n=3			n=4					
	CIC									
Tracer CICi-c-Fos	VCN			n=3		n=3				
	DCN			n=4		n=3				
	LSO			n=3		n=3				
	CIC			n=3		n=3				
Tracer VCNc-c-Fos	VCN		n=4				n=5			
	DCN		n=6				n=10			
	LSO		n=3				n=3			
	CIC		n=3				n=3			
Tracer VCNi-c-Fos	VCN									
	DCN									
	LSO							n=3	n=4	
	CIC							n=3	n=3	
Tracer cochlea-c-Fos	VCN									
	DCN									
	LSO									n=13
	CIC									

[a] combination of tracer injection site and antibodies. [b] experimental rat number. [c] number of slices counted per animal.

Cell culture experiments have revealed that glial cells may express c-Fos upon excitation (Eun et al., 2004). In order to evaluate this possibility for the set-up used here, sections of stimulated brains were double stained for c-Fos and GFAP serving to identify astrocytes. Even when these markers overlapped regionally, they were nowhere found in the same cell. An up-regulation of c-Fos in microglia could be excluded by the size of the stained nuclei exceeding the size of entire microglial cell bodies. It was therefore concluded that the EIS-induced gene expression observed in this study was restricted to neurons.

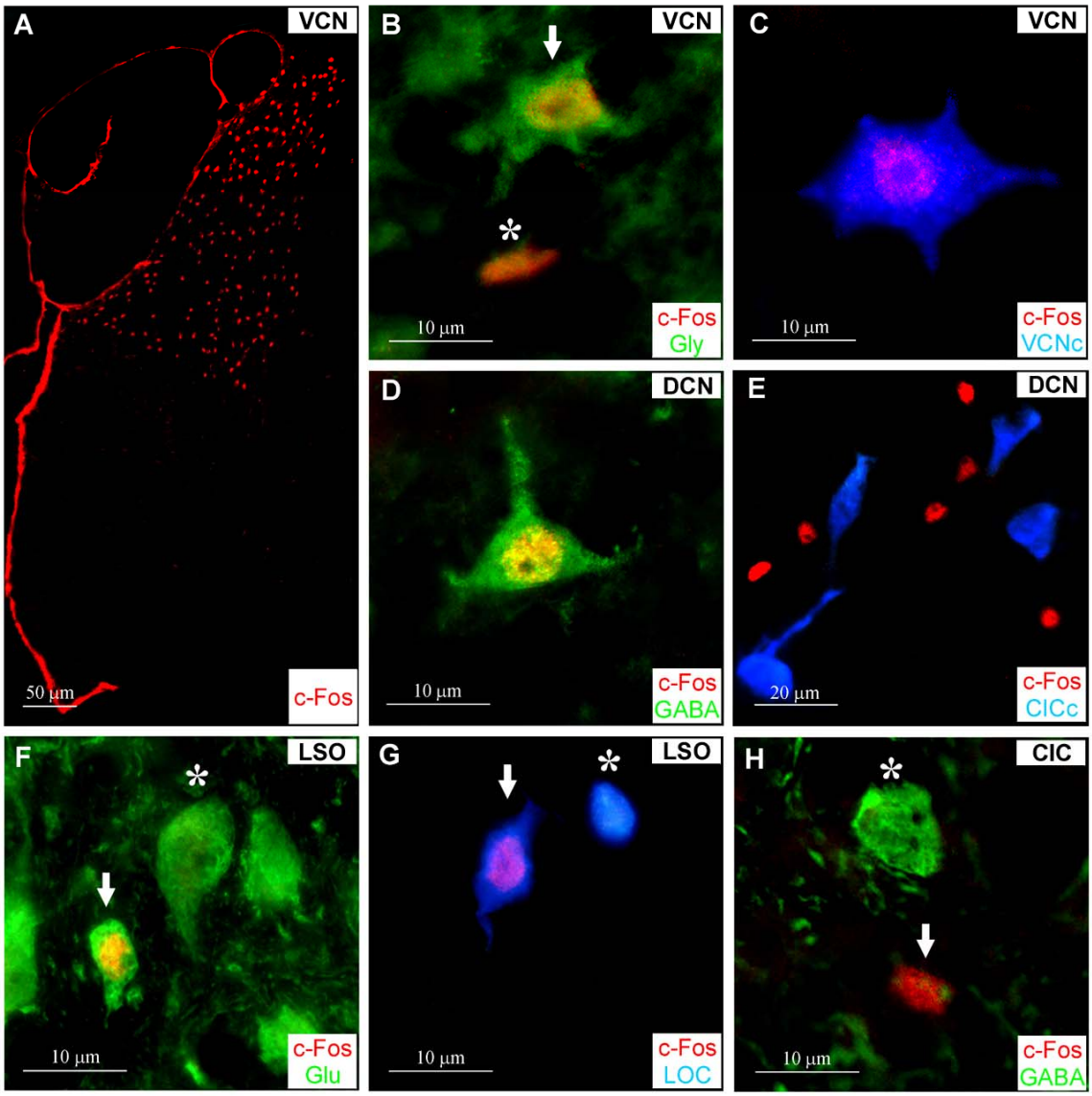

Figure 15: Exemplary illustrations of stimulation-dependent IEG expression in the auditory brainstem. A: The expression of c-Fos after basal EIS was restricted to the corresponding tonotopic area in the dorsal VCN. The ventral area representing the low frequencies of the unstimulated apical cochlea was entirely devoid of c-Fos positive nuclei. B: In the VCN, one half of the c-Fos positive nuclei were localized in glycinergic cells (yellow, arrow) while the other half showed no double labeling with glycine (red, asterisk). C: Expression of c-Fos (red) in a large VCN commissural neuron (blue) after FB injection into the contralateral VCN. D: The DCN was the only area investigated where c-Fos positive nuclei (red) were found in GABA immunoreactive neurons (green). E: c-Fos positive nuclei (red) were never observed in FB positive neurons of DCN (blue) after tracer injection into the contralateral CIC. F: C-Fos positive nuclei in the LSO belonged to small glutamatergic cells (yellow, arrow), but were never found in large principal cells exhibiting glutamate immunoreactivity (green, asterisk). G: Distinct LOC cells (blue) of the LSO that projected back to the cochlea showed co-localization with c-Fos (red, arrow), while others were not affected by the EIS mediated IEG up-regulation (asterisk). H: Like in VCN and LSO, there were no c-Fos positive nuclei (red, arrow) in GABAergic neurons (green, asterisk) in CIC.

5.2.1. C-Fos Expression in the Spiral Ganglion of the Cochlea

Looking for activity-dependent expression of c-Fos in neurons of the spiral ganglion, I failed to find any (Fig. 16A). This finding applied to the unstimulated apical (Fig. 16B) and medial area (Fig. 16C), as well as to the stimulated basal part (Fig. 16D) of the cochlea. The effective activation of these cells by EIS was obvious in the ABR and by the expression of c-Fos immunoreactive nuclei in the corresponding auditory brainstem areas to which these cells communicate their activity (Fig. 16E).

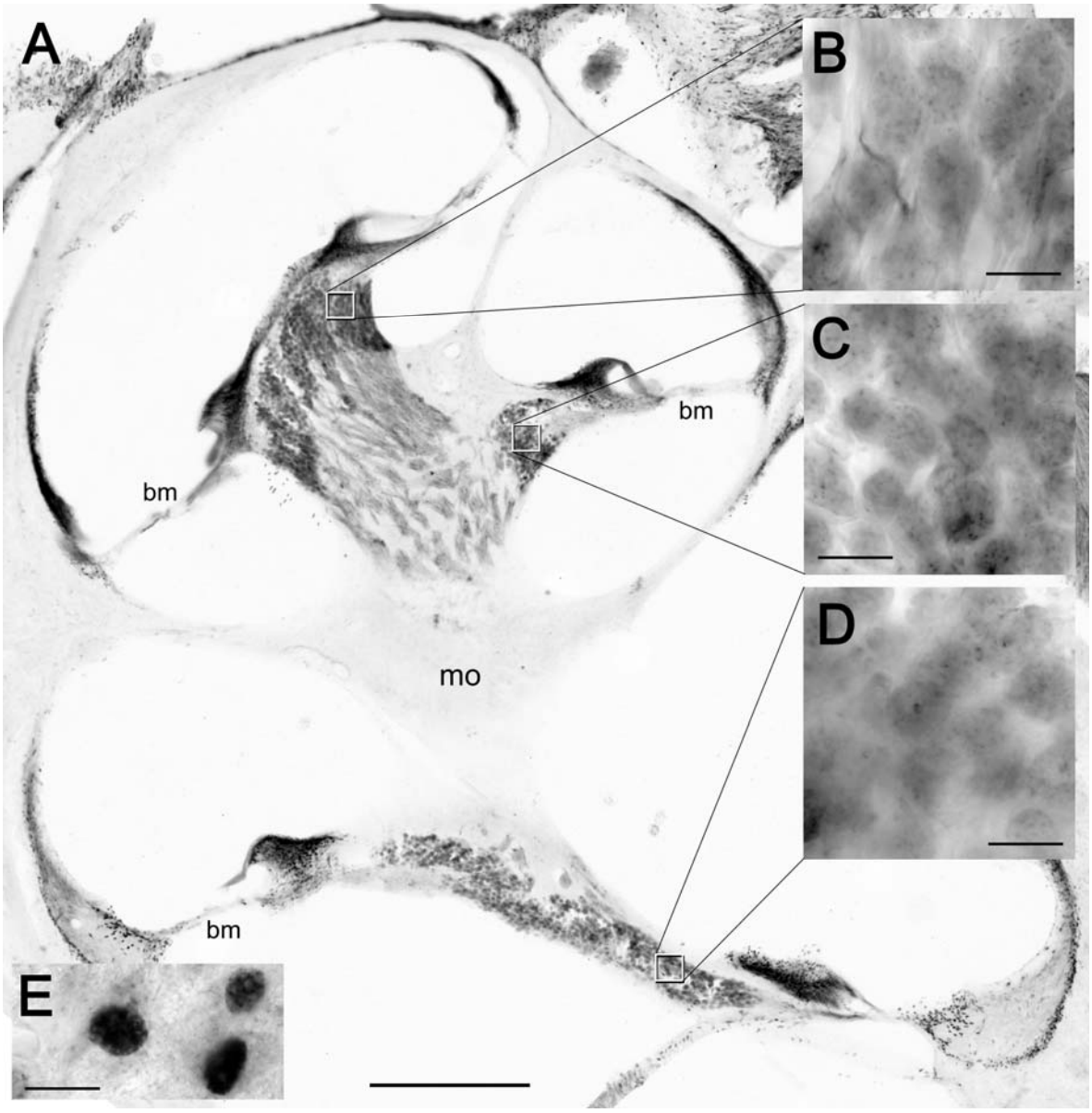

Figure 16: Longitudinal section through a cochlea stained for c-Fos immunoreactivity following EIS. Despite effective stimulation as evident from the emergence of c-Fos immunoreactivity in several auditory brainstem nuclei of the same animal, EIS failed to induce c-Fos expression in the spiral ganglion. A: Cochlear section processed for c-Fos immunoreactivity. Spiral ganglion neurons showed c-Fos neither in areas of the unstimulated apical turn (B), nor in the medial turn (C), nor in regions corresponding to the stimulated basal turn (D). E: Nuclei stained for c-Fos in VCN of the same animal served as positive control and proof of effective stimulation of spiral ganglion cells. bm: basial membrane; mo: modiolus. Scale bars: 200 µm in A, 10 µm in B to E.

5.2.2. C-Fos Expression in the Ventral Cochlear Nucleus

Following unilateral EIS, c-Fos positive cellular nuclei emerged in the ipsilateral but not in the contralateral VCN. Half of them were found in glutamatergic cells and the other half in glycinergic neurons (Fig. 15B) of various size and shape. I never detected c-Fos in CB positive octopus neurons (Fig. 17, sub-population 2), but 50% of the c-Fos positive nuclei were observed in cells that stained for PV. According to the data presented previously (Reisch and Illing, in preparation), these must have been glutamatergic neurons (Fig. 17, sub-population 3). Following EIS, 25% of c-Fos positive nuclei emerged in glutamatergic and PV positive multipolar type I cells with axons projecting across the midline to the contralateral CIC (Fig. 17, sub-population 3i). Since fifty percent of c-Fos positive neurons contained both glutamate and PV, the tracing experiment implied that the other 25% of these IEG positive nuclei must belong to glutamatergic neurons of the VCN that also co-localized with PV (Fig. 17, sub-population 3ii).

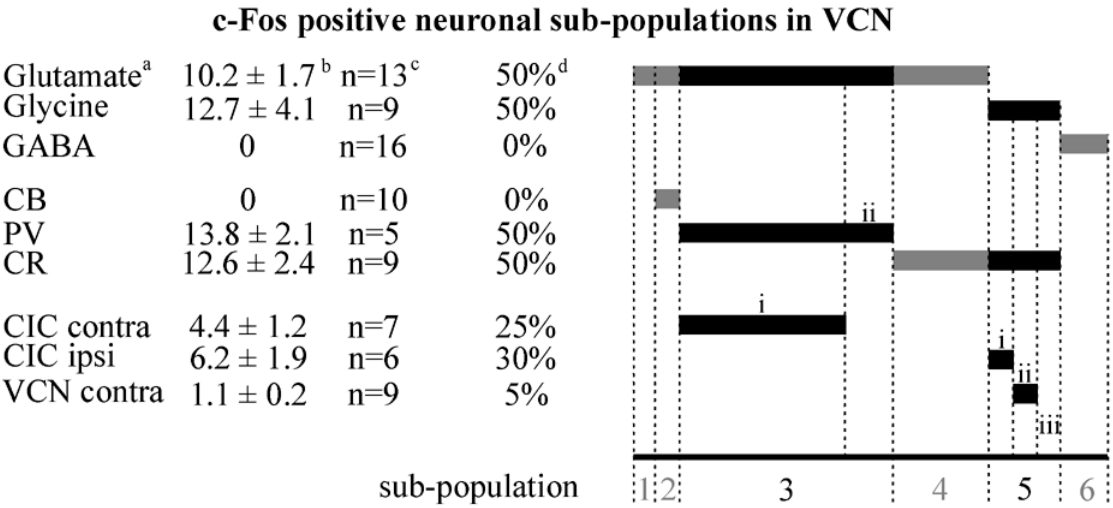

Figure 17: Immunocytochemically identified sub-populations in VCN that responded differentially to EIS. Six major molecular sub-populations of neurons (1 to 6) were identified (Reisch and Illing, in preparation), some of which invoked c-Fos expression upon EIS (black) while others failed to do so (gray). Attributing c-Fos positive neurons to identified sub-populations, they must sum up to 100%. C-Fos expression occurred only in two of these sub-populations (3 and 5). These two sub-populations split up again according to their axonal destination. [a] Marker molecule or site of tracer application, respectively. [b] Number of c-Fos positive nuclei expressed in cells labeled with antibodies or tracer, given as average number of cells per section ± S.E.M. [c] Number of sections on which evaluation was based. [d] Percentage of c-Fos nuclei located in specified sub-populations. Identified cell types: bushy (1, 3ii, 4), octopus (2), multipolar type I (3i, 5i), multipolar type II (5ii), small (5iii, 6).

In double staining experiments, 50% of all c-Fos positive nuclei were found in neurons containing CR matching the morphology of the glycinergic c-Fos positive cells. As it was detailed in a previous study (Reisch and Illing, in preparation), glycinergic VCN somata were always stained for CR. Obviously, then, c-Fos expression was required to show up equally frequent in cells containing glycine or CR, as it was indeed the case (Fig. 17, sub-population 5). I detected thirty percent of the c-Fos positive nuclei in multipolar type I cells projecting to the ipsilateral CIC (Fig. 17, sub-population 5i). The population of multipolar type II neurons that mediate the commissural pathway to the contralateral VCN was also affected by EIS to express c-Fos (Fig. 15C). 5% of all c-Fos positive nuclei were found in these commissural cells (Fig. 17, sub-population 5ii), reflecting the moderate number of neurons participating in this projection (2.2 ± 0.4 cells, averaged from 31 sections) compared to the almost 10 times more numerous multipolar type I neurons that projected to the contralateral CIC (21.6 ± 2.6 cells, averaged from 26 sections). In total, 50% of the c-Fos positive neurons contained both glycine and CR, but only 35% of them projected to the ipsilateral CIC or to the contralateral VCN. It was assumed that the remaining 15% of c-Fos positive nuclei in cells containing glycine and CR must be neurons with so far undetermined axonal destinations (Fig. 17, sub-population 5iii). Remarkably, c-Fos was never localized in neurons singly stained for glutamate (Fig. 17, sub-population 1), nor in glutamatergic bushy cells that co-localized with CR (Fig. 4, sub-population 4), nor in GABAergic cells of the VCN (Fig. 17, sub-population 6). In total, c-Fos was found in two of the six characterized VCN neuronal sub-populations that represented 60% of the complete neuronal population that was identified in VCN.

5.2.3. C-Fos Expression in the Dorsal Cochlear Nucleus

In DCN, a few c-Fos positive nuclei were present even without EIS. Two days after bilateral middle ear bone removal, I observed a ratio between the left and the right DCN of 1.08 for c-Fos immunoreactive nuclei with no significant difference ($p = 0.137$, $n = 9$). After two hours of EIS, a significant increase in the number of c-Fos immunoreactivity was observed in the ipsilateral (*$p = 0.037$) as well as the contralateral DCN (***$p = 0.002$) compared to control animals. However, the rise was stronger ipsilaterally than contralaterally. The number of c-Fos positive nuclei in the ipsilateral DCN was 1.40 times higher than the number of c-Fos positive nuclei on the contralateral side after stimulation (**$p = 0.005$, $n =$

24). The EIS invoked c-Fos expression in neuronal sub-populations was therefore evaluated in the DCN on both sides of the brainstem.

On neither side, c-Fos positive nuclei were seen in PV positive stellate cells (Fig. 18, sub-population 7), nor in CR immunoreactive somata of granule cells and unipolar brush cells (Fig. 18, sub-population 2). Ipsilaterally, 50% of the c-Fos positive nuclei were co-localized with glutamate (Fig 18, sub-popultions 1 and 3). Contralaterally, about every third c-Fos positive neuron also contained glutamate (36.6 ± 6.9%, n = 7). Ipsilaterally, one half of the IEG positive nuclei occurred in GABA positive somata (Fig. 15D), and the same amount was seen in glycinergic neurons. Contralaterally, two thirds of the IEG positive nuclei emerged in GABAergic (63.2 ± 7.1%, n = 6) as well as in glycinergic neurons (64.0 ± 7.1%, n = 6). Since glutamate immunoreactivity was neither co-localized with glycine nor with GABA in the DCN, but GABA was in part co-localized with glycine (Reisch and Illing, in preparation), it was concluded that 50% of c-Fos positive nuclei occurred in the subset of cartwheel neurons (Fig. 18; sub-population 6), but not in GABAergic Golgi cells (Fig. 18; sub-population 8), while the other half of c-Fos immunostained nuclei occurred in glutamatergic neurons.

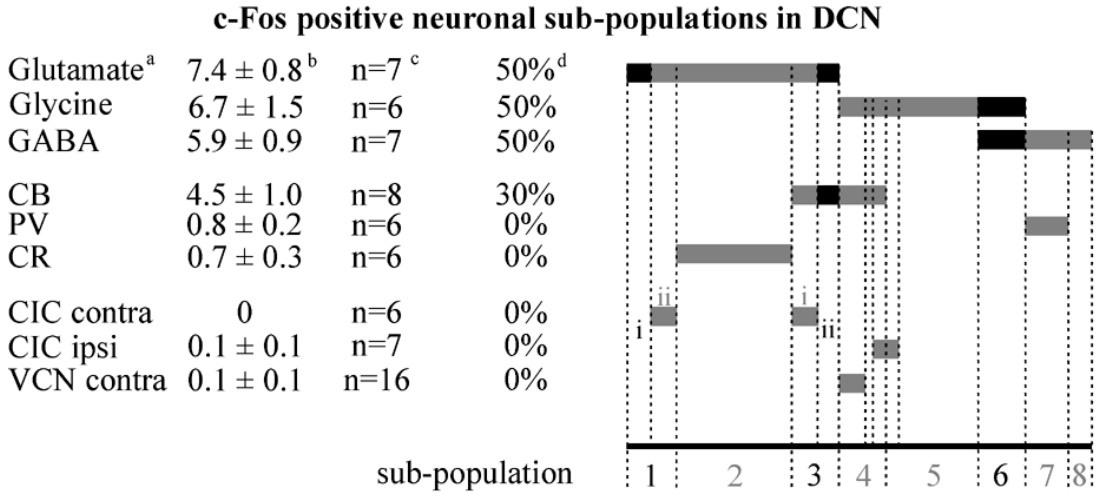

Figure 18: Immunocytochemically identified sub-populations in DCN that responded differentially to EIS.Eight major molecular sub-populations of neurons (1 to 8) were identified in previous studies (Reisch and Illing, in preparation), some of which invoked c-Fos expression upon EIS (black) while others failed to do so (gray). Three sub-populations expressed c-Fos (1, 3 and 6). [a] Marker molecule or site of tracer application, respectively. [b] Number of c-Fos positive nuclei expressed in cells labeled with antibodies or tracer, given as average number of cells per section ± S.E.M. [c] Number of sections on which evaluation was based. [d] Percentage of c-Fos nuclei located in specified sub-populations. Identified cell types: medium fusiform (1), granule and unipolar brush (2), small fusiform (3), giant (4), vertical (5), cartwheel (6), superficial stellate (7), Golgi (8).

There was a notable difference between the staining patterns in ipsilateral and contralateral DCN. Thirty percent of c-Fos positive nuclei were located in CB positive neurons (Fig. 18, sub-population 3) in the ipsiliateral, but none in the contralateral DCN. An equal number of CB immunoreactive neurons in the ipsilateral (12.8 ± 3.1 cells, n = 5) as well as the contralateral DCN (13.0 ± 3.1 cells, n = 5) indicated, that the CB expression itself did not change upon stimulation. This observation therefore implies that a distinct CB positive population of ipsilateral, but not contralateral DCN neurons responded to EIS with IEG expression. The higher number of c-Fos immunoreactive nuclei in ipsilateral DCN, represented by the ipsilateral-to-contralateral ratio of 1.40, can be fully accounted by the c-Fos nuclei that were found in the CB positive neurons. This is strongly suggestive for the higher number of IEG positive nuclei in the ipsilateral DCN to be due to the CB positive neuronal sub-population.

When characterizing neuronal subsets, it was shown that DCN neurons stained for CB exhibited co-localization with glutamate or with glycine, but not with GABA (Reisch and Illing, in preparation). The c-Fos positive nuclei residing in neurons containing CB must therefore be attributed to the glutamatergic subset of small fusiform cells (Fig. 5, sub-population 3), while the remaining c-Fos positive nuclei apparently resided in neurons immunoreactive for glutamate only (Fig. 18, sub-population 1).

Stimulation-dependent IEG up-regulation was never observed in neurons of the DCN projecting to the contalateral CIC (Fig. 15D), ipsilateral CIC, or contralateral VCN (Fig. 18, sub-populations 1ii, 3i, 4, 5). Therefore, glutamatergic and glycinergic cells that expressed c-Fos upon stimulation appear to be locally projecting neurons. More specifically, they are likely to be DCN interneurons since neurons projecting to VCN on the same side did not develop c-Fos immunoreactivity. In total, I found only three of the eight identified neuronal sub-populations to express c-Fos upon stimulation, amounting to 25% of all characterized DCN neurons.

5.2.4. C-Fos Expression in the Lateral Superior Olive

Activity-dependent gene expression in the ipsilateral LSO occurred, as in the CNC, to 50% in glycine positive cell bodies of various shape and size. Most c-Fos positive nuclei were observed in glycinergic neurons with small and round somata (Fig. 19, sub-population 6), being about twice as numerous as IEG expression in the larger principal cells. These small glycinergic neurons were shown to project to the ipsilateral VCN previously (Reisch and Illing, in preparation). The number of c-Fos stained nuclei observed in PV positive neurons, amounting to 15% of the total, matched the number of nuclei in glycinergic principal neurons, projecting to the ipsilateral CIC (Fig. 19, sub-population 5).

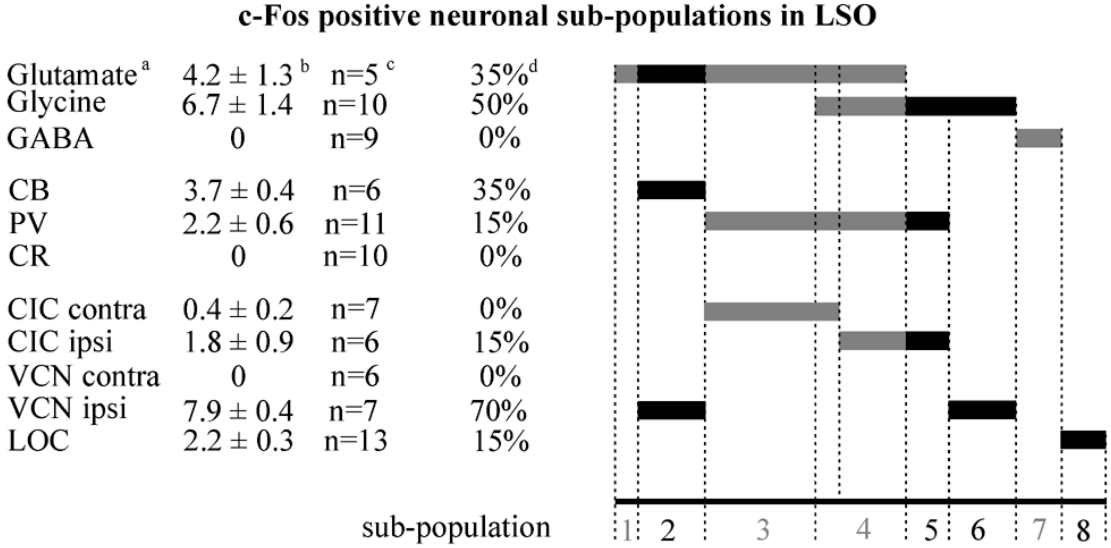

Figure 19: Immunocytochemically identified sub-populations in LSO that responded differentially to EIS. Seven major molecular sub-populations of neurons (1 to 7) were identified, some of which invoked c-Fos expression upon EIS (black) while others failed to do so (gray). I observed four sub-populations that expressed c-Fos (2, 5, 6, 8). Neurons on which the major ascending glutamatergic pathway was based were unaffected by EIS, whereas neurons forming descending connections to the VCN (2, 6) and to the cochlea (8) strongly expressed c-Fos after EIS. [a] Marker molecule or site of tracer application, respectively. [b] Number of c-Fos positive nuclei expressed in cells labeled with antibodies or tracer, given as average number of cells per section ± S.E.M. [c] Number of sections on which evaluation was based. [d] Percentage of c-Fos nuclei located in specified sub-populations. Identified cell types: cells projecting to VCN (2, 6), principal (3, 4, 5), LOC (7, 8).

About every third c-Fos positive nucleus resided in a glutamatergic neuron. In these cases, IEG expression was restricted to small cells, whereas the large glutamatergic principal neurons did not reveal c-Fos positive nuclei (Fig. 15E). The same number of c-Fos immunoreactive nuclei, amounting to 35%, was found in small CB positive cells (Fig. 19, sub-population 2), which were shown to be glutamatergic (Reisch and Illing, in preparation).

Since only 15% of IEG positive nuclei occurred in neurons that mediated ascending projections, I wondered where the remaining c-Fos positive neurons project to and investigated descending projections of the LSO. One such descending projection is destined for the ipsilateral VCN. This system was found to be constituted of both glutamatergic and glycinergic neurons. Seventy percent of c-Fos positive nuclei were expressed in LSO projection neurons to the ipsilateral VCN. Based on double staining experiments, 35% of the c-Fos positive cells were found to be associated to the glutamatergic and CB positive neurons (Fig. 19, sub-population 2) and the remaining 35% to glycinergic cells projecting to the VCN (Fig. 19, sub-population 6).

Another descending projection originating in LSO that was affected by the stimulation-dependent c-Fos upregulation was found to be constituted by LOC neurons (Fig. 15G), which send their axon to the ipsilateral cochlea (White and Warr, 1983; Aschoff and Ostwald, 1988; Horváth et al., 2000). A tracer injection was made into the cochlea to prelabel LOC neurons. Subsequently, EIS was applied to the same cochlea. Of all c-Fos immunoreactivity nuclei 54.4 ± 5.4% (n = 13) were seen to belong to LOC neurons. However, since these experiments required that the same cochlea was filled with FB before being stimulated, it has to be taken into account that interference might occur between these treatments. Indeed, a reduced number of neurons expressing c-Fos was observed in the studies combining cochlear tracer injection and EIS as compared to the other experiments of this study. This reduction might be due to an auditory nerve mildly intoxicated by FB, or to intracochlear damage inflicted by tracer application into the cochlea. Correspondingly, a sub-optimal resolution of the ABR curve during these experiments was observed. Neurons transsynaptically triggered to express c-Fos were therefor likely to be underestimated and every second of all c-Fos positive cells in the LSO to be LOC neurons must be classified as an overestimation. The number of c-Fos positive LOC neurons may not exceed 15% (Fig. 19, sub-population 8) since 85% of c-Fos positive neurons were already attributed to projections towards CIC (15%) and VCN (70%). Since c-Fos was never observed in GABAergic cells (Fig. 19, sub-population 7), the LOC neurons found to turn c-Fos positive through EIS must

be of the cholinergic type (Fig. 19, sub-population 8). In total, I found only four of the identified LSO sub-populations to turn c-Fos positive upon EIS, amounting to 50%, while the remaining four did not.

5.2.5. C-Fos Expression in the Central Nucleus of the Inferior Colliculus

Stimulation-dependent gene expression in CIC was prominent in neurons that exhibited glutamate or glycine immunoreactivity. Half of all c-Fos positive nuclei were found in glutamatergic cells (Fig. 20, sub-population 1), and almost one third in glycinergic neurons (Fig. 20, sub-population 2). Cell bodies containing PV that turned up c-Fos expression upon stimulation in VCN and in LSO did not do so in CIC, although PV positive cells represented a CIC sub-population of considerable size (Fig. 20, sub-populations 3, 4, 5). Like in VCN and LSO, GABAergic CIC neurons never showed a stimulation-dependent IEG up-regulation (Fig. 15H). As only 80% of the c-Fos positive nuclei could be ascribed to neurons of characterized sub-populations, it must be concluded that an as yet unidentified subset was affected by EIS, amounting to 20% of all responding neurons in CIC (Fig. 20, sub-population 6).

Neurons projecting through the inferior collicular commissure mediate inhibitory as well as excitatory effects on their contralateral targets (Malmierca et al., 2005). C-Fos positive nuclei were not found in these projection neurons. Descending projections of CIC aim for SOC and CNC (Caicedo and Herbert, 1993). While I did not obtain data concerning the pathway towards the olive, cell bodies in CIC retrogradely traced from VCN were found to lack c-Fos after stimulation.

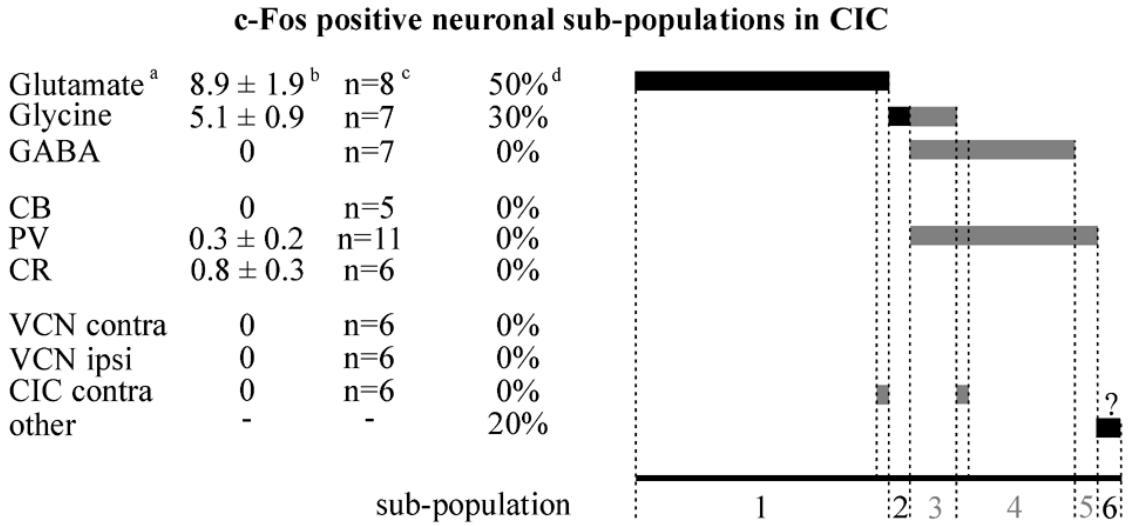

Figure 20: Immunocytochemically identified sub-populations in CIC that responded differentially to EIS. Five major sub-populations were identified in the CIC (1 to 5), some of which invoked c-Fos expression upon EIS (black) while others failed to do so (gray). Glutamatergic (1), glycinergic (2) and at least one yet unidentified subset of neurons (6) responded to EIS with c-Fos up-regulation. [a] Marker molecule or site of tracer application, respectively. [b] Number of c-Fos positive nuclei expressed in cells labeled with antibodies or tracer, given as average number of cells per section ± S.E.M. [c] Number of sections on which evaluation was based. [d] Percentage of c-Fos nuclei located in specified sub-populations. Identified cell types: flat neurons (1), less-flat neurons (3, 4).

5.3. Structural Synaptic Rearrangements in the Adult Auditory Brainstem Mediated by GAP-43 and PSA-NCAM After Chronic Electrical Intracochlear Stimulation

To investigate activity-dependent plasticity beyond IEG expression, stimulation was extended from two hours to seven days. EIS was applied unilaterally in the basal cochlea, using the same stimulation parameters as in acute experiments. Investigations focused on the high-frequency areas of VCN, DCN, and LSO, where IEGs were tonotopically upregulated upon EIS for two hours. Stimulation-dependent IEG upregulation was no longer detected in the chronic experiment, but activity-dependent changes occurred on the level of proteins mediating structural rearrangements of synapses. In this study, the plasticity markers GAP-43 and PSA-NCAM were used to obtain quantitative data (Table 5).

Table 5
Immunocytochemical staining in the experimental animals after chronic EIS and control implantation

	Area	M869[b]	M888	M997	M1003	M1014	M1047
7 days EIS GAP-43[a]	AVCN	n=9[c]			n=6	n=7	
	LSO	n=6			n=4	n=3	
7 days EIS PSA-NCAM	AVCN	n=8			n=7	n=7	
	LSO	n=5			n=5	n=3	
7 days control GAP-43	AVCN		n=9	n=6			n=7
	LSO		n=5	n=5			n=8
7 days control PSA-NCAM	AVCN		n=8	n=7			n=10
	LSO		n=5	n=5			n=7

[a] experimental procedure and antibodies used. [b] experimental rat number. [c] number of slices counted per animal.

5.3.1. GAP-43 and PSA-NCAM in the Anteroventral Cochlear Nucleus

After seven days of EIS, GAP-43 was dramatically up-regulated in the AVCN on the stimulated side, while remaining at control levels on the unstimulated side (Fig. 21A). Remarkably, this stimulation-dependent expression of GAP-43 was not restricted to the dorsal AVCN corresponding to the high frequency area of the basal cochlea, where the stimulation electrode was placed. GAP-43 positive boutons were dispersed over the whole AVCN, with an even denser staining in the ventral part than in the dorsal area. Up-regulation of PSA-NCAM (Fig. 21B) was locally corresponding to the activity-dependent GAP-43 expression. Immunoreactivity against PSA-NCAM was highly increased in the whole AVCN ipsilateral to EIS, but remained at control levels contralaterally.

Up-regulation of the two plasticity-associated molecules GAP-43 and PSA-NCAM was clearly dependent on EIS and not caused by cochlear damage induced by the implantation. In animals that received an implant but were not stimulated, GAP-43 (Fig. 21C) and PSA-NCAM (Fig. 21D) immunostaining was identical in ipsilateral and contralateral AVCN, remaining at control levels on both sides. The comparison of stimulated with unstimulated animals was highly significant. Gray-value density measurements were performed in the dorsal part of AVCN, corresponding to the placement of the stimulating electrode in the cochlea. After EIS, gray-value density ratio between ipsilateral and contralateral AVCN was 1.22 ± 0.03, while in control animals levels in ipsi- and contralateral AVCN were equal with a ratio of 0.99 ± 0.04 (Fig. 21E). Gray-value density measurements of PSA-NCAM stained sections revealed similar results with ipsilateral/contralateral ratios of 1.30 ± 0.05 in stimulated and 1.02 ± 0.03 in unstimulated animals (Fig. 21F). For both

plasticity markers, the increased ipsilateral/contralateral ratio upon EIS was highly significant compared to controls (GAP-43: ***p = 1.40×10^{-4}; PSA-NCAM: ***p = 6.78×10^{-5}).

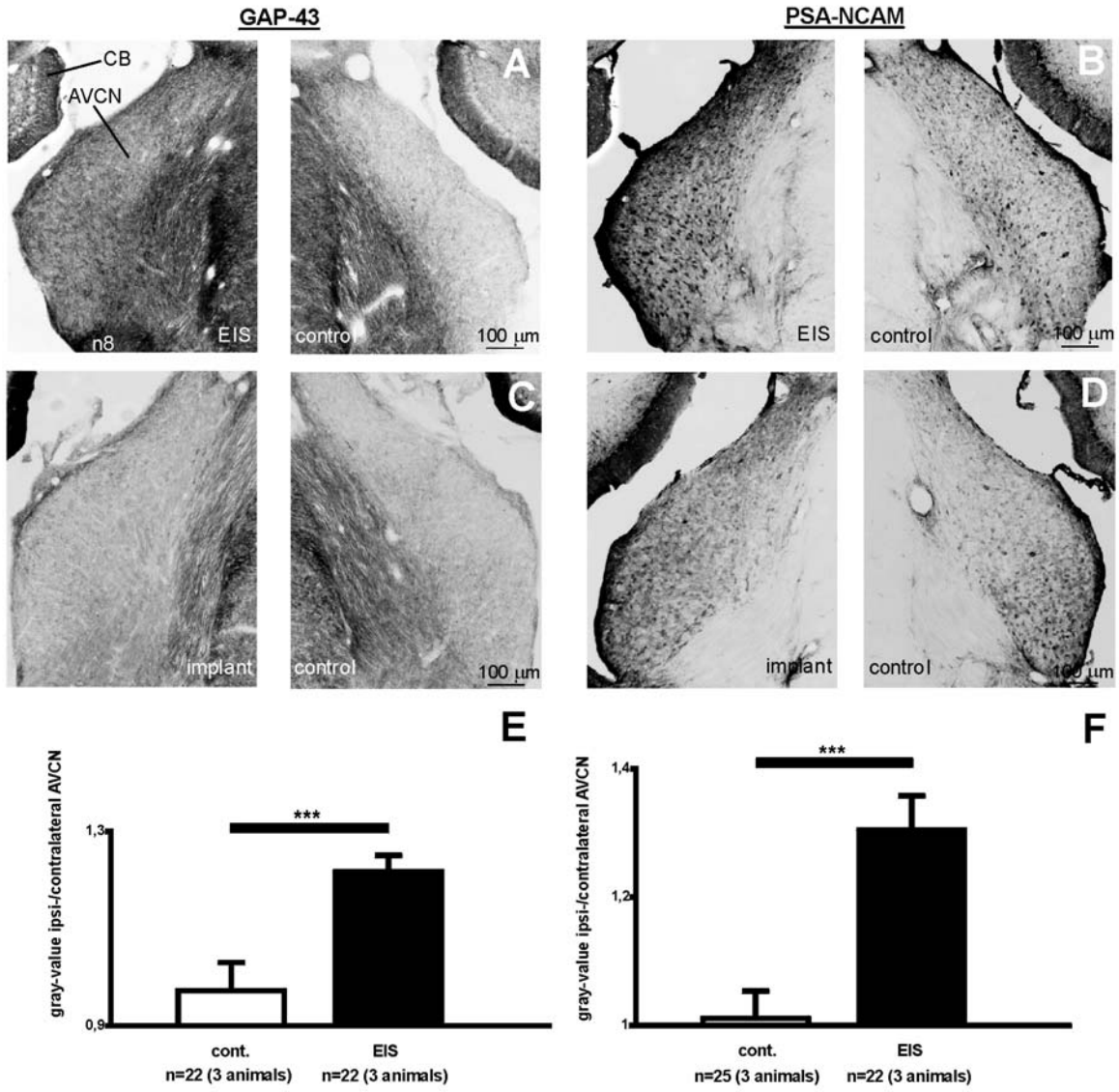

Figure 21: Stimulation-dependent GAP-43 and PSA-NCAM up-regulation in AVCN. A: GAP-43 and B: PSA-NCAM was up-regulated in AVCN on the stimulated side after seven days of EIS. On the unstimulated side, AVCN showed comparable staining intensities as in implanted but unstimulated control animals for C: GAP-43 and D: PSA-NCAM. A significant difference (***p < 0.005) was observed when comparing ipsi- and contralateral gray-value density between control and stimulated rats for E: GAP-43 and F: PSA-NCAM. n8 = 8th cranial nerve, CB = cerebellum.

To show that implantation and whereabouts of the stimulation electrode in the cochlea for seven days did not induce any degeneration, comparisons were made with animals deafened by cochleotomy. During cochleotomy, the whole interior of the cochlea, including organ of Corti and spiral ganglion, was removed and neurons forming the auditory nerve were axotomized (Illing and Horváth, 1995; Illing and Reisch, 2006). The induced unilateral deafness also leads to up-regulation of GAP-43 in the ipsilateral, but not in the contralateral AVCN (Illing et al. 1997; Fig. 22A). The increase in GAP-43 expression is accompanied by a decrease of CR staining in AVCN on the deafened side (Illing et al., 2005; Fig. 22B), resulting from loss of spiral ganglion fibers forming the auditory nerve. In implanted but unstimulated animals, GAP-43 (Fig. 22C) and CR (Fig. 22D) expression in AVCN remained at control levels on both sides. Severe damage of cochlea and spiral ganglion caused by implantation or overstimulation could be excluded, since no degeneration processes were observed in AVCN.

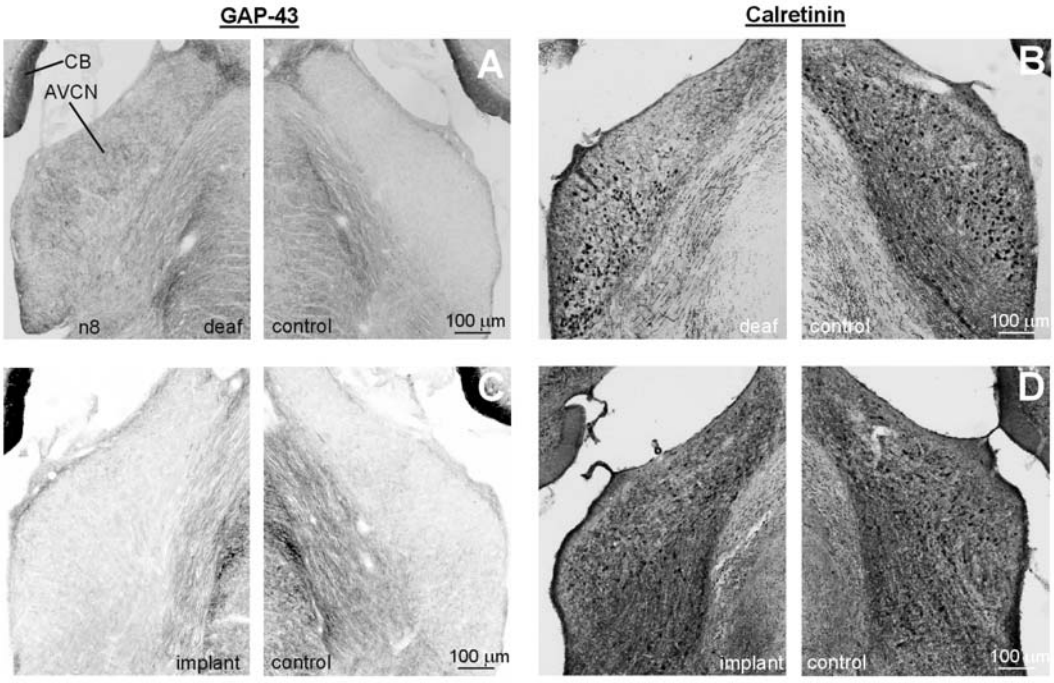

Figure 22: Comparison of artificially induced deafness and implantation. A: GAP-43 was up-regulated in AVCN on the deafened side seven days after cochleotomy. On the unstimulated side, AVCN immunoreactivity remained at control levels. B: CR decreased to in AVCN locally corresponding to GAP-43 increase in the unilateral deaf animal. C: Implanted but unstimulated rats showed no increased GAP-43 expression in AVCN. D: Implantation caused no degeneration of auditory nerve fibers, manifesting in CR staining at control levels in ipsilateral as well as contralateral AVCN. n8 = 8th cranial nerve, CB = cerebellum.

5.3.2. GAP-43 and PSA-NCAM in the Dorsal and Posteroventral Cochlear Nucleus

Cochleotomy-induced GAP-43 expression is not only restricted to AVCN, but the whole CNC on the non-hearing side is affected (Illing et al. 1997; Illing et al., 2005). GAP-43 is dramatically up-regulated in ipsilateral, but not in contralateral DCN upon cochleotomy (Fig. 23A). Interestingly, upon EIS, GAP-43 was not upregulated in DCN and its expression remained at control levels on both sides (Fig. 23B). In PVCN, GAP-43 up-regulation similar to DCN and AVCN is observed seven days after cochleotomy. Expression of GAP-43 is increased on ipsilateral side, but not contralaterally to the deaf ear (Fig. 23C). Again, no such activity-dependent GAP-43 upregulation was observed in PVCN after stimulation for seven days (Fig. 23D). In all experiments, upon cochleotomy as well as upon EIS, PSA-NCAM was locally co-regulated with GAP-43.

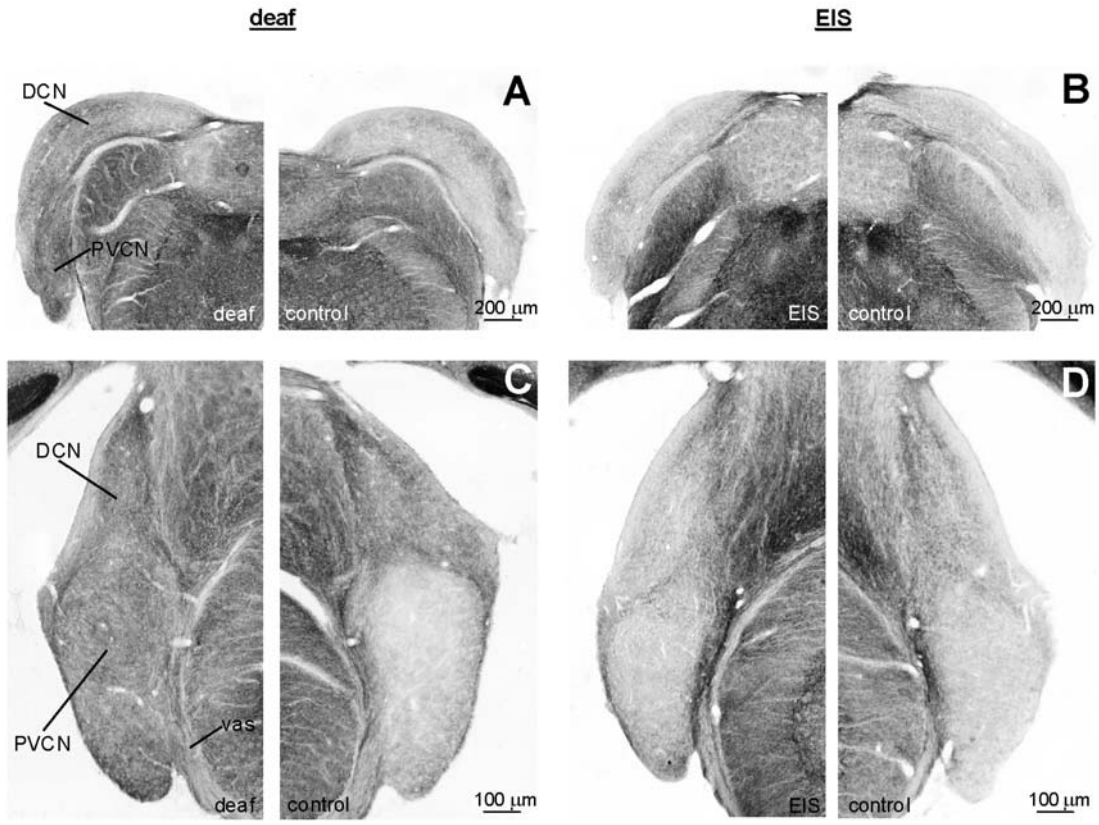

Figure 23: GAP-43 immunostaining in DCN and PVCN after EIS and induced deafness. A: Seven days after induced deafness by cochleotomy, GAP-43 levels increase dramatically in the DCN of the affected side. B: GAP-43 staining remained at control levels after seven days of EIS. C: Upon cochleotomy-induced hearing loss, GAP-43 levels increase in PVCN of the deaf, but not of the normal hearing control side. D: Similar to DCN, GAP-43 immunoreactivity remained low after chronic EIS in PVCN.

5.3.3. GAP-43 and PSA-NCAM in the Lateral Superior Olive

In the LSO, activity-dependent up-regulation of GAP-43 was observed upon EIS lasting seven days. In contrast to AVCN, stimulation-dependent GAP-43 up-regulation in LSO was restricted to the medial part (Fig. 24A), representing the high frequency area that corresponds to the basal cochlea, where the electrode was placed. This frequency-specific GAP-43 increase resulted in a gray-value density ratio between medial and lateral LSO of 1.12 ± 0.02 (Fig. 24B). On the unstimulated control side, GAP-43 expression remained at control levels in the entire LSO, resulting in a gray-value density ratio of 1.03 ± 0.01 between medial and lateral LSO. Gray-value density ratio from contralateral LSO in stimulated rats showed no difference compared to density ratio in ipsilateral (1.04 ± 0.01; $p = 0.71$) and contralateral LSO (1.03 ± 0.01; $p = 0.86$) in implanted but unstimulated control animals. Gray-value density measurements in ipsilateral LSO of stimulated animals revealed significantly higher medial to lateral ratios compared with contralateral LSO in the same animal (***$p = 4.49 \times 10^{-4}$), ipsilateral (***$p = 2.48 \times 10^{-4}$), and contralateral LSO (***$p = 1.25 \times 10^{-4}$) in rats receiving implantation without EIS.

Contrarily to AVCN, PSA-NCAM showed no locally correlated expression with GAP-43 in LSO upon chronic EIS. PSA-NCAM immunostaining remained low in both, ipsilateral and contralateral LSO of animals unilaterally stimulated for seven days (Fig. 24C). Gray-value density measurements revealed medial/lateral ratios upon EIS (1.06 ± 0.01) and after implantation without stimulation (1.06 ± 0.01), that showed no significant difference ($p = 0.90$) in ipsilateral LSO (Fig. 24D). Interestingly, medial to lateral ratio of gray-value density in contralateral LSO of stimulated rats (0.99 ± 0.02) was significantly lower compared with ipsilateral LSO in the same animal (***$p = 0.003$), as well as in ipsilateral (*$p = 0.011$) and contralateral LSO (1.03 ± 0.01; *$p = 0.03$) of control animals. Medial/lateral ratio in contralateral LSO of control animals was identical with ratios in ipsilateral control ($p = 0.084$) and ipsilateral EIS ($p = 0.21$) for PSA-NCAM gray-value density measurements.

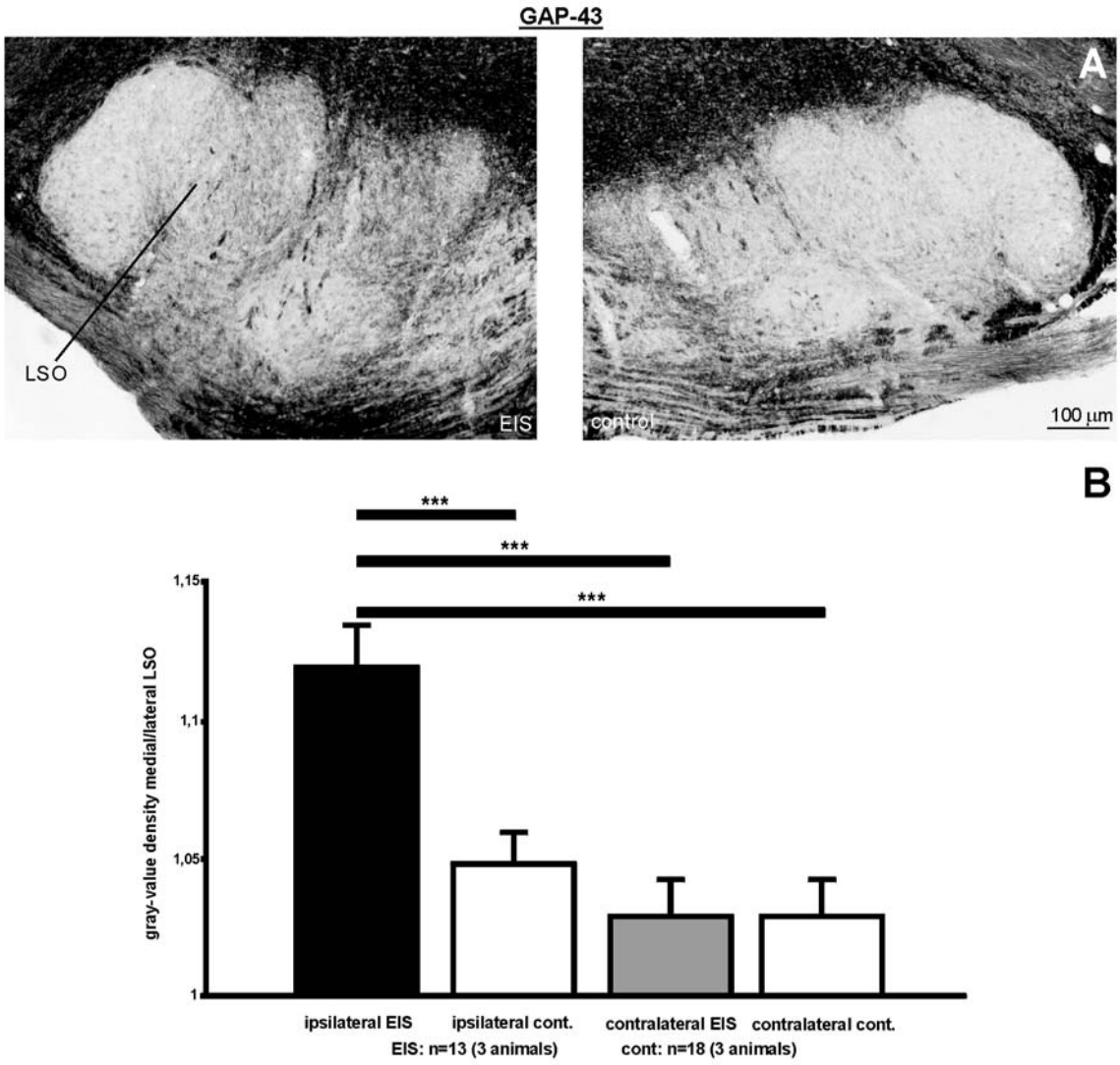
GAP-43
LSO
EIS
control
A
100 µm
B
***
***
***
1,15
1,1
1,05
1
gray-value density medial/lateral LSO
ipsilateral EIS
ipsilateral cont.
contralateral EIS
contralateral cont.
EIS: n=13 (3 animals)
cont: n=18 (3 animals)

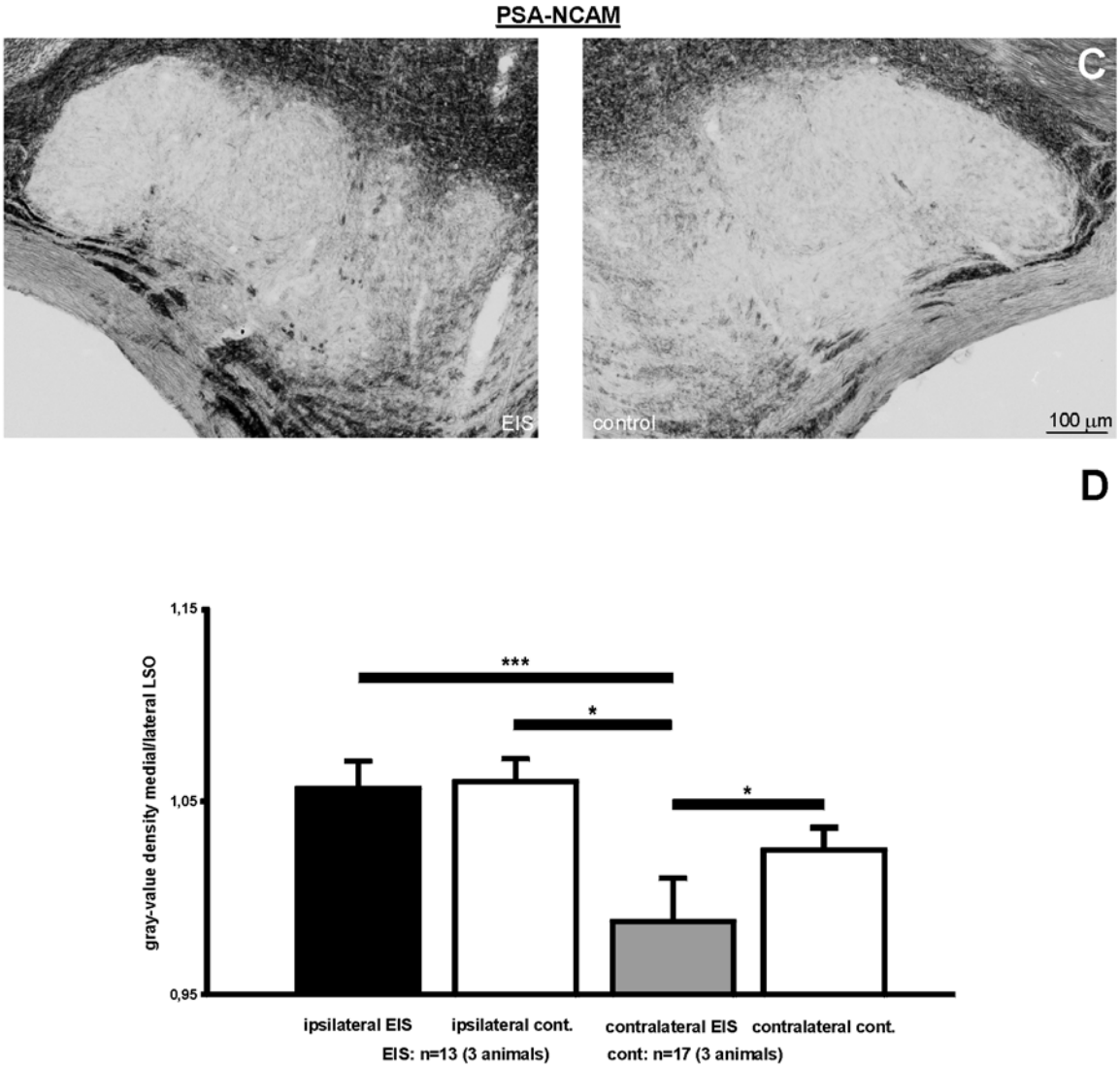

Figure 24: Stimulation-dependent effects in LSO. A: GAP-43 was up-regulated only in the medial limb of the ipsilateral LSO upon EIS. B: This GAP-43 increase was significant (***$p < 0.005$) compared to control animals and to the contralateral LSO. C: PSA-NCAM remained at low levels in ipsilateral and contralateral LSO after EIS. D: There was no significant difference in gray-value density ratio in ipsilateral LSO of stimulated rats compared with control animals. Medial/lateral ratio of PSA-NCAM on the unstimulated side was significantly reduced compared stimulated side and control.

Upon chronic EIS for seven days, GAP-43 expression in ipsilateral LSO was located in fibers, but cell bodies were devoid of GAP-43 staining (Fig. 25A). Seven days after cochleotomy, GAP-43 is not only up-regulated in ipsilateral CNC, but also in ipsilateral LSO (Illing et al., 1997). Contrarily to EIS mediated GAP-43 expression, not only the medial part, but the entire LSO showes immunoreactivity. A remarkable difference compared to

stimulation is the expression of GAP-43 in somata of LOC neurons after induction of deafness by cochleotomy (Fig. 25B). As shown previously (Kraus and Illing, 1998; 2005), axotomy leads to expression of c-Jun in LOC neurons. Since no damage occurred to the auditory nerve during chronic EIS, c-Jun was not induced in LSO upon chronic stimulation (Fig. 25C), but is expressed in LOC neurons after cochleotomy (Fig. 25D).

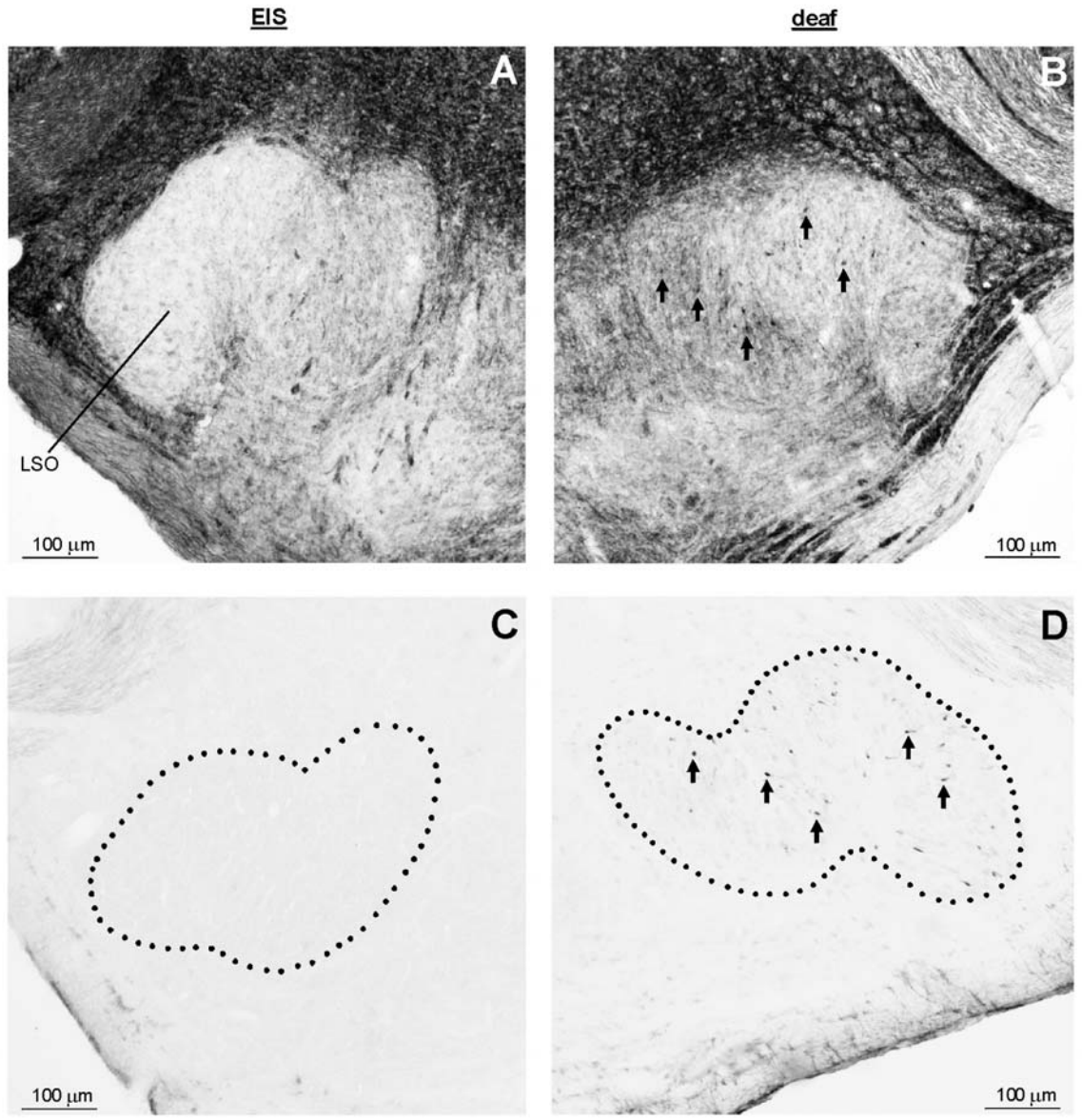

Figure 25: Differential response of LOC neurons upon EIS and upon cochleotomy. A: The medial limb of the LSO showed increased GAP-43 staining in the neuropil upon EIS. GAP-43 positive neuronal cell bodies were never detected. B: The small somata of LOC neurons are intensely GAP-43 labeled (arrows) after axotomy. C: Neurons of the LSO never showed c-Jun upregulation that indicates axotomy, upon EIS. D: Axotomized LOC neurons that upregulate GAP-43 upon cochleotomy also expresse c-Jun (arrows).

Since GAP-43 protein is quickly transported out of the soma into the axon, the identification of neuronal cells that responded to chronic EIS had to be done with in situ hybridization against GAP-43 mRNA. Neurons with somata positively stained for GAP-43 mRNA are very likely to be responsible for the increased GAP-43 immunostaining in boutons in the ipsilateral AVCN and fibers in the LSO. Recent experiments indicated that small neurons only in the medial, but not the lateral limb of the ipsilateral LSO dramatically up-regulated GAP-43 mRNA upon chronic EIS (Fig. 26A). In the entire contralateral LSO of the unstimulated side, no such GAP-43 mRNA up-regulation was detected and in situ hybridization signals remained at control levels (Fig. 26B). In all other auditory brainstem areas; the entire CNC, the rest of the SOC, the NLL, and the IC, stimulation-dependent up-regulation of GAP-43 mRNA was never detected.

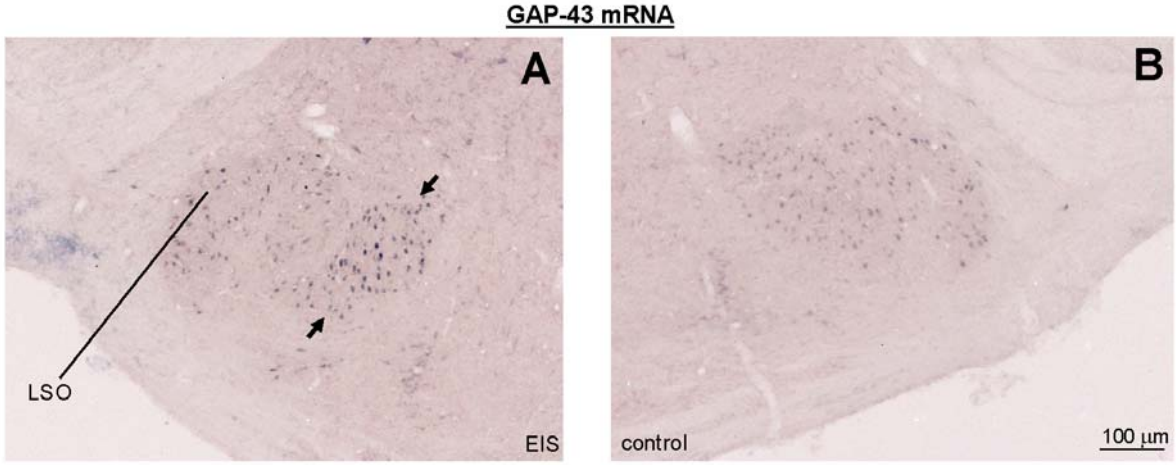

Figure 26: Detection of GAP-43 mRNA in the LSO by in situ hybridization. A: Increased levels of GAP-43 mRNA was detected only in small neuronal somata in the medial limb (arrows), but not in the lateral limb of the ipsilateral LSO upon EIS. B: GAP-43 mRNA levels remained at control levels in the entire LSO on the unstimulated side.

6. Discussion

6.1. Neuronal Cell Types in the Auditory Brainstem of the Adult Rat

With the first study, a wealth of data concerning molecular profiles related to connectional patterns of neurons in the auditory brainstem nuclei VCN, DCN, LSO, MSO, and CIC was obtained. The underlying concern was to associate the major morphological types of neurons in the auditory brainstem nuclei to an unequivocal pattern of molecular components present in their cell bodies.

6.1.1. Neuronal Sub-Populations in the Ventral Cochlear Nucleus

In the VCN, six main cell types are generally recognized: spherical bushy, globular bushy, octopus, multipolar type I, multipolar type II, and small cells. The most detailed studies on VCN cell types comes from the cat (Osen, 1969; Brawer et al., 1974), but there appeared to be no fundamental differences compared to the rat as reviewed (Malmierca, 2003). By position, size, and shape of their cell body, octopus cells in the rat were easily identified as CB positive (Friauf, 1994; Förster and Illing, 2000) glutamatergic neurons (Fig. 9, sub-population 2). Spherical bushy cells project to the ipsilateral LSO to provide excitatory input (cat: Harrison and Warr, 1962; rat: Friauf and Ostwald, 1988). Globular bushy cells also mediate excitation and project to the contralateral MNTB (cat: Harrison and Irving, 1965; rat: Alibardi, 1998b).

In accordance to a previous study (Alibardi, 1998b), I identified the glutamatergic sub-population that did not send axonal projections to the CIC as constituted by bushy cells (Fig. 9, sub-populations 1, 3ii, and 4). The data are inconclusive for distinguishing globular bushy cells from spherical bushy cells. However, it is known that the VCN of the rat contains a relatively small spherical bushy cell area and a comparatively large globular bushy cell area (for review c.p. Malmierca, 2003). Therefore it is suggested that the population of globular bushy cells is composed of CR positive neurons (Fig. 9, sub-population 4, 20%), together with either cells singly stained for glutamate (Fig. 9, sub-population 1, 5%) or the PV containing sub-population (Fig. 9, sub-population 3ii, 10%), representing 25-30% of all VCN

neurons. The spherical bushy cells would then represent the remaining sub-population of 5-10% of all VCN neurons.

Small multipolar type I neurons of the cat (Smith and Rhode, 1989) that are equivalent to planar cells in rat (Doucet and Ryugo, 1997) mainly project to the contralateral CIC, but some of them send their axons to the ipsilateral CIC (cat: Adams, 1979; Oliver, 1987; rat: Malmierca et al., 1999). Sub-population 3i (Fig. 9) was identified as multipolar type I neurons projecting to the contralateral CIC and sub-population 5i (Fig. 9) as multipolar type I neurons projecting ipsilaterally. Multipolar type I cells of the VCN were previously described to form excitatory presynaptic endings in the ipsilateral as well as in the contralateral CIC of the cat (Oliver, 1987). Multipolar type I neurons projecting to the contralateral CIC indeed contained glutamate, but not glycine as already suggested by a study performed in rat (Alibardi, 1998b). I showed here that multipolar type I cells sending their axons to the ipsilateral CIC were glycinergic and therefore probably mediate inhibition in the rat, whereas these cells might mediate excitation in the cat.

Glycinergic multipolar type II neurons (Doucet et al., 1999) connect the VCN to the VCN on the other side of the rhombencephalon in rat (Alibardi, 1998a) as well as in guinea-pig (Wenthold 1987) and mediate inhibition (guinea-pig: Shore et al., 1992; Babalian et al., 2002; rat: Alibardi, 1998a). Like all other glycinergic VCN neurons, the commissural cells representing sub-population 5ii (Fig. 9) always co-localized CR.

GABAergic VCN neurons with small somata (guinea-pig: Wenthold et al., 1986; Roberts and Ribak, 1987a) represented a sub-population of the small cells (Fig. 9, sub-population 6), always devoid of any CaBP. Another sub-population that was identified as small cells were the glycinergic neurons that projected neither to contralateral VCN nor to CIC (Fig. 9; sub-population 5iii).

6.1.2. Neuronal Sub-Populations in the Dorsal Cochlear Nucleus

In DCN, eight major morphological classes of neurons were recognized in previous studies (e.g. Osen, 1969). Excitation-mediating fusiform cells (cat: Oliver, 1985) that are mostly connected to the contralateral CIC (cat: Osen, 1972; Oliver, 1984; rat: Beyerl, 1978) displayed no immunoreactivity for GABA (rat: Mugnaini, 1985; guinea-pig: Wenthold et al., 1986) and glycine (Gates et al., 1996). DCN neurons singly stained for glutamate were

identified as medium-sized fusiform cells (Fig. 11, sub-population 1). Cells that co-localized glutamate and CB (Friauf, 1994; Förster and Illing, 2000) were identified as small fusiform cells (Fig. 11, sub-population 3). In both sub-populations of fusiform cells, half of the neurons projected to the contralateral CIC, while the other half did not. These findings indicate that only part of the DCN fusiform cells were connected to the CIC. The other part of the fusiform cell population possibly represents neurons that bypass the CIC and project directly to the medial geniculate body of the thalamus (Malmierca et al., 2002).

Granular and unipolar brush cells are glutamatergic neurons with small and round somata located in the DCN granular layer (Weedman et al., 1996; Mugnaini et al., 1997; Malmierca, 2003). Both of them were reported to be CR positive (Floris et al., 1994; Lohmann and Friauf, 1996), but negative for glycine (Mugnaini et al., 1994; Gates et al., 1996) and GABA (guinea-pig: Wenthold et al., 1986; rat: Mugnaini et al., 1994). By these criteria they were identified as sub-population 2 (Fig. 11).

Giant cells of the deep layer of DCN that project to the contralateral VCN (cat: Cant and Gaston, 1982; guinea-pig: Shore et al., 1992) as well as to the CIC (cat: Osen, 1972; Oliver, 1984; rat: Beyerl, 1978) represent sub-population 4 (Fig. 11). Giant cells are known to be CB positive in rat (Friauf, 1994; Förster and Illing, 2000) as well as glycine positive in cat (Adams, 1979), guinea-pig (Kolston et al., 1992), and rat (Alibardi, 2000).

Vertical or tuberculoventral cells are characterized by small somata that are located in the deep layers of the DCN (mouse: Zhang and Oertel, 1993; guinea-pig: Hackney et al., 1990) and were immunostained for glycine in guinea-pig (Saint Marie et al., 1991; Kolston et al., 1992). Soma size, position, and molecular profile indicate that they match sub-population 5 (Fig. 11).

Cartwheel cells at the boundary between granular and superficial cell layer displayed immunoreactivity for GABA as well as glycine (guinea-pig: Wenthold et al., 1987; cat: Osen et al., 1990; rat: Gates et al., 1996), were shown to act as inhibitory interneurons (guinea-pig: Wenthold et al., 1986), and correspond to sub-population 6 (Fig. 11).

Stellate cells of the superficial layer are GABA positive (Mugnaini, 1985) and contain PV (Lohmann and Friauf, 1996), suggesting that they match sub-population 7 (Fig. 11). These cells were described as glycinergic in mice (Wickesberg et al., 1994), but as glycine negative in rat (Gates et al., 1996). The data indicate that they do not stain for glycine.

Golgi cells were reported to be immunostained for GABA as well as glycine in guinea-pig (Kolston et al., 1992). Golgi neurons (Fig. 11, sub-population 8) were found to be singly stained for GABA, consistent with other studies showing that DCN neurons that were stained for GABA in rat (Mugnaini, 1985) and cat (Adams and Mugnaini, 1987), but are glycine negative in rat (Gates et al., 1996) are likely to be medium-sized Golgi cells.

6.1.3. Neuronal Sub-Populations in the Lateral Superior Olive

In the rat's LSO, seven different morphological classes of neurons were characterized by intracellular labeling studies (Rietzel and Friauf, 1998). Bipolar, multipolar, and banana-like cells form sub-groups of the large LSO principal neurons, whereas small multipolar cells, bushy cells, unipolar cells, and marginal cells have smaller somata and are less frequent. Neuronal somata containing CR were absent from the entire LSO as reported previously (Lohmann and Friauf, 1996).

Small CB positive cells (Celio, 1990; Friauf, 1993) always also contained glutamate but no other markers used (Fig. 12, sub-population 2). These neurons constituted one part of the newly identified descending pathway from the LSO to the ipsilateral VCN. The second part of this connection was mediated by glycinergic neurons (Fig. 12, sub-population 6). Various descending pathways heading for VCN originate in the SOC either ipsilaterally or contralaterally and were previously described in various species (cat: Elverland, 1977; guinea-pig: Ostapoff et al., 1990; Schofield, 1991; rat: Horváth et al., 2000), but none of them was reported to originate from neurons of the LSO. Neurons of the LOC system project to the ipsilateral cochlea (cat: Warr, 1975; rat: Horváth et al., 2000). The neurons projecting to the ipsilateral VCN were with a mean diameter of 5.2 ± 0.2 μm (ranges: 5.9 – 4.2 μm) significantly (***$p < 0.001$) smaller than LOC neurons of 6.3 ± 0.2 μm (ranges: 9.1 – 4.2 μm) mean diameter. Since LOC neurons consist of a GABAergic and a cholinergic subset (Aschoff and Ostwald, 1988; Vetter et al., 1991), but the cells projecting to VCN were glutamatergic and glycinergic, they could therefore not be LOC neurons that picked up tracer from the injection site in VCN as passing fibers. Since no other LSO neurons are known to be GABAergic, I suggest that sub-population 7 (Fig. 12) constitutes LOC neurons. These GABAergic cells with a mean soma size of 6.8 ± 0.2 μm were not significantly larger ($p =$

0.051) than LOC neuronal somata of 6.3 ± 0.2 μm mean diameter, stained after tracer application to the cochlea.

The glutamatergic sub-population of cells projecting to VCN was positively stained for CB. In previous reports (Friauf, 1993; Förster and Illing, 2000), small neurons immunostained for CB were already observed in the LSO, but in none of these studies they were related to LOC neurons. Further support for the finding, that the CB positive LSO cells could not be LOC neurons comes from the observation that no CB positive fibers were observed beneath the inner hair cells of the cochlea where the axons of LOC neurons terminate (data not shown). Clear and multiple evidence for a pathway to the VCN originating in the ipsilateral LSO is provided in this study. Why this pathway was not observed previously remains unclear. Since LSO neurons sending their axons to the ipsilateral VCN were of relatively small size and only few in number, it might be possible that they were overlooked in previous studies.

Principal cells of the LSO projecting to the CIC (cat: Elverland, 1978; Shneiderman and Henkel, 1985; rat: Kelly and Li, 1997) always expressed PV (Fig. 12, sub-populations 3, 4, 5). The projection to the contralateral CIC (Fig. 12, sub-populations 3, 4i) rests on glutamatergic, and therefore excitatory, principal cells (guinea-pig: Saint Marie and Baker, 1990). The projection to the ipsilateral CIC (Fig. 12, sub-populations 4ii, 5) was mostly glycinergic and therefore inhibitory (guinea-pig: Saint Marie and Baker, 1990; rat: Kelly and Li, 1997). Additionally, there is an uncrossed projection that is neither glycinergic nor GABAergic and probably excitatory. These findings neatly correspond to previous observations. A glutamatergic sub-population of principal neurons projecting to the contralateral CIC as well as a glycinergic sub-set of cells that project to the ipsilateral CIC was identified. No connections to the ipsilateral CIC that were singly stained for glutamate were detected, but the number of neurons co-localizing glutamate with glycine was clearly higher for the uncrossed than for the crossed projection.

6.1.4. Neuronal Sub-Populations in the Medial Superior Olive

The MSO of the rat is small and has not been considered previously in detail. In the cat, the probably excitatory MSO neurons project mainly to DNLL (Oliver and Shneiderman, 1989) and CIC (Henkel and Spangler, 1983) on the ipsilateral side. I showed in this studies that the neurons of the rats MSO were all glutamatergic and project mainly to the ipsilateral CIC, with the possibility of axon collaterals reaching DNLL as well. These neurons were to some part positive for PV (Fig. 13, sub-population 2), to some part not (Fig. 13, sub-population 1). How these two different sub-populations differ in their physiology could not be determined in this study. Few glutamatergic and PV positive MSO neurons send their axon to the CIC on the contralateral side.

6.1.5. Neuronal Sub-Populations in the Central Nucleus of the Inferior Colliculus

The CIC is characterized by disc-shaped and stellate cells of various sizes, or by smaller flat and larger less flat neurons. As reviewed by Malmierca (2003), the largest neuronal sub-population in CIC is immunopositive for glutamate, probably flat cells (Merchan et al., 2005), exclusively singly stained in my experiments (Fig. 14, sub-population 1). Flat cells of the CIC were shown to be GABA negative and to have smaller somata than GABAergic less flat cells (Merchan et al., 2005).

In the rat CIC, stellate cells of different size, but also medium sized disc-shaped neurons are GABAergic (Roberts and Ribak, 1987b), estimated to make up about one third of the total population of neurons in CIC (guinea-pig: Thompson et al., 1985; rat: Merchan et al., 2005). The counts of these studies corresponded very well with the finding of 35% GABAergic neurons, represented by the sub-populations 2 and 3 (Fig. 14) which were identify as less-flat cells (Merchan et al., 2005) in this study. An important detail of these data not described before was the co-expression of PV in all GABAergic CIC neurons. This is noteworthy since GABAergic neurons never co-localized with any of the CaBPs in VCN and LSO. In DCN, GABAergic stellate cells, but not cartwheel and Golgi cells, contained PV.

For the first time, I found glycine positive neuronal somata in the CIC, some of which also contained GABA (Fig. 14, sub-population 3) but others did not (Fig. 8, sub-population 2). A previous study did not mention glycine-containing neuronal cell bodies in the rat (Merchan et al., 2005). In this study, brain slices were postfixed and were therefore harder to penetrate for the antibodies. It might be, that the antibody only recognized synaptic terminals where glycine is higher concentrated than in the soma. To assess the selectivity of the immunoreactivity in this study, the investigators compared structures of known immunostaining patterns. This was done only for GABA, but not for glycine and the investigators showed no prove that their antibody was able to label glycinergic neuronal somata in the rat brain. However, considering the specific glycine staining in other areas investigated here, that match the findings of several studies published previously, I felt confident about the dependability of this finding. In this study, multipolar type II neurons of the VCN (Alibardi, 1998a; Doucet et al., 1999), giant cells (Alibardi, 2000) and cartwheel cells (Gates et al., 1996) of the DCN, a sub-population of LSO principal cells (Kelly and Li, 1997), and neurons of the MNTB (Kulesza and Berrebi, 2000) were identified as glycinergic.

In the dorsal and external cortex of the IC, cell bodies that were stained for CR or CB were encountered at high densities, but such cells were seen only sporadically in CIC. This was consistent with previous work reporting a complementary distribution of PV immunoreactive somata compared with CR (Lohmann and Friauf, 1996) and CB immunoreactive cells (Friauf, 1994) in various collicular sub-regions. Therefore, neither CR nor CB positive neurons constitute major neuronal sub-populations in the CIC.

6.1.6. Overview Over the Identified Neuronal Cell Types

The goal of this study was to relate established morphologically characterized neuronal cell types of the rat auditory brainstem to their molecular and connectional profile. This goal was achieved. A near-complete list of this morpho-molecular matching (Table 1) is provided here. Several findings from previous studies in the rat were confirmed, showing the specificity of the methods that were used here. Other data were obtained previously from different species, especially cat and guinea-pig. Even in a recent review about the structure and physiology of the rat auditory system (Malmierca, 2003), several major points feature only work from these two species, but not from rat. It was shown that most, but not all,

findings from cat and guinea-pig can be transferred to rat. Beneath that, I obtained data that have not been presented in previous studies, neither in rat, nor in other species. First, multipolar type I cells of the VCN projecting to the ipsilateral CIC exhibited glycine immunoreactivity. Second, a descending pathway of the SOC to the ipsilateral VCN that was not described before was discovered. Third, glycine positive neurons do occur in the CIC. Finally, GABAergic neurons of the CIC always co-localize PV.

Table 1
Matching of morphological cell types and molecular sub-populations in the rat auditory brainstem

	morphological cell type	molecular sub-population	markers	projections
VCN (Fig. 9)	globular bushy	4, 1 or 3ii	Glu + CR, Glu or Glu + PV	SOC[a]
	spherical bushy	3ii or 1	Glu + PV or Glu	SOC[a]
	octopus	2	Glu + CB	SOC, VNLL[a]
	multipolar type I	3i, 5i	Glu + PV, Gly + CR	CIC
	multipolar type II	5ii	Gly + CR	VCNc
	small	5iii, 6	Gly + CR, GABA	?
DCN (Fig. 11)	fusiform	1 (medium-sized)	Glu	CICc, ?
	fusiform	3 (small-sized)	Glu + CB	CICc, ?
	granule	2	Glu + CR	Interneuron[a]
	unipolar brush	2	Glu + CR	?
	giant	4	Gly + CB	VCNc, CIC
	tuberculoventral	5	Gly	VCNi[a], ?
	cartwheel	6	Gly + GABA	Interneuron[a]
	stellate	7	GABA + PV	Interneuron[a]
	Golgi	8	GABA	Interneuron[a]
LSO (Fig. 12)	principal	3, 4, 5	Glu + PV, Glu + Gly + PV, Gly + PV	CIC
	lateral olivocochlear	7	GABA	Cochlea[a]
	VCN projecting	2, 6	Glu + CB, Gly	VCNi
MSO (Fig. 13)	principal	1, 2ii	Glu, Glu + PV,	CICi, DNLL[a]
	-	2i	Glu + PV	CICc
CIC (Fig. 14)	flat	1	Glu	?
	less-flat	3, 4	GABA + Gly + PV, GABA + PV	?

[a] according to previous studies, see Discussion. Glu = glutamate, Gly = glycine, PV = parvalbumin, CR = calretinin, CB = calbindin-D28k, VNLL = ventral nucleus of the lateral lemniscus

6.2. Activity-Dependent Immediate Early Gene Expression in Distinct Neuronal Sub-Populations After Acute EIS

There has been a vigorous dispute on what an increased expression of c-Fos signifies. Contrary to the earlier understanding, the increased presence of c-Fos in a particular neuron cannot be taken as evidence for its particular high electrophysiological activity. The local and cellular mismatch between stimulation-dependence of c-Fos expression and 2-desoxyglucose uptake (Duncan et al., 1993; Reimer, 1993; White and Price, 1993; Kearney et al., 1997) indicates that these markers monitor neuronal activity on different levels. The finding that spiral ganglion cells altogether failed to express c-Fos despite their effective driving of other neurons to do so is striking evidence against equating c-Fos expression with electrophysiological activity. Instead of reflecting spiking intensity, emergence of c-Fos may rather be implied in intracellular signal cascades triggered to induce a remodeling of the affected neuron.

A widely occurring type of activity-dependent neuronal plasticity is known as LTP. It consists of a persistent functional modification that includes an increased synaptic strength (Bliss and Lomo, 1973) and involves the interaction of a large variety of molecular players. Several transcription factor coding IEGs are involved in signaling cascades crucial for the induction and/or maintenance of LTP, and up-regulation of c-fos and egr-1 mRNA is related to the stimulation-dependent synaptic enhancement (Cole et al., 1989). Whereas egr-1 mRNA is already strongly transcribed upon stimuli near the threshold of LTP induction, c-fos mRNA requires a stronger stimulation for being recruited in the processes of synaptic remodeling (Worley et al., 1993). Many studies (Kaczmarek, 1992; Demmer et al., 1993; Jones et al., 2001; Fleischmann et al., 2003) imply that strong stimulation evokes different signaling events than weak stimuli do. It was shown that inhibition of c-fos mRNA expression prevented egr-1 expression (Dragunow et al., 1994; Yasoshima et al., 2006).

The expression of both c-Fos and Egr-1 was found to be up-regulated along the ascending auditory system in regions tonotopically corresponding to the intracochlear site of stimulation (Illing and Michler, 2001; Illing et al., 2002). Under the stimulation conditions used here, Egr-1 immunoreactivity was always co-localized with c-Fos immunostaining, indicating that neuronal activation by EIS was well above threshold for induction of activity-dependent plasticity.

6.2.1. IEG Up-Regulation in the Spiral Ganglion of the Cochlea

Induction of IEGs in cochlear spiral ganglion neurons has been seen to occur upon acoustic overstimulation (Cho et al., 2004) or EIS at very high levels (Saito et al., 2000). In my experiments, the absence of EIS-induced IEG expression in the cochlea corresponded to the moderate ABR response elicited, indicating a physiological level of stimulation. As a consequence, stimulation-dependent IEG up-regulation was only seen in distinct regions of the auditory brainstem. For instance, IEG positive nuclei were not observed in the ventral superior olive and MSO. Within the affected areas, only individual neuronal sub-populations related to specific axonal projection systems responded with IEG up-regulation to the unilateral patterned sensory input (Fig. 26).

6.2.2. IEG Up-Regulation in the Ventral Cochlear Nucleus

In VCN, only two of six neuronal sub-populations characterized by their profile of molecular markers responded to EIS with c-Fos expression. Fifty percent of all c-Fos positive cells in VCN were glutamatergic. Half of these, and 25% of the total, were identified by their axonal destinations to be multipolar type I neurons projecting to the contralateral CIC (Fig. 26). The remaining 25% must have been bushy cells, because CB positive octopus cells were never found to express c-Fos, consistent with a previous study (Saint Marie et al., 1999b). Bushy cells split up in spherical and globular bushy cells. Both types of bushy cells are specialized for the transmission of temporal information essential for the binaural computation of sound localization (Young et al., 1988).

Inhibitory glycinergic multipolar type I neurons projecting to the ipsilateral CIC and commissural multipolar type II neurons (Shore et al., 1992; Doucet et al., 1999) together comprised 35% of the total c-Fos population induced by EIS (Fig. 17). However, as I also found c-Fos in glycinergic cells other than type I and type II neurons these may belong to glycinergic interneurons and may mediate subtle side band inhibition (Wu and Oertel, 1986), or they belong to glycinergic cells projecting to the ipsilateral DCN, possibly enhancing the spectral contrast sensitivity of the targeted DCN neurons (Doucet et al., 1999). By sharp contrast, GABAergic neurons that comprise a recognizable share of VCN interneurons were never seen to express c-Fos in a stimulation-dependent manner.

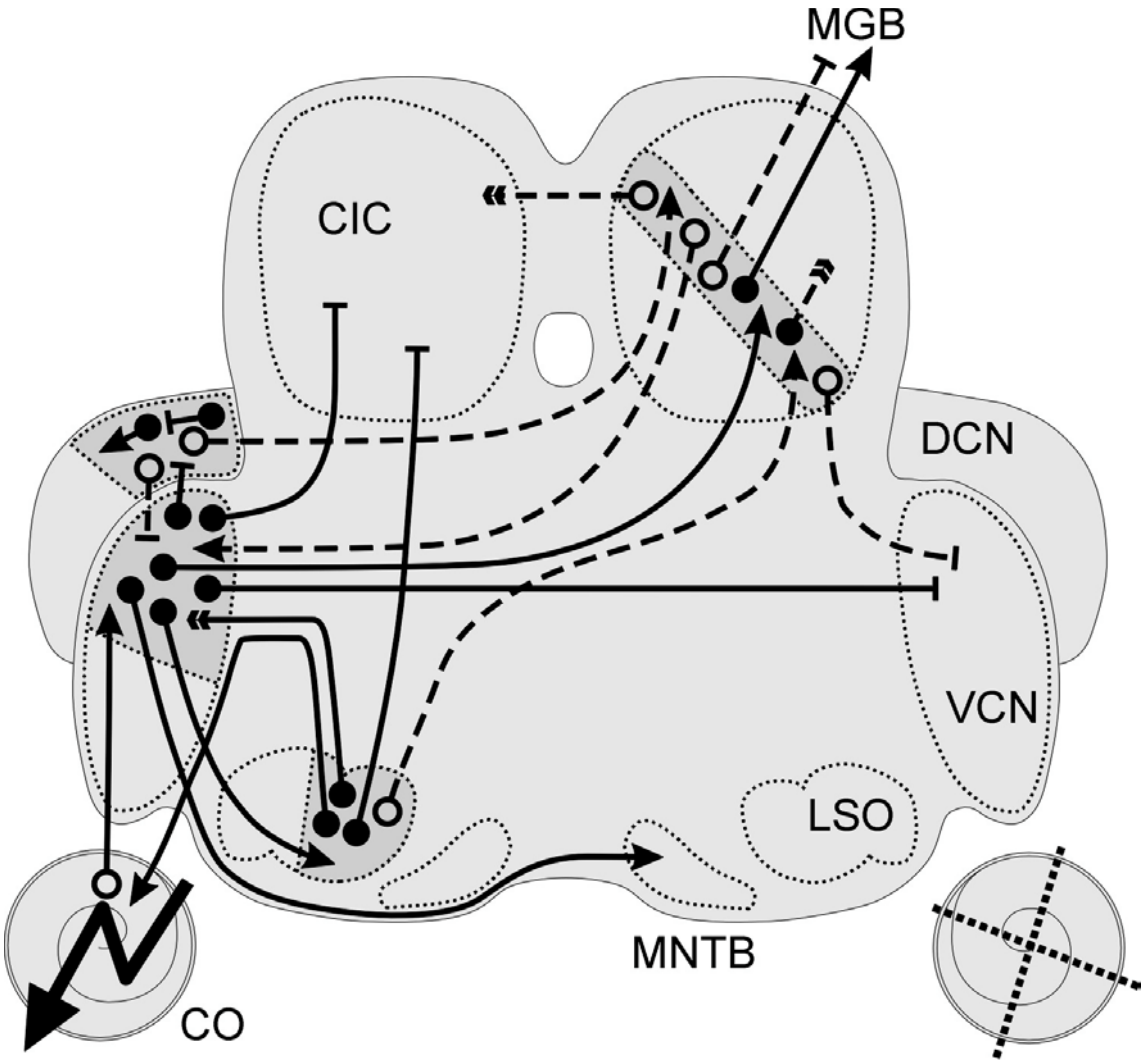

Figure 27: The set of auditory brainstem projections that were selectively affected by c-Fos expressed upon EIS. Expression of c-Fos corresponded tonotopically to the intracochlear position of the stimulation electrode (dark gray areas). Excitatory neurons that project to higher order auditory areas (arrows) exhibited IEG positive nuclei (solid circles, continuous lines) in the VCN and in CIC but not in DCN and LSO. From VCN, an inhibitory (T-shaped end) commissural pathway arises that also responded with c-Fos expression. In the DCN, only interneurons, excitatory as well as inhibitory, responded to unilateral EIS. In the LSO, inhibitory cells projecting to the ipsilateral CIC, but also neurons sending their collaterals downstream to lower auditory centers, up-regulated IEGs upon EIS. From CIC, a glutamatergic projection ascends to the MGB of the diencephalon that developed c-Fos immunoreactivity. Altogether, excitatory pathways of the ascending auditory system originating in the stimulated ear as well as inhibitory pathways extenuating pathways serving the unstimulated ear expressed c-Fos.

6.2.3. IEG Up-Regulation in the Dorsal Cochlear Nucleus

In the ipsilateral DCN, only three of eight neuronal cell types that were identified by their molecular marker profile showed IEG positive nuclei. Fifty percent of the IEG expression was restricted to cartwheel cells that colocalize GABA with glycine and act as inhibitory interneurons (Wenthold et al., 1986; Golding and Oertel, 1996; Zhang and Oertel, 1994).

Since fusiform and giant cells projecting to the CIC as well as vertical cells that send their axons to VCN never responded with IEG expression to EIS, it was concluded that the remaining half of IEG positive nuclei was mainly, if not completely, also expressed in interneurons. 20% of the IEG positive nuclei were found in glutamatergic medium sized fusiform cells, and I identified CB positive neurons that upregulated IEGs upon EIS as small fusiform cells, neither of which forming connections to CIC. These neurons must either act as excitiatory interneurons, or they may project directly to the MGB (Malmierca et al., 2002). Although it was recently shown that the threshold for sound-induced c-Fos activation in granule cells is lower than in other DCN neurons (Yang et al., 2005), there were no c-Fos positive granule cells in the study. This discrepancy suggests that granule cells may have a greater vulnerability towards anesthesia, or, alternatively, that the specific acoustic and electrical modes of stimulation elicit different programs of gene activation in these auditory neurons.

6.2.4. IEG Up-Regulation in the Lateral Superior Olive

In LSO, glycinergic principal cells that form an inhibitory projection to the ipsilateral CIC, but not glutamatergic principal neurons that form an excitatory ascending pathway to the contralateral CIC (Glendenning and Baker, 1988), responded to the EIS with IEG up-regulation (Fig. 27). Additionally, activity-dependent IEG expression was detected in neurons that form descending connections. Glutamatergic as well as glycinergic neurons that project back to ipsilateral VCN each comprised 35% of the c-Fos expressing cells.

Another countercurrent pathway originating from the LSO is build by LOC neurons that send their axon collaterals to the inner spiral bundle to terminate beneath the IHCs in the ipsilateral cochlea (Warr and Guinan, 1979; Warr et al., 1997; Horváth et al., 2000). LOC

neurons consist of two chemically distinct sub-populations, a GABAergic and a cholinergic subset (Vetter et al., 1991) and two functional subsets of LOC neurons are known. One subset mediates suppression, the other sub-population elicits enhancement of cochlear neuronal responses (Groff and Liberman, 2003). It seems likely that GABAergic neurons mediate inhibition, probably to protect the auditory system from overstimulation, whereas the neurotransmitter acetylcholine could cause excitation in cochlear cells. In tracing studies it was observed that LOC neurons responded with stimulation-dependent IEG expression to EIS, as previously suggested (Adams, 1995), but IEG up-regulation was never found in GABAergic neurons. It was therefore concluded that only cholinergic LOC cells displayed activity-dependent IEG up-regulation. This is consistent with the physiological ABR response and the lack of EIS-mediated IEG expression in spiral ganglion neurons and indicates that no over-stimulation the system occurred, forcing it to protect itself by turning down cellular excitation on cochlear systems.

6.2.5. IEG Up-Regulation in the Central Nucleus of the Inferior Colliculus

Only half of the neuronal sub-sets identified by their profile of molecular markers showed IEG up-regulation upon stimulation in CIC. 50% of EIS-dependent IEG expression were detected in glutamatergic neurons. Glutamatergic CIC neurons mainly form commissural projections (Saint Marie, 1996; Zhang et al., 1998) or send their axons to the ipsilateral MGB of the thalamus (Calford and Aitkin, 1983; Malmierca, 2003). Neurons that form connections to the contralateral CIC were devoid of activity-dependent IEG up-regulation. Therefore, the glutamatergic cells expressing IEGs upon EIS must have been neurons projecting towards the thalamus (Fig. 27).

There is also a GABAergic population of neurons projecting to the MGB (Winer et al., 1996; Peruzzi et al., 1997) and another forming collaterals to the contralateral CIC (Gonzalez-Hernandez et al., 1996; Malmierca et al., 2005). Under different circumstances, GABAergic cells in CIC prove to be capable of expressing c-Fos (Ishida et al., 2002). However, with the stimulation set-up and settings used here, the large population of GABAergic neurons in CIC never up-regulated IEGs. I ascribed the remaining 50% of non-glutamatergic cells expressing IEGs to specific cellular subsets of the many CIC interneurons (Osen, 1972).

6.2.6. Functional Relevance of Stimulation-Dependent IEG Expression

In the study presented here, it was shown that only distinct neuronal sub-populations of the auditory brainstem neurons respond within two hours EIS of specific strength and temporal structure (Reisch and Illing, 2005). The response consisted of IEG expression that is not straightforwardly related to spiking activity but probably to an initial phase of longer-term modifications of neurons and their synapses. The affected neurons were found to constitute excitatory pathways related to the stimulated side, as well as inhibitory projections reaching to neurons and pathways serving the unstimulated side of the auditory brainstem (Fig. 27). Increase in synaptic efficacy of the affected pathways would entail strengthened excitation of the stimulated side, while the signaling in the unstimulated side appears to be actively extenuated (Illing and Reisch, 2006). Therefore, the early phase of plastic remodeling studied here appears to initiate processes that would, if completed, result in a readjustment of auditory brainstem networks to account for the changed pattern of sensory activation and to optimize the exploitation of the now-available resources.

6.3. GAP-43 and PSA-NCAM Mediate Synaptic Rearrangements in the Adult Auditory Brainstem Upon Chronic EIS

Unilaterally increased or decreased hearing intensity entails specific molecular and morphological changes in the central auditory system (Illing and Reisch, 2006). So far, experiments on deafening and stimulation operated on different time scales. Re-expression of GAP-43 is observed seven days after induced deafness (Illing et al., 1995; 1997) while up-regulation of IEG transcription factors such as c-Fos occurs upon two hours of EIS (Illing and Michler, 2001; Illing et al., 2002). While it is well established that LTP activates IEGs encoding transcription factors (Cole et al., 1989; Wisden et al., 1990), there is no evidence indicating what target genes are directly activated by these transcription factors. C-Fos may dimerize with c-Jun to form the AP-1 transcription factor complex (Halazonetis et al., 1988; Wisdom, 1999) which can bind to the promoter region of the GAP-43 gene (de Groen et al., 1995). Therefore, GAP-43 is a prospering candidate molecule to be induced in c-Fos expressing cells. Overexpression of GAP-43 dramatically enhances learning and LTP

(Routtenberg et al., 2000) and induces nerve sprouting in the adult nervous system (Aigner et al., 1995). GAP-43 protein is found in the auditory brainstem of the rat exclusively in developing animals (Horváth et al., 1997) and therefore its re-expression in the adult is indicative for ongoing plasticity (Gispen et al., 1991; Aigner et al., 1992; Kruger et al., 1993; Alonso et al., 1997). GAP-43 expression is often associated with PSA-NCAM (Bonfanti et al., 1992; Benowitz and Routtenberg, 1997) exhibiting remarkable capacities for morphological plasticity in these particular brain areas. Removal of PSA from the NCAM molecule leads to impairment of LTP (Becker et al., 1996; Muller et al., 1996; Eckhardt et al., 2000) underlining the importance of PSA-NCAM for activity-dependent plasticity. To investigate stimulation-dependent plasticity beyond IEG expression, chronic EIS lasting seven days was performed.

6.3.1. Expression of GAP-43 and PSA-NCAM in the Anteroventral Cochlear Nucleus

After seven days of EIS, up-regulation of GAP-43 and PSA-NCAM was observed in the ipsilateral AVCN. Interestingly, both molecules were expressed in the entire AVCN and not only in the dorsal area, tonotopically corresponding to the basal cochlea where the stimulating electrode was placed. After two hours of EIS, c-Fos up-regulation was restricted to dorsal AVCN, while ventral AVCN was always devoid of IEG expression upon basal stimulation of the cochlea (see above; Illing et al., 2002). After chronic EIS, GAP-43 was never observed in cell bodies, but restricted to fibers and boutons that formed characteristic ring-like structures around neuronal somata (Fig. 28A), as observed after cochleotomy (Illing et al., 1997; 2005). From electron microscopic studies, it is known that GAP-43 is expressed in presynaptic terminals and neuronal growth cones, seven days after cochleotomy-induced deafness (Illing et al., 2005; Meidinger et al., 2006). Light microscopic analysis at high magnifications indicated that GAP-43 expression after chronic EIS was also restricted to presynaptic structures. If GAP-43 was restricted to already existing presynaptic endings which underwent structural rearrangements, or weather it was also expressed in growth cones of newly forming synapses and outgrowing axons upon EIS remains to be determined by ultrastructural analysis.

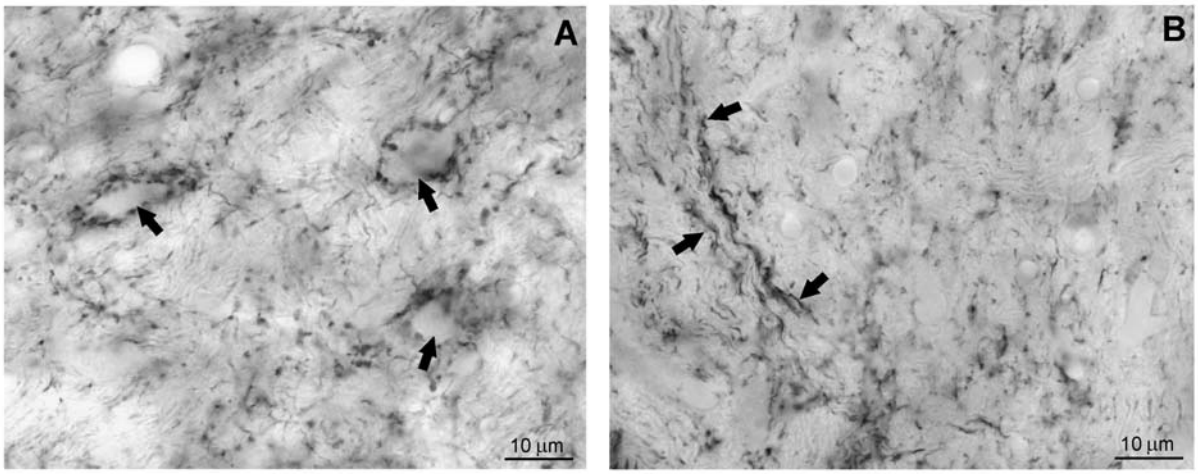

Figure 28: High-magnification images of GAP-43 immunostainings. A: In AVCN, GAP-43 was located in boutons forming characteristic ring-like structures around GAP-43 negative neuronal somata (arrows). B: LSO was devoid of GAP-43 stained ring-like presynaptic structures, but GAP-43 was found to be located in fibers (arrows).

In Hippocampus, only granule cells receiving direct input from perforant path, but not mossy cells in dentate gyrus express c-Fos mRNA (Dragunow et al., 1989; Jeffery et al., 1990; Worley et al., 1993), Fos-related proteins (Demmer et al., 1993), and Egr-1 mRNA (Cole et al., 1989; Wisden et al., 1990; Richardson et al., 1992) upon LTP-inducing stimulation. Mossy cells receive major excitatory input from granule cells (Scharfman et al., 1990) and express GAP-43 mRNA three days after LTP-inducing perforant path stimulation (Namgung et al., 1997). This increase is positively correlated with the level of enhancement and restricted to mossy cells on the side of the stimulation, while granule cells are devoid of GAP-43 mRNA. Mossy cell axons form synapses on granule cells. The study shows that GAP-43 is not increased in neurons expressing IEGs upon stimulation, but in neurons synapsing on such IEG up-regulating cells in hippocampal dentate gyrus. Similarly, in AVCN GAP-43 positive presynaptic endings connect to neurons expressing IEGs upon acute EIS. Most likely, these AVCN neurons do not up-regulate GAP-43 after chronic EIS. However, so far there is no explanation why GAP-43 positive boutons occur throughout whole AVCN and are not restricted to the dorsal area, to which IEG up-regulation was restricted.

PSA-NCAM was locally correlated with GAP-43 in the same area, but co-expression in the same structures was not observed. GAP-43 was located in fibers and boutons, whereas PSA-NCAM occurred in and possibly on the surface of neuronal cell bodies in AVCN. PSA appears to be synthesized in a conventional manner in the Golgi (Scheidegger et al., 1994) and PSA-NCAM can then be rapidly translocated to the cell surface via regulated exocytosis (Kiss et al., 1994). Suggestions are that PSA-NCAM was located in postsynaptic structures corresponding to GAP-43 expressing presynaptic boutons. Deadhesive properties of PSA-NCAM (Rutishauser et al., 1988; Rutishauser and Landmesser, 1996) would promote remodeling of those synapses where GAP-43 is responsible for presynaptic structural plasticity. Expression of PSA-NCAM in only those cells that up-regulated c-Fos upon two hours of EIS could be excluded by the locally uncorrelated expression. C-Fos was restricted to the dorsal AVCN tonotopically corresponding to stimulation in the basal cochlea, whereas PSA-NCAM positive cells were observed in the entire AVCN.

6.3.2. Expression of GAP-43 and PSA-NCAM in the Dorsal and Posteroventral Cochlear Nucleus

GAP-43 and PSA-NCAM were both not increased upon chronic stimulation but remained at control levels in DCN and PVCN. After cochleotomy, GAP-43 (Illing et al., 1995; 1997) and PSA-NCAM (unpublished data) are both increased in these two nuclei after survival times of seven days. Upon cochleotomy, GAP-43 expression in CNC depends on MOC neurons from contralateral VNTB (Kraus and Illing, 2004). Auditory nerve fibers from the cochlea are axotomized, degenerate, and therefore presynaptic terminals of the auditory nerve disappear from CNC. Corresponding postsynaptic structures are “empty” now, and presynaptic auditory nerve terminals could be “replaced” by MOC collaterals (Illing et al., 2005). After cochleotomy synaptic plasticity possibly has the purpose of compensating ill-balanced hearing, achieved by rewiring neurons of the entire CNC (Kraus and Illing, 2004; Illing and Reisch, 2006). After chronic EIS, the auditory nerve is still intact as shown by unchanged CR staining (Fig. 22D) and therefore, there is neither space nor need for “novel” MOC synapses in CNC. After seven days of chronic stimulation, only AVCN was affected by structural rearrangements mediated by GAP-43 and PSA-NCAM, although the entire CNC responded with IEG expression to acute EIS of two hours (see above, Illing et al., 2002).

There may be two possible explanations for this observation. First, structural rearrangements might have occurred on different time scales in AVCN compared to the rest of the CNC. Rewiring might either have occurred earlier and therefore molecules mediating structural plasticity were already down-regulated to control conditions after seven days. Alternatively, structural rearrangements in DCN and PVCN were delayed compared to AVCN and will occur later. Second, activity-dependent synaptic plasticity in CNC was completely restricted to AVCN. Since stimulation-dependent up-regulation of IEG transcription factors occurred in the whole CNC after two hours, it seems very likely that structural rearrangements triggered by these transcription factors will also occur in the same time window throughout whole CNC. These findings strongly favor the second explanation indicating that processes directed fundamentally different occur upon increased or decreased sensory activation.

6.3.3. Expression of GAP-43 and PSA-NCAM in the Lateral Superior Olive

GAP-43 and PSA-NCAM showed uncorrelated activity-dependent regulation in LSO upon chronic EIS for seven days. Up-regulation of GAP-43 was restricted to the medial limb in the ipsilateral LSO, corresponding to the basal cochlea where stimulation occurred. Similar to AVCN, increased GAP-43 expression was never observed in cell bodies. In LSO, GAP-43 immunoreactivity was restricted to fibers, but characteristic ring-like staining pattern was missing here (Fig. 28B), indicating that GAP-43 positive presynaptic terminals were restricted to AVCN. PSA-NCAM remained at control levels in ipsilateral LSO upon stimulation, but was decreased in the medial limb of the contralateral LSO. This uncorrelated up-regulation of GAP-43 and PSA-NCAM in LSO is indicative that different processes occured in AVCN and LSO on the stimulated side upon EIS. AVCN synapses, where PSA-NCAM is possibly located at the postsynapse face to face with GAP-43 expressing presynaptic boutons, are very like to undergo structural plasticity. Missing PSA-NCAM up-regulation in LSO suggested that no synaptic rearrangements occurred here. Increased GAP-43 staining might be due to immunoreactive fibers of LSO neurons where GAP-43 was transported towards presynaptic endings in ipsilateral AVCN. PSA-NCAM was significantly decreased ipsilaterally in the medial LSO upon chronic EIS, which might be associated with decreased synaptic efficacy (Bouzioukh et al., 2001).

In neurons poised to survive their axotomy, c-Jun is often co-expressed with GAP-43 (Schmitt et al., 1999), as LOC neurons do after cochleotomy (Kraus and Illing, 1998; 2005). LOC neurons exhibit GAP-43 immunoreactivity upon cochleotomy, but they are not the source of GAP-43 staining in ipsilateral CNC (Illing et al., 2005). MOC neurons of VNTB have immunonegative somata for GAP-43 protein, but are positively stained for GAP-43 mRNA (Illing et al., 1999) and were shown to be the source of GAP-43 positive synaptic boutons in CNC upon cochleotomy. After chronic EIS, LSO was devoid of GAP-43 positive LOC neurons, clearly showing that these cells were not axotomized, since the auditory nerve was not injured or degenerated. This observation is highly suggestive that fundamental different processes of structural synaptic rearrangements occur upon increased or decreased hearing intensity. Missing GAP-43 immunoreactive cell bodies in SOC does not exclude the SOC to be the source of GAP-43 positive boutons in AVCN. In situ hybridization experiments indeed indicated that small neurons in the medial limb of the ipsilateral LSO dramatically up-regulated GAP-43 mRNA upon chronic EIS. It is very likely that these LSO neurons responding with GAP-43 mRNA up-regulation to chronic EIS are those cells, which form the newly discovered descending pathway to the ipsilateral VCN (Reisch and Illing, in preparation), since they corresponded in size, shape, and location. This up-regulation of GAP-43 mRNA upon chronic EIS in the LSO neurons projecting to the ipsilateral VCN perfectly fits to the detection of increased GAP-43 immunostaining in boutons of the AVCN and in fibers in the medial limb of the LSO on the stimulated side. These findings are highly suggestive that GAP-43 protein was expressed in small LSO neurons and was rapidly transported to the presynaptic terminals of these neurons in the AVCN to execute its function in stimulation-dependent synaptic rearrangements.

Furthermore, these particular LSO neurons responded with c-Fos expression to acute stimulation. To my knowledge, this is the first and so far only observation that the same neurons which expressed c-Fos immediately after stimulation also up-regulated GAP-43, a longer time period after stimulation. Of course, these findings have to be proven by further experiments. Identification of the responding neuronal sup-population could by further verified by combining in situ hybridization against GAP-43 mRNA with immunostaining against CB after seven days of chronic EIS. Chronic stimulation might not be combined with tracer injection into VCN since both procedures are already difficult and long-lasting operations for their own. In situ hybridization against GAP-43 mRNA should also be combined with immunostaining against c-Fos to verify if the same individual cell really up-

regulated both molecules upon electrical stimulation. Here, the time window for chronic EIS should be reduced, since c-Fos expression was no more detected after seven days of stimulation.

6.3.4. Activity-Dependent Plasticity Mediated by Chronic EIS

By switching from two hours of EIS in the anesthetized animal to chronic stimulation for seven days in the awake an freely behaving animal, activity-dependent plasticity beyond IEG up-regulation was detected. Specific plastic responses of the auditory brainstem to unilaterally decreased or increased hearing intensity (Illing and Reisch, 2006) now operate on the same time scale. Although the same molecules GAP-43 and PSA-NCAM mediate plasticity after cochleotomy and stimulation, the processes are directed fundamentally different. The thesis provides evidence that presynaptic terminals of small LSO cells synapsing on AVCN neurons underwent structural plasticity upon seven days of stimulation. It is very likely that these LSO neurons up-regulating GAP-43 upon chronic EIS lasting seven days also up-regulated c-Fos upon acute EIS of two hours. This is a strong and to my knowledge the first hint that c-Fos indeed activates the gap-43 gene, possibly via the AP-1 transcription factor complex, after stimulation in vivo. However, c-Fos seems not to induce the gap-43 gene in all neurons where it was expressed after acute EIS, since GAP-43 mRNA was never detected in neurons of CNC and CIC. The factors and circumstances which led distinct c-Fos expressing neurons up-regulate GAP-43, while others did not remain to be determined in further studies.

6.4. Main Conclusions

A large variety of neuronal cell types exists in the central nuclei of the auditory brainstem. In this thesis, six of the most relevant neuronal markers were linked to these different morphological cell types, partially identified by their connections and a previously unrecognized pathway was discovered: Small neurons of the superior olive send their axons towards the lower-order auditory center of the cochlear nucleus. Identification of these

specific neuronal cell types will contribute to a better understanding of both physiological and anatomical observations.

Novel sensory inputs may induce plastic reconstruction processes of adult neuronal communication networks. Activity-dependent plasticity was induced here by acute electrical stimulation of the auditory nerve in the cochlea and the affected neurons were related to the previously identified specific neuronal cell types. In total, less than 50% of the identified neurons turned up expression of immediate early gene transcription factors, which served as markers for these stimulation-dependent plastic changes. One of the neuronal cell types that were affected, were the small neurons of the superior olive forming the newly identified descending projection to the cochlear nucleus. The immediate early gene expression pattern in the auditory brainstem, caused by unilateral stimulation, suggests that novel sensory activity may quickly initiate a facilitation of central pathways serving the active ear at the expense of those serving the unstimulated ear.

Immediate early gene transcription factors trigger, as the initial step of neuronal remodeling, cascades of activity-dependent protein synthesis crucial for structural synaptic rearrangements. After chronic electrical intracochlear stimulation molecular changes beyond immediate early expression were detected. It seems very likely that superior olivary neurons forming the newly identified pathway towards the cochlear nucleus mediate structural plasticity caused by novel sensory afferent activity. The model of electrically stimulating the hearing nerve in the cochlea that was used here provides the unique opportunity to study activity-dependent plasticity in the adult brain from few hours to several days, with the possibility to increase the time window to several weeks. Understanding the specific molecular, ultrastructural, and morphological changes to central auditory neurons entailed by the substitution for physiological sensory activation by this electrical stimulation may enormously help perfecting cochlear implant therapy.

7. Abbreviations

ABR	auditory brainstem response
AC	auditory cortex
AP-1	activator protein 1
AVCN	anteroventral cochlear nucleus
CaBP	calcium-binding protein
CB	calbindin-D28k
CGRP	calcitonin gene-related peptide
CI	cochlear implant
CIC	central nucleus of the inferior colliculus
CNC	cochlear nucleus complex
CNS	central nervous system
CR	calretinin
DAB	diaminobenzidine
DAS	dorsal acoustic stria
DCN	dorsal cochlear nucleus
DNLL	dorsal nucleus of the lateral lemniscus
EABR	electrically evoked auditory brainstem response
EIS	electrical intracochlear stimulation
FB	fast blue
GAP-43	growth and plasticity-associated protein
GFAP	glial fibrillary acidic protein
IAS	intermediate acoustic stria
IC	inferior colliculus
IEG	immediate early gene
IHC	inner hair cell
LNTB	lateral nucleus of the trapezoid body
LOC	lateral olivocochlear
LSO	lateral superior olive
LTP	long-term potentiation
MGB	medial geniculate body

MGBd	dorsal medial geniculate body
MGBm	medial medial geniculate body
MGBv	ventral medial geniculate body
MNTB	medial nucleus of the trapezoid body
MOC	medial olivocochlear
MSO	medial superior olive
NCAM	neural cell adhesion molecule
NLL	nuclei of the lateral lemniscus
OHC	outer hair cell
PBS	phosphate buffered saline
PKC	protein kinase C
PSA	polysialic acid
PV	parvalbumin
PVCN	posteroventral cochlear nucleus
SOC	superior olivary complex
TB	trapezoid body
TEA	triethanol amine
VAS	ventral acoustic stria
VCN	ventral cochlear nucleus
VNLL	ventral nucleus of the lateral lemniscus
VNTB	ventral nucleus of the trapezoid body

8. References

Abraham, W. C., Williams, J. M. 2003. Properties and mechanisms of LTP maintenance. Neuroscientist. 9, 463-474.

Adams, J. C., 1979. Ascending projections to the inferior colliculus. J.Comp.Neurol. 183, 519-538.

Adams, J. C., 1995. Sound stimulation induces Fos-related antigens in cells with common morphological properties throughout the auditory brainstem. J.Comp.Neurol. 361, 645-668.

Adams, J. C., Mugnaini, E., 1987. Patterns of glutamate decarboxylase immunostaining in the feline cochlear nuclear complex studied with silver enhancement and electron microscopy. J.Comp.Neurol. 262, 375-401.

Adams, J. C., Mugnaini, E. 1990. Immunocytochemical evidence for inhibitory and disinhibitory circuits in the superior olive. Hear.Res. 49, 281-298.

Aigner, L., Arber, S., Kapfhammer, J. P., Laux, T., Schneider, C., Botteri, F., Brenner, H. R., Caroni, P. 1995. Overexpression of the neural growth-associated protein GAP-43 induces nerve sprouting in the adult nervous system of transgenic mice. Cell 83, 269-278.

Aigner, L., Caroni, P. 1993. Depletion of 43-kD growth-associated protein in primary sensory neurons leads to diminished formation and spreading of growth cones. J.Cell Biol. 123, 417-429.

Alibardi, L., 1998a. Ultrastructural and immunocytochemical characterization of commissural neurons in the ventral cochlear nucleus of the rat. Ann.Anat. 180, 427-438.

Alibardi, L., 1998b. Ultrastructural and immunocytochemical characterization of neurons in the rat ventral cochlear nucleus projecting to the inferior colliculus. Ann.Anat. 180, 415-426.

Alibardi, L., 2000. Cytology, synaptology and immunocytochemistry of commissural neurons and their putative axonal terminals in the dorsal cochlear nucleus of the rat. Ann.Anat. 182, 207-220.

Alonso, G., Prieto, M., Legrand, A., Chauvet, N., 1997. PSA-NCAM and B-50/GAP-43 are coexpressed by specific neuronal systems of the adult rat mediobasal hypothalamus that exhibit remarkable capacities for morphological plasticity. J.Comp.Neurol. 384, 181-199.

Arndt, K., Fink, G. R., 1986. GCN4 protein, a positive transcription factor in yeast, binds general control promoters at all 5' TGACTC 3' sequences. Proc.Natl.Acad.Sci.U.S.A 83, 8516-8520.

Aschoff, A., Ostwald, J., 1988. Distribution of cochlear efferents and olivo-collicular neurons in the brainstem of rat and guinea pig. A double labeling study with fluorescent tracers. Exp Brain Res 71, 241-251.

Ausubel, F.M. et al., 1992. Short protocols in molecular biology, 2nd Edition,. (J. Wiley and Sons, eds.) pp. 14-24. 14-30.

Babalian, A. L., Jacomme, A. V., Doucet, J. R., Ryugo, D. K., Rouiller, E. M., 2002. Commissural glycinergic inhibition of bushy and stellate cells in the anteroventral cochlear nucleus. Neuroreport 13, 555-558.

Barea-Rodriguez, E. J., Rivera, D. T., Jaffe, D. B., Martinez, J. L., Jr. 2000. Protein synthesis inhibition blocks the induction of mossy fiber long-term potentiation in vivo. J.Neurosci. 20, 8528-8532.

Becker, C. G., Artola, A., Gerardy-Schahn, R., Becker, T., Welzl, H., Schachner, M., 1996. The polysialic acid modification of the neural cell adhesion molecule is involved in spatial learning and hippocampal long-term potentiation. J.Neurosci.Res. 45, 143-152.

Benowitz, L. I., Apostolides, P. J., Perrone-Bizzozero, N., Finklestein, S. P., Zwiers, H. 1988. Anatomical distribution of the growth-associated protein GAP-43/B-50 in the adult rat brain. J.Neurosci. 8, 339-352.

Benowitz, L. I., Routtenberg, A. 1997. GAP-43: an intrinsic determinant of neuronal development and plasticity. Trends Neurosci. 20, 84-91.

Beyerl, B. D., 1978. Afferent projections to the central nucleus of the inferior colliculus in the rat. Brain Res. 145, 209-223.

Bledsoe, S. C., Jr., Nagase, S., Miller, J. M., Altschuler, R. A. 1995. Deafness-induced plasticity in the mature central auditory system. Neuroreport 7, 225-229.

Bliss, T. V., Collingridge, G. L. 1993. A synaptic model of memory: long-term potentiation in the hippocampus. Nature 361, 31-39.

Bliss, T. V., Lomo, T., 1973. Long-lasting potentiation of synaptic transmission in the dentate area of the anaesthetized rabbit following stimulation of the perforant path. J.Physiol. 232, 331-356.

Bonfanti, L., Olive, S., Poulain, D. A., Theodosis, D. T. 1992., Mapping of the distribution of polysialylated neural cell adhesion molecule throughout the central nervous system of the adult rat: an immunohistochemical study. Neuroscience 49, 419-436.

Bordi, F., LeDoux, J. E., 1994. Response properties of single units in areas of rat auditory thalamus that project to the amygdala. I. Acoustic discharge patterns and frequency receptive fields. Exp.Brain Res. 98, 261-274.

Bouzioukh, F., Tell, F., Jean, A., Rougon, G., 2001. NMDA receptor and nitric oxide synthase activation regulate polysialylated neural cell adhesion molecule expression in adult brainstem synapses. J.Neurosci. 21, 4721-4730.

Bramham, C. R., Southard, T., Sarvey, J. M., Herkenham, M., Brady, L. S. 1996. Unilateral LTP triggers bilateral increases in hippocampal neurotrophin and trk receptor mRNA expression in behaving rats: evidence for interhemispheric communication. J.Comp.Neurol. 368, 371-382.

Brawer, J. R., Morest, D. K., Kane, E. C., 1974. The neuronal architecture of the cochlear nucleus of the cat. J.Comp.Neurol. 155, 251-300.

Bredderman, P. J., Wasserman, R. H., 1974. Chemical composition, affinity for calcium, and some related properties of the vitamin D dependent calcium-binding protein. Biochemistry 13, 1687-1694.

Buchwald J.S., Huang C., 1975. Far-field acoustic response: origins in the cat. Science 189, 382-384.

Caicedo, A., Herbert, H., 1993. Topography of descending projections from the inferior colliculus to auditory brainstem nuclei in the rat. J.Comp.Neurol. 328, 377-392.

Caillard, O., Moreno, H., Schwaller, B., Llano, I., Celio, M. R., Marty, A., 2000. Role of the calcium-binding protein parvalbumin in short-term synaptic plasticity. Proc.Natl.Acad.Sci.U.S.A. 97, 13372-13377.

Calford, M. B., Aitkin, L. M., 1983. Ascending projections to the medial geniculate body of the cat: evidence for multiple, parallel auditory pathways through thalamus. J.Neurosci. 3, 2365-2380.

Cant, N. B. 1984. The fine structure of the lateral superior olivary nucleus of the cat. J.Comp.Neurol. 227, 63-77.

Cant, N. B., Gaston, K. C., 1982. Pathways connecting the right and left cochlear nuclei. J.Comp.Neurol. 212, 313-326.

Carretta, D., Herve-Minvielle, A., Bajo, V. M., Villa, A. E., Rouiller, E. M.. 1999. c-Fos expression in the auditory pathways related to the significance of acoustic signals in rats performing a sensory-motor task. Brain Res. 841, 170-183.

Casseday, J. H., Fremouw, T., Covey, E., 2002. The inferior colliculus. In “The mammalian auditory pathway: Neuroatonomy” (D. Oertel, R. R. Fay, A. N. Popper, eds.) pp. 239-308. Springer Verlag, New York

Celio, M. R., 1990. Calbindin D-28k and parvalbumin in the rat nervous system. Neuroscience 35, 375-475.

Celio, M. R., Baier, W., Scharer, L., de Viragh, P. A., Gerday, C., 1988. Monoclonal antibodies directed against the calcium binding protein parvalbumin. Cell Calcium 9, 81-86.

Celio, M. R., Heizmann, C. W., 1982. Calcium-binding protein parvalbumin is associated with fast contracting muscle fibres. Nature 297, 504-506.

Chaudhuri, A., 1997. Neural activity mapping with inducible transcription factors. Neuroreport 8, iii-vii.

Chirwa, S., Aduonum, A., Pizarro, J., Reasor, J., Kawai, Y., Gonzalez, M., McAdory, B. S., Onaivi, E., Barea-Rodriguez, E. J., 2005. Dopaminergic DA1 signaling couples growth-associated protein-43 and long-term potentiation in guinea pig hippocampus. Brain Res.Bull. 64, 433-440.

Cho, Y., Gong, T. W., Kanicki, A., Altschuler, R. A., Lomax, M. I., 2004. Noise overstimulation induces immediate early genes in the rat cochlea. Mol.Brain.Res. 130, 134-148.

Christy, B. A., Lau, L. F., Nathans, D., 1988. A gene activated in mouse 3T3 cells by serum growth factors encodes a protein with "zinc finger" sequences. Proc.Natl.Acad.Sci.U.S.A. 85, 7857-7861.

Clark, S. A., Allard, T., Jenkins, W. M., Merzenich, M. M., 1988. Receptive fields in the body-surface map in adult cortex defined by temporally correlated inputs. Nature 332, 444-445.

Clerici, W. J., McDonald, A. J., Thompson, R., Coleman, J. R., 1990. Anatomy of the rat medial geniculate body: II. Dendritic morphology. J.Comp.Neurol. 297, 32-54.

Cole, A. J., Saffen, D. W., Baraban, J. M., Worley, P. F., 1989. Rapid increase of an immediate early gene messenger RNA in hippocampal neurons by synaptic NMDA receptor activation. Nature 340, 474-476.

Coleman, J. R., Clerici, W. J. 1987. Sources of projections to subdivisions of the inferior colliculus in the rat. J.Comp.Neurol. 262, 215-226.

Darlington, C. L., Flohr, H., Smith, P. F., 1991. Molecular mechanisms of brainstem plasticity. The vestibular compensation model. Mol.Neurobiol. 5, 355-368.

de Graan, P. N., Van Hooff, C. O., Tilly, B. C., Oestreicher, A. B., Schotman, P., Gispen, W. H., 1985. Phosphoprotein B-50 in nerve growth cones from fetal rat brain. Neurosci.Lett. 61, 235-241.

de Groen, P. C., Eggen, B. J., Gispen, W. H., Schotman, P., Schrama, L. H., 1995. Cloning and promoter analysis of the human B-50/GAP-43 gene. J.Mol.Neurosci. 6, 109-119.

Demmer, J., Dragunow, M., Lawlor, P. A., Mason, S. E., Leah, J. D., Abraham, W. C., Tate, W. P., 1993. Differential expression of immediate early genes after hippocampal long-term potentiation in awake rats. Mol.Brain.Res. 17, 279-286.

Doucet, J. R., Ross, A. T., Gillespie, M. B., Ryugo, D. K., 1999. Glycine immunoreactivity of multipolar neurons in the ventral cochlear nucleus which project to the dorsal cochlear nucleus. J.Comp.Neurol. 408, 515-531.

Doucet, J. R., Ryugo, D. K., 1997. Projections from the ventral cochlear nucleus to the dorsal cochlear nucleus in rats. J.Comp.Neurol. 385, 245-264.

Dragunow, M., Abraham, W. C., Goulding, M., Mason, S. E., Robertson, H. A., Faull, R. L. 1989. Long-term potentiation and the induction of c-fos mRNA and proteins in the dentate gyrus of unanesthetized rats. Neurosci.Lett. 101, 274-280.

Duncan, G. E., Johnson, K. B., Breese, G. R., 1993. Topographic patterns of brain activity in response to swim stress: assessment by 2-deoxyglucose uptake and expression of Fos-like immunoreactivity. J.Neurosci. 13, 3932-3943.

Eckhardt, M., Bukalo, O., Chazal, G., Wang, L., Goridis, C., Schachner, M., Gerardy-Schahn, R., Cremer, H., Dityatev, A., 2000. Mice deficient in the polysialyltransferase ST8SiaIV/PST-1 allow discrimination of the roles of neural cell adhesion molecule protein and polysialic acid in neural development and synaptic plasticity. J.Neurosci. 20, 5234-5244.

Ehret, G., Fischer, R., 1991. Neuronal activity and tonotopy in the auditory system visualized by c-fos gene expression. Brain Res. 567, 350-354.

Elverland, H. H., 1977. Descending connections between superior olivary and cochlear nuclear complexes in the cat studied by autoradiographic and horseradish peroxidase methods. Exp.Brain Res. 27, 397-12.

Elverland,, H. H., 1978. Ascending and intrinsic projections of the superior olivary complex in the cat. Exp.Brain Res. 32, 117-134.

Eun, S. Y., Hong, Y. H., Kim, E. H., Jeon, H., Suh, Y. H., Lee, J. E., Jo, C., Jo, S. A., Kim, J. 2004. Glutamate receptor-mediated regulation of c-fos expression in cultured microglia. Biochem.Biophys.Res.Commun. 325, 320-327.

Faye-Lund, H., Osen, K. K. 1985. Anatomy of the inferior colliculus in rat. Anat.Embryol.(Berl) 171, 1-20.

Finlayson, P. G., Adam, T. J., 1997. Excitatory and inhibitory response adaptation in the superior olive complex affects binaural acoustic processing. Hear.Res. 103, 1-18.

Fleischmann, A., Hafezi, F., Elliott, C., Reme, C. E., Ruther, U., Wagner, E. F. 2000. Fra-1 replaces c-Fos-dependent functions in mice. Genes Dev. 14, 2695-2700.

Fleischmann, A., Hvalby, O., Jensen, V., Strekalova, T., Zacher, C., Layer, L. E., Kvello, A., Reschke, M., Spanagel, R., Sprengel, R., Wagner, E. F., Gass, P., 2003. Impaired long-term memory and NR2A-type NMDA receptor-dependent synaptic plasticity in mice lacking c-Fos in the CNS. J.Neurosci. 23, 9116-9122.

Floris, A., Dino, M., Jacobowitz, D. M., Mugnaini, E., 1994. The unipolar brush cells of the rat cerebellar cortex and cochlear nucleus are calretinin-positive: a study by light and electron microscopic immunocytochemistry. Anat.Embryol.(Berl) 189, 495-520.

Förster, C. R., Illing, R. B., 2000. Plasticity of the auditory brainstem: cochleotomy-induced changes of calbindin-D28k expression in the rat. J.Comp.Neurol. 416, 173-187.

Friauf, E. 1992. Tonotopic Order in the Adult and Developing Auditory System of the Rat as Shown by c-fos Immunocytochemistry. Eur.J.Neurosci. 4, 798-812.

Friauf, E., 1993. Transient appearance of calbindin-D28k-positive neurons in the superior olivary complex of developing rats. J.Comp.Neurol. 334, 59-74.

Friauf, E., 1994. Distribution of calcium-binding protein calbindin-D28k in the auditory system of adult and developing rats. J.Comp.Neurol. 349, 193-211.

Friauf, E., 1995. C-fos immunocytochemical evidence for acoustic pathway mapping in rats. Behav.Brain.Res 66, 217-224.

Friauf, E., Ostwald, J., 1988. Divergent projections of physiologically characterized rat ventral cochlear nucleus neurons as shown by intra-axonal injection of horseradish peroxidase. Exp.Brain Res. 73, 263-284.

Games, K. D., Winer, J. A., 1988. Layer V in rat auditory cortex: projections to the inferior colliculus and contralateral cortex. Hear.Res. 34, 1-25.

Gates, T. S., Weedman, D. L., Pongstaporn, T., Ryugo, D. K., 1996. Immunocytochemical localization of glycine in a subset of cartwheel cells of the dorsal cochlear nucleus in rats. Hear.Res. 96, 157-166.

Geissler, D. B., Ehret, G., 2004. Auditory perception vs. recognition: representation of complex communication sounds in the mouse auditory cortical fields. Eur.J.Neurosci. 19, 1027-1040.

Gianotti, C., Nunzi, M. G., Gispen, W. H., Corradetti, R., 1992. Phosphorylation of the presynaptic protein B-50 (GAP-43) is increased during electrically induced long-term potentiation. Neuron 8, 843-848.

Gispen, W. H., Nielander, H. B., de Graan, P. N., Oestreicher, A. B., Schrama, L. H., Schotman, P. 1991. Role of the growth-associated protein B-50/GAP-43 in neuronal plasticity. Mol.Neurobiol. 5, 61-85.

Glendenning, K. K., Baker, B. N., 1988. Neuroanatomical distribution of receptors for three potential inhibitory neurotransmitters in the brainstem auditory nuclei of the cat. J.Comp.Neurol. 275, 288-308.

Golding, N. L., Oertel, D., 1996. Context-dependent synaptic action of glycinergic and GABAergic inputs in the dorsal cochlear nucleus. J.Neurosci. 16, 2208-2219.

Gonzalez-Hernandez, T., Mantolan-Sarmiento, B., Gonzalez-Gonzalez, B., Perez-Gonzalez, H., 1996. Sources of GABAergic input to the inferior colliculus of the rat. J.Comp.Neurol. 372, 309-326.

Goodman, C. S., Shatz, C. J. 1993. Developmental mechanisms that generate precise patterns of neuronal connectivity. Cell 72 Suppl, 77-98.

Goslin, K., Schreyer, D. J., Skene, J. H., Banker G., 1988. Development of neuronal polarity: GAP-43 distinguishes axonal from dendritic growth cones. Nature 336, 672-674.

Groff, J. A., Liberman, M. C., 2003. Modulation of cochlear afferent response by the lateral olivocochlear system: activation via electrical stimulation of the inferior colliculus. J.Neurophysiol. 90, 3178-3200.

Guinan, J. J., Jr., Warr, W. B., Norris, B. E., 1983. Differential olivocochlear projections from lateral versus medial zones of the superior olivary complex. J.Comp Neurol. 221, 358-370.

Hackney, C. M., Osen, K. K., Kolston, J., 1990. Anatomy of the cochlear nuclear complex of guinea pig. Anat.Embryol.(Berl) 182, 123-149.

Halasy, K., Miettinen, R., Szabat, E., Freund, T. F., 1992. GABAergic Interneurons are the major postsynaptic targets of median raphe afferents in the rat dentate gyrus. Eur.J.Neurosci. 4, 144-153.

Halazonetis, T. D., Georgopoulos, K., Greenberg, M. E., Leder, P. 1988. c-Jun dimerizes with itself and with c-Fos, forming complexes of different DNA binding affinities. Cell 55, 917-924.

Harrison, J. M., Irving, R., 1965. The anterior ventral cochlear nucleus. J.Comp.Neurol. 124, 15-41.

Harrison, J. M., Warr, W. B., 1962. A study of the cochlear nuclei and ascending auditory pathways of the medulla. J.Comp.Neurol. 119, 341-379.

Hartshorn, D. O., Miller, J. M., Altschuler, R. A. 1991. Protective effect of electrical stimulation in the deafened guinea pig cochlea. Otolaryngol.Head Neck Surg. 104, 311-319.

He, Q., Dent, E. W., Meiri, K. F. 1997. Modulation of actin filament behavior by GAP-43 (neuromodulin) is dependent on the phosphorylation status of serine 41, the protein kinase C site. J.Neurosci. 17, 3515-3524.

Hebb, D. O., 1949. The organization of behavior: A neuropsychological theory. Wiley, New York

Hefti, B. J., Smith, P. H., 2000. Anatomy, physiology, and synaptic responses of rat layer V auditory cortical cells and effects of intracellular GABA(A) blockade. J.Neurophysiol. 83, 2626-2638.

Heizmann, C. W., 1984. Parvalbumin, a relaxing factor in muscle and a neuronal marker in brain. Prog.Clin.Biol.Res. 168, 205-210.

Henkel, C. K., Gabriele, M. L., 1999. Organization of the disynaptic pathway from the anteroventral cochlear nucleus to the lateral superior olivary nucleus in the ferret. Anat.Embryol.(Berl) 199, 149-160.

Henkel, C. K., Spangler, K. M. 1983. Organization of the efferent projections of the medial superior olivary nucleus in the cat as revealed by HRP and autoradiographic tracing methods. J.Comp.Neurol. 221, 416-428.

Herdegen, T., Leah, J. D., 1998. Inducible and constitutive transcription factors in the mammalian nervous system: control of gene expression by Jun, Fos and Krox, and CREB/ATF proteins. Brain Res.Brain Res.Rev. 28, 370-490.

Herkenham, M., 1980. Laminar organization of thalamic projections to the rat neocortex. Science 207, 532-535.

Hess, U. S., Lynch, G., Gall, C. M. 1995. Regional patterns of c-fos mRNA expression in rat hippocampus following exploration of a novel environment versus performance of a well-learned discrimination. J.Neurosci. 15, 7796-7809.

Hillman, D. E., Gordon, C. E., Troublefield, Y., Stone, E., Giacchi, R. J., Chen, S., 1997. Effect of unilateral tympanotomy on auditory induced c-fos expression in cochlear nuclei. Brain Res. 748, 77-84.

Horváth, M., Forster, C. R., Illing, R. B. 1997. Postnatal development of GAP-43 immunoreactivity in the auditory brainstem of the rat. J.Comp Neurol. 382, 104-115.

Horváth, M., Kraus, K. S., Illing, R. B., 2000. Olivocochlear neurons sending axon collaterals into the ventral cochlear nucleus of the rat. J.Comp.Neurol. 422, 95-105.

Huang, Y. Y., Li, X. C., Kandel, E. R. 1994. cAMP contributes to mossy fiber LTP by initiating both a covalently mediated early phase and macromolecular synthesis-dependent late phase. Cell 79, 69-79.

Hubel, D. H., Wiesel, T. N., 1970. The period of susceptibility to the physiological effects of unilateral eye closure in kittens. J.Physiol. 206, 419-436.

Hughes, P. E., Alexi, T., Walton, M., Williams, C. E., Dragunow, M., Clark, R. G., Gluckman, P. D. 1999. Activity and injury-dependent expression of inducible transcription factors, growth factors and apoptosis-related genes within the central nervous system. Prog.Neurobiol. 57, 421-450.

Illing, R. B., Cao, Q. L., Förster, C. R., Laszig, R. 1999. Auditory brainstem: development and plasticity of GAP-43 mRNA expression in the rat. J.Comp.Neurol. 412, 353-372.

Illing, R. B., Horváth, M. 1995. Re-emergence of GAP-43 in cochlear nucleus and superior olive following cochlear ablation in the rat. Neurosci.Lett. 194, 9-12.

Illing, R. B., Horváth, M., Laszig, R., 1997. Plasticity of the auditory brainstem: effects of cochlear ablation on GAP-43 immunoreactivity in the rat. J.Comp.Neurol. 382, 116-138.

Illing, R. B., Michler, S. A., Kraus, K. S., Laszig, R., 2002. Transcription factor modulation and expression in the rat auditory brainstem following electrical intracochlear stimulation. Exp.Neurol. 175, 226-244.

Illing, R. B., Michler, S. A., 2001. Modulation of P-CREB and expression of c-fos in cochlear nucleus and superior olive following electrical intracochlear stimulation. Neuroreport 12, 875-878.

Illing, R.B., Reisch, A., 2006. Specific plasticity responses to unilaterally decreased or increased hearing intensity in the adult cochlear nucleus and beyond. Hear.Res. 216-217, 189-197.

Ishida, Y., Nakahara, D., Hashiguchi, H., Nakamura, M., Ebihara, K., Takeda, R., Nishimori, T., Niki, H., 2002. Fos expression in GABAergic cells and cells immunopositive for NMDA receptors in the inferior and superior colliculi following audiogenic seizures in rats. Synapse 46, 100-107.

Jain, N., Florence, S. L., Qi, H. X., Kaas, J. H., 2000. Growth of new brainstem connections in adult monkeys with massive sensory loss. Proc.Natl.Acad.Sci.U.S.A. 97, 5546-5550.

Jeffery, K. J., Abraham, W. C., Dragunow, M., Mason, S. E. 1990. Induction of Fos-like immunoreactivity and the maintenance of long-term potentiation in the dentate gyrus of unanesthetized rats. Brain Res.Mol.Brain Res. 8, 267-274.

Jones, M. W., Errington, M. L., French P. J., Fine, A., Bliss, T. V., Garel, S., Charnay, P., Bozon, B., Laroche, S., Davis, S., 2001. A requirement for the immediate early gene Zif268 in the expression of late LTP and long-term memories. Nat.Neurosci. 4, 289-296.

Kaas, J. H., Merzenich, M. M., Killackey, H. P., 1983. The reorganization of somatosensory cortex following peripheral nerve damage in adult and developing mammals. Annu.Rev.Neurosci. 6, 325-356.

Kaczmarek, L., 1992. Expression of c-fos and other genes encoding transcription factors in long-term potentiation. Behav.Neural.Biol. 57, 263-266.

Kalloniatis, M., Fletcher, E. L., 1993. Immunocytochemical localization of the amino acid neurotransmitters in the chicken retina. J.Comp.Neurol. 336, 174-193.

Kandel, E. R., Schwartz, J. H., Jessel, T. M., 2000. Principles of neural science. McGraw-Hill, 4th edition

Kaplan, I. V., Guo, Y., Mower, G. D. 1995. Developmental expression of the immediate early gene EGR-1 mirrors the critical period in cat visual cortex. Brain Res.Dev.Brain Res. 90, 174-179.

Kearney, J. A., Frey, K. A., Albin, R. L., 1997. Metabotropic glutamate agonist-induced rotation: a pharmacological, FOS immunohistochemical, and [14C]-2-deoxyglucose autoradiographic study. J.Neurosci. 17, 4415-4425.

Keilmann, A., Herdegen, T., 1996. Decreased expression of the c-Fos, but not Jun B, transcription factor in the auditory pathway of the rat after repetitive acoustic stimulation. ORL J.Otorhinolaryngol.Relat Spec. 58, 262-265.

Keilmann, A., Herdegen, T., 1997. The c-Fos transcription factor in the auditory pathway of the juvenile rat: effects of acoustic deprivation and repetitive stimulation. Brain Res. 753, 291-298.

Kelly, J. B., Glenn, S. L., Beaver, C. J. 1991. Sound frequency and binaural response properties of single neurons in rat inferior colliculus. Hear.Res. 56, 273-280.

Kelly, J. B., Li, L., 1997. Two sources of inhibition affecting binaural evoked responses in the rat's inferior colliculus: the dorsal nucleus of the lateral lemniscus and the superior olivary complex. Hear.Res. 104, 112-126.

Kim, J., Morest, D. K., Bohne, B. A. 1997. Degeneration of axons in the brainstem of the chinchilla after auditory overstimulation. Hear.Res. 103, 169-191.

King, S. M., Shehab, S., Dean, P., Redgrave, P. 1996. Differential expression of fos-like immunoreactivity in the descending projections of superior colliculus after electrical stimulation in the rat. Behav.Brain Res. 78, 131-145.

Kiss, J. Z., Rougon, G., 1997. Cell biology of polysialic acid. Curr.Opin.Neurobiol. 7, 640-646.

Kiss, J. Z., Wang, C., Olive, S., Rougon, G., Lang, J., Baetens, D., Harry, D., Pralong, W. F. 1994. Activity-dependent mobilization of the adhesion molecule polysialic NCAM to the cell surface of neurons and endocrine cells. EMBO J. 13, 5284-5292.

Kleschevnikov, A. M., Routtenberg, A., 2001. PKC activation rescues LTP from NMDA receptor blockade. Hippocampus 11, 168-175.

Kolston, J., Osen, K. K., Hackney, C. M., Ottersen, O. P., Storm-Mathisen, J., 1992. An atlas of glycine- and GABA-like immunoreactivity and colocalization in the cochlear nuclear complex of the guinea pig. Anat.Embryol.(Berl) 186, 443-465.

Kral, A., Hartmann, R., Mortazavi, D., Klinke, R., 1998. Spatial resolution of cochlear implants: the electrical field and excitation of auditory afferents. Hear.Res. 121, 11-28.

Kraus, K. S., Illing, R. B., 1998. Cochleotomy induces c-Jun expression in the auditory brainstem. Eur. J. Neurosci. Suppl. 10, 222-222.

Kraus, K. S., Illing, R. B., 2004. Superior olivary contributions to auditory system plasticity: medial but not lateral olivocochlear neurons are the source of cochleotomy-induced GAP-43 expression in the ventral cochlear nucleus. J.Comp.Neurol. 475, 374-390.

Kraus, K. S., Illing, R. B. 2005. Cell death or survival: Molecular and connectional conditions for olivocochlear neurons after axotomy. Neuroscience 134, 467-481.

Kruger, L., Bendotti, C., Rivolta, R., Samanin, R., 1993. Distribution of GAP-43 mRNA in the adult rat brain. J.Comp.Neurol. 333, 417-434.

Kujawa, S. G., Liberman, M. C., 1997. Conditioning-related protection from acoustic injury: effects of chronic deefferentation and sham surgery. J.Neurophysiol. 78, 3095-3106.

Kulesza, R. J., Jr., Berrebi, A. S., 2000. Superior paraolivary nucleus of the rat is a GABAergic nucleus. J.Assoc.Res. Otolaryngol. 1, 255-269.

Leake, P. A., Hradek, G. T., Snyder, R. L. 1999. Chronic electrical stimulation by a cochlear implant promotes survival of spiral ganglion neurons after neonatal deafness. J.Comp.Neurol. 412, 543-562.

Lemaire, P., Revelant, O., Bravo, R., Charnay, P., 1988. Two mouse genes encoding potential transcription factors with identical DNA-binding domains are activated by growth factors in cultured cells. Proc.Natl.Acad.Sci.U.S.A. 85, 4691-4695.

LeDoux, J. E., Ruggiero, D. A., Forest, R., Stornetta, R., Reis, D. J., 1987. Topographic organization of convergent projections to the thalamus from the inferior colliculus and spinal cord in the rat. J.Comp Neurol. 264, 123-146.

LeDoux, J. E., Ruggiero, D. A., Reis, D. J., 1985. Projections to the subcortical forebrain from anatomically defined regions of the medial geniculate body in the rat. J.Comp.Neurol. 242, 182-213.

Linden, D. J., Routtenberg, A. 1989. The role of protein kinase C in long-term potentiation: a testable model. Brain Res.Brain Res.Rev. 14, 279-296.

Linke, R., 1999. Organization of projections to temporal cortex originating in the thalamic posterior intralaminar nucleus of the rat. Exp.Brain Res. 127, 314-320.

Lohmann, C., Friauf, E., 1996. Distribution of the calcium-binding proteins parvalbumin and calretinin in the auditory brainstem of adult and developing rats. J.Comp.Neurol. 367, 90-109.

Lousteau, R. J. 1987. Increased spiral ganglion cell survival in electrically stimulated, deafened guinea pig cochleae. Laryngoscope 97, 836-842.

Lovinger, D. M., Colley, P. A., Akers, R. F., Nelson, R. B., Routtenberg, A., 1986. Direct relation of long-term synaptic potentiation to phosphorylation of membrane protein F1, a substrate for membrane protein kinase C. Brain Res. 399, 205-211.

Lynch, M. A. 2004. Long-term potentiation and memory. Physiol. Rev. 84, 87-136.

Mahalik, T. J., Carrier, A., Owens, G. P., Clayton, G., 1992. The expression of GAP43 mRNA during the late embryonic and early postnatal development of the CNS of the rat: an in situ hybridization study. Brain Res.Dev.Brain Res. 67, 75-83.

Malenka, R. C., Nicoll, R. A. 1999. Long-term potentiation--a decade of progress? Science 285, 1870-1874.

Malmierca, M. S., 2003. The structure and physiology of the rat auditory system: an overview. Int.Rev.Neurobiol. 56, 147-211.

Malmierca, M. S., Blackstad, T. W., Osen, K. K., Karagulle, T., Molowny, R. L., 1993. The central nucleus of the inferior colliculus in rat: a Golgi and computer reconstruction study of neuronal and laminar structure. J.Comp.Neurol. 333, 1-27.

Malmierca, M. S., Hernandez, O., Rees, A., 2005. Intercollicular commissural projections modulate neuronal responses in the inferior colliculus. Eur.J.Neurosci. 21, 2701-2710.

Malmierca, M. S., Merchan, M. A., Henkel, C. K., Oliver, D. L., 2002. Direct projections from cochlear nuclear complex to auditory thalamus in the rat. J.Neurosci. 22, 10891-10897.

Malmierca, M. S., Merchan, M. A., Oliver, D. L., 1999. Concergence of dorsal and ventral cochlear nuclei input onto frequency-band laminae of the IC, a double tracer study in rat and cat. ARO Abstr. 22, 221.

Malmierca, M. S., Seip, K. L., Osen, K. K., 1995. Morphological classification and identification of neurons in the inferior colliculus: a multivariate analysis. Anat.Embryol.(Berl) 191, 343-350.

Marangos, N., Laszig, R., 1996. Restoration of hearing with multichannel prostheses: 10 years' experience. Folia Phoniatr.Logop. 48, 131-136.

Masterton, B., Thompson, G. C., Bechtold, J. K., RoBards, M. J., 1975. Neuroanatomical basis of binaural phase-difference analysis for sound localization: a comparative study. J.Comp.Physiol.Psychol. 89, 379-386.

Matsushima, J. I., Shepherd, R. K., Seldon, H. L., Xu, S. A., Clark, G. M. 1991. Electrical stimulation of the auditory nerve in deaf kittens: effects on cochlear nucleus morphology. Hear.Res. 56, 133-142.

Meidinger, M. A., Hildebrandt-Schoenfeld, H., Illing, R. B. 2006. Cochlear damage induces GAP-43 expression in cholinergic synapses of the cochlear nucleus in the adult rat: a light and electron microscopic study. Eur.J.Neurosci. 23, 3187-3199.

Meiri, K. F., Gordon-Weeks, P. R. 1990. GAP-43 in growth cones is associated with areas of membrane that are tightly bound to substrate and is a component of a membrane skeleton subcellular fraction. J.Neurosci. 10, 256-266.

Meiri, K. F., Saffell, J. L., Walsh, F. S., Doherty, P., 1998. Neurite outgrowth stimulated by neural cell adhesion molecules requires growth-associated protein-43 (GAP-43) function and is associated with GAP-43 phosphorylation in growth cones. J.Neurosci. 18, 10429-10437.

Merchan, M., Aguilar, L. A., Lopez-Poveda, E. A., Malmierca, M. S., 2005. The inferior colliculus of the rat: Quantitative immunocytochemical study of GABA and glycine. Neuroscience 136, 907-925.

Michler, S. A., Illing, R. B., 2002. Acoustic trauma induces reemergence of the growth- and plasticity-associated protein GAP-43 in the rat auditory brainstem. J.Comp.Neurol. 451, 250-266.

Milbrandt, J., 1987. A nerve growth factor-induced gene encodes a possible transcriptional regulatory factor. Science 238, 797-799.

Molinari, S., Battini, R., Ferrari, S., Pozzi, L., Killcross, A. S., Robbins, T. W., Jouvenceau, A., Billard, J. M., Dutar, P., Lamour, Y., Baker, W. A., Cox, H., Emson, P. C., 1996. Deficits in memory and hippocampal long-term potentiation in mice with reduced calbindin D28K expression. Proc.Natl.Acad.Sci.U.S.A. 93, 8028-8033.

Moore, J. K., Niparko, J. K., Perazzo, L. M., Miller, M. R., Linthicum, F. H., 1997. Effect of adult-onset deafness on the human central auditory system. Ann.Otol.Rhinol.Laryngol. 106, 385-390.

Moore, M. J., Caspary, D. M. 1983. Strychnine blocks binaural inhibition in lateral superior olivary neurons. J.Neurosci. 3, 237-242.

Morgan, J.I., Curran, T., 1989. Stimulus-transcription coupling in neurons: role of cellular immediate-early genes. Trends Neurosci 12, 459-462.

Morest, D. K., Kim, J., Potashner, S. J., Bohne, B. A. 1998. Long-term degeneration in the cochlear nerve and cochlear nucleus of the adult chinchilla following acoustic overstimulation. Microsc.Res.Tech. 41, 205-216.

Moriizumi, T., Hattori, T., 1991. Pyramidal cells in rat temporoauditory cortex project to both striatum and inferior colliculus. Brain Res.Bull. 27, 141-144.

Mugnaini, E., 1985. GABA neurons in the superficial layers of the rat dorsal cochlear nucleus: light and electron microscopic immunocytochemistry. J.Comp.Neurol. 235, 61-81.

Mugnaini, E., Dino, M. R., Jaarsma, D., 1997. The unipolar brush cells of the mammalian cerebellum and cochlear nucleus: cytology and microcircuitry. Prog.Brain.Res. 114, 131-150.

Mugnaini, E., Floris, A., Wright-Goss, M., 1994. Extraordinary synapses of the unipolar brush cell: an electron microscopic study in the rat cerebellum. Synapse 16, 284-311.

Muller, D., Wang, C., Skibo, G., Toni, N., Cremer, H., Calaora, V., Rougon, G., Kiss, J. Z., 1996. PSA-NCAM is required for activity-induced synaptic plasticity. Neuron 17, 413-422.

Namgung, U., Matsuyama, S., Routtenberg, A. 1997. Long-term potentiation activates the GAP-43 promoter: selective participation of hippocampal mossy cells. Proc.Natl.Acad.Sci.U.S.A 94, 11675-11680.

Nguyen, P. V., Abel, T., Kandel, E. R. 1994. Requirement of a critical period of transcription for induction of a late phase of LTP. Science 265, 1104-1107.

Oehrlein, S. A., Parker, P. J., Herget, T., 1996. Phosphorylation of GAP-43 (growth-associated protein of 43 kDa) by conventional, novel and atypical isotypes of the protein kinase C gene family: differences between oligopeptide and polypeptide phosphorylation. Biochem.J. 317 (Pt 1), 219-224.

Oliver, D. L., 1984. Dorsal cochlear nucleus projections to the inferior colliculus in the cat: a light and electron microscopic study. J.Comp.Neurol. 224, 115-172.

Oliver, D. L., 1985. Quantitative analyses of axonal endings in the central nucleus of the inferior colliculus and distribution of 3H-labeling after injections in the dorsal cochlear nucleus. J.Comp.Neurol. 237, 343-359.

Oliver, D. L., 1987. Projections to the inferior colliculus from the anteroventral cochlear nucleus in the cat: possible substrates for binaural interaction. J.Comp.Neurol. 264, 24-46.

Oliver, D. L., Ostapoff, E. M., Beckius, G. E., 1999. Direct innervation of identified tectothalamic neurons in the inferior colliculus by axons from the cochlear nucleus. Neuroscience 93, 643-658.

Oliver, D. L., Shneiderman, A. 1989. An EM study of the dorsal nucleus of the lateral lemniscus: inhibitory, commissural, synaptic connections between ascending auditory pathways. J.Neurosci. 9, 967-982.

Osen, K. K., 1969. Cytoarchitecture of the cochlear nuclei in the cat. J.Comp.Neurol. 136, 453-484.

Osen, K. K., 1972. Projection of the cochlear nuclei on the inferior colliculus in the cat. J.Comp.Neurol. 144, 355-372.

Osen, K. K., 1988. Anatomy of the mammalian cochlear nuclei, a review. In “Auditory pathway, structure and function” (J. Skyla and R. B. Masterton, eds.), pp. 66-75. Plenum Press, New York

Osen, K. K., Ottersen, O. P., Storm-Mathisen, J., 1990. Colocalization of glycine-like and GABA-like immunoreactivites, a semiquantitative study of individual neurons in the dorsal cochlear nucleus of the cat. In “Glycine Neurotransmission” (O. P. Ottersen and J. Storm-Mathisen, eds.) pp. 417-451. Wiley, Chester.

Ostapoff, E. M., Morest, D. K., Potashner, S. J., 1990. Uptake and retrograde transport of [3H]GABA from the cochlear nucleus to the superior olive in the guinea pig. J.Chem.Neuroanat. 3, 285-295.

Ottersen, O. P., Hjelle, O. P., Osen, K., K., Laake, J. H., 1995. Amino acid transmitters. In “The rat nervous system”, 2nd ed. (G. Paxinos, ed.), pp. 1017-1037. Academic Press, San Diego

Ottersen, O. P., Storm-Mathisen, J., 1985. Different neuronal localization of aspartate-like and glutamate-like immunoreactivities in the hippocampus of rat, guinea-pig and Senegalese baboon (Papio papio), with a note on the distribution of gamma-aminobutyrate. Neuroscience 16, 589-606.

Palmer, C. V., Nelson, C. T., Lindley, G. A., 1998. The functionally and physiologically plastic adult auditory system. J.Acoust.Soc.Am. 103, 1705-1721.

Paxinos, G., Watson, C., 1982. The rat brain in stereotaxic coordinates. Academic Press

Peruzzi, D., Bartlett, E., Smith, P. H., Oliver, D. L., 1997. A monosynaptic GABAergic input from the inferior colliculus to the medial geniculate body in rat. J.Neurosci. 17, 3766-3777.

Pittenger, C., Kandel, E. R. 2003. In search of general mechanisms for long-lasting plasticity: Aplysia and the hippocampus. Philos.Trans.R.Soc.Lond.B.Biol.Sci. 358, 757-763.

Platenik, J., Kuramoto, N., Yoneda, Y. 2000. Molecular mechanisms associated with long-term consolidation of the NMDA signals. Life Sci. 67, 335-364.

Ponton, C. W., Moore, J. K., Eggermont, J. J., 1999. Prolonged deafness limits auditory system developmental plasticity: evidence from an evoked potentials study in children with cochlear implants. Scand.Audiol.Suppl 51, 13-22.

Rampon, C., Jiang, C. H., Don, H., Tan, Y. P., Lockhart, D., Schultz, P., Tsien, J. Z., Hu, Y., 2000. Effects of environmental enrichment on gene expression in the brain. Proc.Natl.Acad.Sci.U.S.A. 97, 12880-12884.

Reimer, K., 1993. Simultaneous demonstration of Fos-like immunoreactivity and 2-deoxy-glucose uptake in the inferior colliculus of the mouse. Brain Res. 616, 339-343.

Reisch, A., Illing, R. B., 2005. Electrical intracochlear stimulation induces c-Fos expression in specific neuronal populations of the cochlear nucleus. Proc. 6th German Neuroscience Conference Göttingen, 378B.

Reisch ,A., Illing, R. B., 2006. Neuronal cell types in the rat auditory brainstem as defined by molecular profile and axonal projection. In preparation.

Rhode, W. S., 1991. Physiological-morphological properties of the cochlear nucleus. In "Neurobiology of Hearing: The Central Auditory System" (R. A. Altschuler et al., eds.) pp 47-77. Raven Press Ltd., New York.

Richardson, C. L., Tate, W. P., Mason, S. E., Lawlor, P. A., Dragunow, M., Abraham, W. C. 1992. Correlation between the induction of an immediate early gene, zif/268, and long-term potentiation in the dentate gyrus. Brain Res. 580, 147-154.

Rietzel, H. J., Friauf, E., 1998. Neuron types in the rat lateral superior olive and developmental changes in the complexity of their dendritic arbors. J.Comp.Neurol. 390, 20-40.

Robinson, K., 1998. Implications of developmental plasticity for the language acquisition of deaf children with cochlear implants. International Journal of Pediatric Otorhinolaryngology 46, 71-80

Roberts, R. C., Ribak, C. E., 1987a. GABAergic neurons and axon terminals in the brainstem auditory nuclei of the gerbil. J.Comp.Neurol. 258, 267-280.

Roberts, R. C., Ribak, C. E., 1987b. An electron microscopic study of GABAergic neurons and terminals in the central nucleus of the inferior colliculus of the rat. J.Neurocytol. 16, 333-345.

Robertson, D., Anderson, C. J., 1994. Acute and chronic effects of unilateral elimination of auditory nerve activity on susceptibility to temporary deafness induced by loud sound in the guinea pig. Brain Res. 646, 37-43.

Rogers J. 1989. Calcium-binding proteins: the search for functions. Nature 339, 661-662.

Rogers, J. H., 1987. Calretinin: a gene for a novel calcium-binding protein expressed principally in neurons. J Cell Biol. 105, 1343-1353.

Ronn, L. C., Berezin, V., Bock, E., 2000. The neural cell adhesion molecule in synaptic plasticity and ageing. Int.J.Dev.Neurosci. 18, 193-199.

Rougon, G., Deagostini-Bazin, H., Hirn, M., Goridis, C. 1982. Tissue- and developmental stage-specific forms of a neural cell surface antigen linked to differences in glycosylation of a common polypeptide. EMBO J. 1, 1239-1244.

Rouiller, E. M., Wan, X. S., Moret, V. Liang, F., 1992. Mapping of c-fos expression elicited by pure tones stimulation in the auditory pathways of the rat, with emphasis on the cochlear nucleus. Neurosci. Lett. 144, 19-24.

Routtenberg, A., Cantallops, I., Zaffuto, S., Serrano, P., Namgung, U. 2000. Enhanced learning after genetic overexpression of a brain growth protein. Proc.Natl.Acad.Sci.U.S.A 97, 7657-7662.

Rutishauser, U., Acheson, A., Hall, A. K., Mann, D. M., Sunshine, J., 1988. The neural cell adhesion molecule (NCAM) as a regulator of cell-cell interactions. Science 240, 53-57.

Rutishauser, U., Landmesser, L., 1996. Polysialic acid in the vertebrate nervous system: a promoter of plasticity in cell-cell interactions. Trends Neurosci. 19, 422-427.

Ryan, A. F., Furlow, Z., Woolf, N. K., Keithley, E. M. 1988. The spatial representation of frequency in the rat dorsal cochlear nucleus and inferior colliculus. Hear.Res. 36, 181-189.

Saint Marie, R. L., 1996. Glutamatergic connections of the auditory midbrain: selective uptake and axonal transport of D-[3H]aspartate. J.Comp.Neurol. 373, 255-270.

Saint Marie, R. L., Baker, R. A., 1990. Neurotransmitter-specific uptake and retrograde transport of [3H]glycine from the inferior colliculus by ipsilateral projections of the superior olivary complex and nuclei of the lateral lemniscus. Brain Res. 524, 244-253.

Saint Marie, R. L., Benson, C. G., Ostapoff, E. M., Morest, D. K., 1991. Glycine immunoreactive projections from the dorsal to the anteroventral cochlear nucleus. Hear.Res. 51, 11-28.

Saint Marie, R. L., Luo, L., Ryan, A. F., 1999a. Spatial representation of frequency in the rat dorsal nucleus of the lateral lemniscus as revealed by acoustically induced c-fos mRNA expression. Hear.Res. 128, 70-74.

Saint Marie, R. L., Luo, L., Ryan, A. F., 1999b. Effects of stimulus frequency and intensity on c-fos mRNA expression in the adult rat auditory brainstem. J.Comp.Neurol. 404, 258-270.

Saint Marie, R. L., Ostapoff, E. M., Morest, D. K., Wenthold, R. J., 1989. Glycine-immunoreactive projection of the cat lateral superior olive: possible role in midbrain ear dominance. J.Comp.Neurol. 279, 382-396.

Saito H., Miller J. M., Altschuler R. A., 2000. Cochleotopic fos immunoreactivity in cochlea and cochlear nuclei evoked by bipolar cochlear electrical stimulation. Hear.Res. 145, 37-51.

Saito, H., Miller, J. M., Pfingst, B. E., Altschuler, R. A. 1999. Fos-like immunoreactivity in the auditory brainstem evoked by bipolar intracochlear electrical stimulation: effects of current level and pulse duration. Neuroscience 91, 139-161.

Saldana, E., Feliciano, M., Mugnaini, E., 1996. Distribution of descending projections from primary auditory neocortex to inferior colliculus mimics the topography of intracollicular projections. J.Comp.Neurol. 371, 15-40.

Sargent, P. B., 1994. Double-label immunofluorescence with the laser scanning confocal microscope using cyanine dyes. Neuroimage. 1, 288-295.

Schachner, M., 1997. Neural recognition molecules and synaptic plasticity. Curr.Opin.Cell Biol. 9, 627-634.

Schaechter, J. D., Benowitz, L. I. 1993., Activation of protein kinase C by arachidonic acid selectively enhances the phosphorylation of GAP-43 in nerve terminal membranes. J.Neurosci. 13, 4361-4371.

Scharfman, H. E., Kunkel, D. D., Schwartzkroin, P. A. 1990. Synaptic connections of dentate granule cells and hilar neurons: results of paired intracellular recordings and intracellular horseradish peroxidase injections. Neuroscience 37, 693-707.

Scheidegger, P., Papay, J., Zuber, C., Lackie, P. M., Roth, J. 1994. Cellular site of synthesis and dynamics of cell surface re-expression of polysialic acid of the neural cell adhesion molecule. Eur.J.Biochem. 225, 1097-1103.

Schmitt, A. B., Breuer, S., Voell, M., Schwaiger, F. W., Spitzer, C., Pech, K., Brook, G. A., Noth, J., Kreutzberg, G. W., Nacimiento, W. 1999. GAP-43 (B-50) and C-Jun are up-regulated in axotomized neurons of Clarke's nucleus after spinal cord injury in the adult rat. Neurobiol.Dis. 6, 122-130.

Schofield, B. R., 1991. Superior paraolivary nucleus in the pigmented guinea pig: separate classes of neurons project to the inferior colliculus and the cochlear nucleus. J.Comp.Neurol. 312, 68-76.

Schofield, B. R., Cant, N. B., 1997. Ventral nucleus of the lateral lemniscus in guinea pigs: cytoarchitecture and inputs from the cochlear nucleus. J.Comp.Neurol. 379, 363-385.

Schwaller, B., Buchwald, P., Blumcke, I., Celio, M. R., Hunziker, W., 1993. Characterization of a polyclonal antiserum against the purified human recombinant calcium binding protein calretinin. Cell Calcium 14, 639-648.

Seki, T., Arai, Y., 1993. Highly polysialylated neural cell adhesion molecule (NCAM-H) is expressed by newly generated granule cells in the dentate gyrus of the adult rat. J.Neurosci. 13, 2351-2358.

Sento, S., Ryugo, D. K. 1989. Endbulbs of held and spherical bushy cells in cats: morphological correlates with physiological properties. J.Comp.Neurol. 280, 553-562.

Shepherd, R. K., Hartmann, R., Heid, S., Hardie, N., Klinke, R., 1997. The central auditory system and auditory deprivation: experience with cochlear implants in the congenitally deaf. Acta Otolaryngol.Suppl. 532, 28-33.

Shneiderman, A., Henkel, C. K., 1985. Evidence of collateral axonal projections to the superior olivary complex. Hear.Res. 19, 199-205.

Shore S. E., Godfrey D. A., Helfert R. H., Altschuler R. A., Bledsoe S. C. Jr., 1992. Connections between the cochlear nuclei in guinea pig. Hear.Res. 62, 16-26.

Skene, J. H., Willard, M., 1981. Axonally transported proteins associated with axon growth in rabbit central and peripheral nervous systems. J.Cell Biol. 89, 96-103.

Smith, P. H., Rhode, W. S., 1989. Structural and functional properties distinguish two types of multipolar cells in the ventral cochlear nucleus. J.Comp.Neurol. 282, 595-616.

Storm-Mathisen, J., Leknes, A. K., Bore, A. T., Vaaland, J. L., Edminson, P., Haug, F. M., Ottersen, O. P., 1983. First visualization of glutamate and GABA in neurones by immunocytochemistry. Nature 301, 517-520.

Strittmatter, S. M., Fankhauser, C., Huang, P. L., Mashimo, H., Fishman, M. C., 1995. Neuronal pathfinding is abnormal in mice lacking the neuronal growth cone protein GAP-43. Cell 80, 445-452.

Sukhatme, V. P., Cao, X. M., Chang, L. C., Tsai-Morris, C. H., Stamenkovich, D., Ferreira, P. C., Cohen, D. R., Edwards, S. A., Shows, T. B., Curran, T., 1988. A zinc finger-encoding gene coregulated with c-fos during growth and differentiation, and after cellular depolarization. Cell 53, 37-43.

Szabat, E., Soinila, S., Happola, O., Linnala, A., Virtanen, I., 1992. A new monoclonal antibody against the GABA-protein conjugate shows immunoreactivity in sensory neurons of the rat. Neuroscience 47, 409-420.

Thompson, G. C., Cortez, A. M., Lam, D. M., 1985. Localization of GABA immunoreactivity in the auditory brainstem of guinea pigs. Brain Res. 339, 119-122.

van Adel, B. A., Kelly, J. B. 1998. Kainic acid lesions of the superior olivary complex: effects on sound localization by the albino rat. Behav.Neurosci. 112, 432-446.

Van Hooff, C. O., de Graan, P. N., Oestreicher, A. B., Gispen, W. H., 1988. B-50 phosphorylation and polyphosphoinositide metabolism in nerve growth cone membranes. J.Neurosci. 8, 1789-1795.

Vetter, D. E., Adams, J. C., Mugnaini, E., 1991. Chemically distinct rat olivocochlear neurons. Synapse 7, 21-43.

Vetter, D. E., Mugnaini, E., 1992. Distribution and dendritic features of three groups of rat olivocochlear neurons. A study with two retrograde cholera toxin tracers. Anat.Embryol.(Berl) 185, 1-16.

Vischer, M. W., Bajo-Lorenzana, V., Zhang, J., Hausler, R., Rouiller, E. M. 1995. Activity elicited in the auditory pathway of the rat by electrical stimulation of the cochlea. ORL J.Otorhinolaryngol.Relat Spec. 57, 305-309.

Walsh, F. S., Doherty, P., 1996. Cell adhesion molecules and neuronal regeneration. Curr.Opin.Cell Biol. 8, 707-713.

Warr, W. B., 1966. Fiber degeneration following lesions in the anterior ventral cochlear nucleus of the cat. Exp.Neurol. 14, 453-474.

Warr, W. B., 1975. Olivocochlear and vestibular efferent neurons of the feline brain stem: their location, morphology and number determined by retrograde axonal transport and acetylcholinesterase histochemistry. J.Comp.Neurol. 161, 159-181.

Warr, W. B., Boche, J. B., Neely, S. T., 1997. Efferent innervation of the inner hair cell region: origins and terminations of two lateral olivocochlear systems. Hear. Res. 108, 89-111.

Warr, W. B., Guinan, J. J., Jr., 1979. Efferent innervation of the organ of corti: two separate systems. Brain Res. 173, 152-155.

Warr, W. B., Guinan, J. J., White, J. S., 1986. Organization of the efferent fibers: The lateral and medial olivocochlear system. In "Neurobiology of hearing: The cochlea" (R. A. Altschuler ed.), pp. 333-348. Raven Press, New York.

Weedman, D. L., Pongstaporn, T., Ryugo, D. K., 1996. Ultrastructural study of the granule cell domain of the cochlear nucleus in rats: mossy fiber endings and their targets. J.Comp.Neurol. 369, 345-360.

Wenthold, R. J., 1987. Evidence for a glycinergic pathway connecting the two cochlear nuclei: an immunocytochemical and retrograde transport study. Brain Res. 415, 183-187.

Wenthold, R. J., Huie, D., Altschuler, R. A., Reeks, K. A., 1987. Glycine immunoreactivity localized in the cochlear nucleus and superior olivary complex. Neuroscience 22, 897-912.

Wenthold, R. J., Zempel, J. M., Parakkal, M. H., Reeks, K. A., Altschuler, R. A., 1986. Immunocytochemical localization of GABA in the cochlear nucleus of the guinea pig. Brain Res. 380, 7-18.

White, L. E., Price, J. L., 1993. The functional anatomy of limbic status epilepticus in the rat. I. Patterns of 14C-2-deoxyglucose uptake and Fos immunocytochemistry. J.Neurosci. 13, 4787-4809.

White, J. S., Warr, W. B., 1983. The dual origins of the olivocochlear bundle in the albino rat. J.Comp.Neurol. 219:203-214.

Wickesberg, R. E., Whitlon, D., Oertel, D., 1994. In vitro modulation of somatic glycine-like immunoreactivity in presumed glycinergic neurons. J.Comp.Neurol. 339, 311-327.

Williams, S., Mmbaga, N., Chirwa, S., 2006. Dopaminergic D(1) receptor agonist SKF 38393 induces GAP-43 expression and long-term potentiation in hippocampus in vivo. Neurosci.Lett. 402, 46-50.

Winer, J. A., Kelly, J. B., Larue, D. T., 1999. Neural architecture of the rat medial geniculate body. Hear.Res. 130, 19-41.

Winer, J. A., Saint Marie, R. L., Larue, D. T., Oliver, D. L., 1996. GABAergic feedforward projections from the inferior colliculus to the medial geniculate body. Proc.Natl.Acad.Sci.U.S.A. 93, 8005-8010.

Wisden, W., Errington, M. L., Williams, S., Dunnett, S. B., Waters, C., Hitchcock, D., Evan, G., Bliss, T. V., Hunt, S. P. 1990. Differential expression of immediate early genes in the hippocampus and spinal cord. Neuron 4, 603-614.

Wisdom, R. 1999. AP-1: one switch for many signals. Exp.Cell Res. 253, 180-185.

Worley, P. F., Bhat, R. V., Baraban, J. M., Erickson, C. A., McNaughton, B. L., Barnes CA. 1993. Thresholds for synaptic activation of transcription factors in hippocampus: correlation with long-term enhancement. J. Neurosci. 13, 4776-4786.

Wu, S. H., Oertel, D., 1986. Inhibitory circuitry in the ventral cochlear nucleus is probably mediated by glycine. J.Neurosci. 6, 2691-2706.

Yang, Y., Saint Marie, R. L., Oliver, D. L., 2005. Granule cells in the cochlear nucleus sensitive to sound activation detected by Fos protein expression. Eur.J.Neursci 136, 865-882.

Yasoshima, Y., Sako, N., Senba, E., Yamamoto, T. 2006. Acute suppression, but not chronic genetic deficiency, of c-fos gene expression impairs long-term memory in aversive taste learning. Proc.Natl.Acad.Sci.U.S.A 103, 7106-7111.

Young, E. D., Robert, J. M., Shofner, W. P., 1988. Regularity and latency of units in ventral cochlear nucleus: implications for unit classification and generation of response properties. J.Neurophysiol. 60:1-29.

Yuste, R., Bonhoeffer, T. 2001. Morphological changes in dendritic spines associated with long-term synaptic plasticity. Annu.Rev.Neurosci. 24, 1071-1089.

Zhang, D. X., Li, L., Kelly, J. B., Wu, S. H., 1998. GABAergic projections from the lateral lemniscus to the inferior colliculus of the rat. Hear. Res. 117, 1-12.

Zhang, S., Oertel, D., 1993. Tuberculoventral cells of the dorsal cochlear nucleus of mice: intracellular recordings in slices. J.Neurophysiol. 69, 1409-1421.

Zhang, S., Oertel, D., 1994. Neuronal circuits associated with the output of the dorsal cochlear nucleus through fusiform cells. J.Neurophysiol. 71, 914-930.

Zhu, X. O., Brown, M. W., McCabe, B. J., Aggleton, J. P. 1995. Effects of the novelty or familiarity of visual stimuli on the expression of the immediate early gene c-fos in rat brain. Neuroscience 69, 821-829.

Zhu, X. O., McCabe, B. J., Aggleton, J. P., Brown, M. W. 1997. Differential activation of the rat hippocampus and perirhinal cortex by novel visual stimuli and a novel environment. Neurosci.Lett. 229, 141-143.

Zuschratter, W., Gass, P., Herdegen, T., Scheich, H., 1995. Comparison of frequency-specific c-Fos expression and fluoro-2-deoxyglucose uptake in auditory cortex of gerbils (Meriones unguiculatus). Eur.J.Neurosci. 7, 1614-1626.